



HAL
open science

Platelets from HIV-infected individuals on antiretroviral drug therapy with poor CD4 + T cell recovery can harbor replication-competent HIV despite viral suppression

Fernando Real, Claude Capron, Alexis Sennepin, Riccardo Arrigucci, Aiwei Zhu, Gérémy Sannier, Jonathan Zheng, Lin Xu, Jean-Marc Massé, Ségolène Greffe, et al.

► **To cite this version:**

Fernando Real, Claude Capron, Alexis Sennepin, Riccardo Arrigucci, Aiwei Zhu, et al.. Platelets from HIV-infected individuals on antiretroviral drug therapy with poor CD4 + T cell recovery can harbor replication-competent HIV despite viral suppression. *Science Translational Medicine*, 2020, 12, pp.eaat6263. 10.1126/scitranslmed.aat626 . hal-03000932

HAL Id: hal-03000932

<https://hal.science/hal-03000932>

Submitted on 20 Nov 2020

HAL is a multi-disciplinary open access archive for the deposit and dissemination of scientific research documents, whether they are published or not. The documents may come from teaching and research institutions in France or abroad, or from public or private research centers.

L'archive ouverte pluridisciplinaire **HAL**, est destinée au dépôt et à la diffusion de documents scientifiques de niveau recherche, publiés ou non, émanant des établissements d'enseignement et de recherche français ou étrangers, des laboratoires publics ou privés.

HIV

Platelets from HIV-infected individuals on antiretroviral drug therapy with poor CD4⁺ T cell recovery can harbor replication-competent HIV despite viral suppression

Fernando Real^{1,2,3}, Claude Capron⁴, Alexis Sennepin^{1,2,3}, Riccardo Arrigucci⁵, Aiwei Zhu^{1,2,3}, G  r  my Sannier^{1,2,3}, Jonathan Zheng^{1,2,3}, Lin Xu^{1,2,3}, Jean-Marc Mass  ^{2,3,6}, S  gol  ne Greffe⁷, Michelle Cazabat⁸, Maribel Donoso⁹, Pierre Delobel^{10,11,12}, Jacques Izopet^{8,10,11}, Eliseo Eugenin⁹, Maria Laura Gennaro⁵, Elisabeth Rouveix⁷, Elisabeth Cramer Bord  ^{1,2,4}, Morgane Bomsel^{1,2,3*}

In addition to hemostasis, human platelets have several immune functions and interact with infectious pathogens including HIV *in vitro*. Here, we report that platelets from HIV-infected individuals on combined antiretroviral drug therapy (ART) with low blood CD4⁺ T cell counts (<350 cells/ μ l) contained replication-competent HIV despite viral suppression. *In vitro*, human platelets harboring HIV propagated the virus to macrophages, a process that could be prevented with the biologic abciximab, an anti-integrin α IIb/ β 3 Fab. Furthermore, in our cohort, 88% of HIV-infected individuals on ART with viral suppression and with platelets containing HIV were poor immunological responders with CD4⁺ T cell counts remaining below <350 cells/ μ l for more than one year. Our study suggests that platelets may be transient carriers of HIV and may provide an alternative pathway for HIV dissemination in HIV-infected individuals on ART with viral suppression and poor CD4⁺ T cell recovery.

INTRODUCTION

The main function of human platelets is in hemostasis, but they also contribute to immunological responses (1) and can engulf viral and nonviral infectious pathogens (2). *In vitro*, platelets directly interact with and internalize HIV, dengue virus, hepatitis C virus, influenza virus, bacteria such as *Staphylococcus aureus*, and other pathogens (3–11). We and others have shown *in vitro* a direct interaction of HIV with platelets and with megakaryocytes, which are platelet precursor cells (5, 7, 10–13). These experimental studies required large quantities of laboratory-adapted cell-free HIV to interact with platelets and megakaryocytes, thus compromising biological relevance (7, 10). Early *in vivo* studies detected HIV RNA without investigation of replication-competent virions in human platelets (12, 13) and in megakaryocytes (14) from untreated HIV-infected individuals. However, evidence for platelets containing infectious HIV *in vivo*, especially in HIV-infected individuals on combined antiretroviral drug therapy (ART), remains elusive.

Here, we investigated the occurrence of replication-competent HIV in platelets from HIV-infected individuals on ART with viral suppression and analyzed whether a correlation existed with their clinical status.

RESULTS

Platelets from HIV-infected individuals on ART harbor HIV

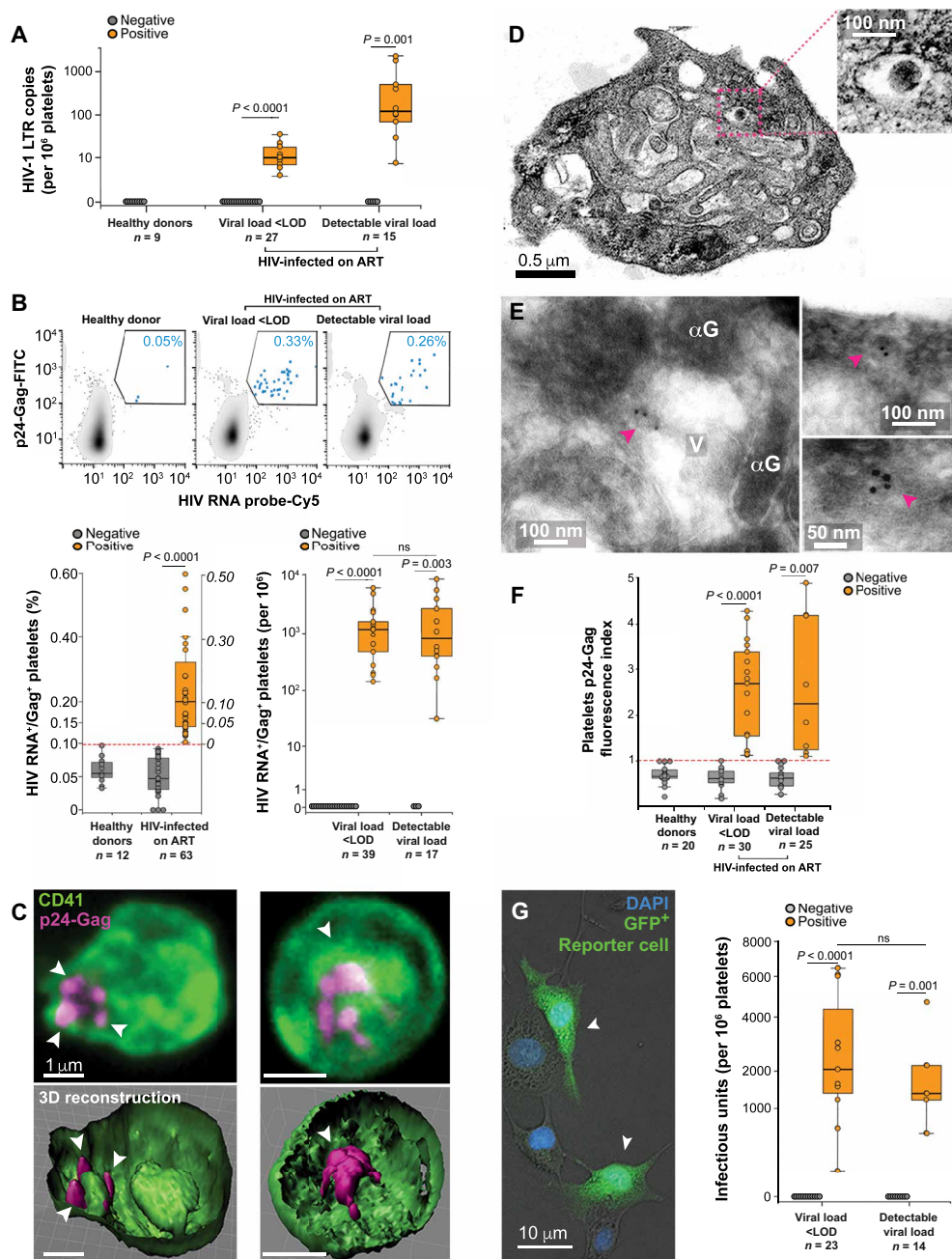
We isolated platelets from HIV-infected individuals on ART (tables S1 and S2), who had either a detectable viral load ($n = 15$) or undetectable virus ($n = 27$) that was below the limit of detection (LOD) of 1.6 log₁₀ HIV RNA copies/ml, and we used quantitative real-time polymerase chain reaction (qPCR) to establish whether the isolated platelets contained HIV. In a subgroup of ART-treated HIV-infected individuals with undetectable blood viral load (10 of 27), platelets were found to contain on average 9.92 HIV RNA copies per million platelets with a confidence interval (CI) of 6.5 to 17.8 (Fig. 1A). A subgroup of ART-treated HIV-infected individuals with detectable viremia (10 of 15) had on average 122.3 HIV RNA copies per million platelets (CI, 65 to 1111) (Fig. 1A). Longitudinal clinical data obtained from these HIV-infected individuals on ART with undetectable viral load at the date of sampling (indicated by an asterisk in table S3) showed that the viral load for six of nine individuals consistently remained below the LOD for more than 1 year (median, 26 months; CI, 14 to 74 months) before the date of sampling (table S3). This finding suggested that circulating HIV had not attached nonspecifically to platelets in the circulation. Furthermore, potential contamination by HIV-infected cells present in the blood of these individuals was evaluated by flow cytometry. Analyses of platelet-rich plasma samples from all assessed HIV-infected individuals on ART detected less than one lymphocyte per sample corresponding to 2.16 CD3⁺ T cells per million platelets (CI, 1.4 to 2.7) (fig. S1, A to C). The likelihood of platelet contamination by HIV-infected T cells was low given that in HIV-infected individuals on ART with undetectable viral load, HIV-infected T cells represented 0.01 to 0.1% of total blood CD4⁺ T cells with 100 to 1000 HIV DNA copies per million CD4⁺ T cells (15).

To identify not only cytosolic HIV RNA but also intact viral particles in platelets, detection of HIV RNA by fluorescence *in situ* hybridization (FISH) was combined with detection of viral protein

¹Mucosal Entry of HIV and Mucosal Immunity, Institut Cochin, Universit   de Paris, Paris, France. ²INSERM U1016, Paris, France. ³CNRS UMR8104, Paris, France. ⁴H  pital Ambroise Par  , Boulogne-Billancourt, France. ⁵Public Health Research Institute, New Jersey Medical School, Rutgers, The State University of New Jersey, Newark, NJ, USA. ⁶Electron Microscopy Platform, Institut Cochin, Universit   de Paris, Paris, France. ⁷Department of Internal Medicine, H  pital Ambroise Par  , Boulogne, France. ⁸CHU de Toulouse, H  pital Purpan, Laboratoire de Virologie, Toulouse, France. ⁹Department of Neuroscience, Cell Biology, and Anatomy, University of Texas Medical Branch (UTMB), Galveston, TX, USA. ¹⁰INSERM U1043, Toulouse, France. ¹¹Universit   Toulouse III Paul-Sabatier, Facult   de M  decine Toulouse-Purpan, Toulouse, France. ¹²CHU de Toulouse, H  pital Purpan, Service des Maladies Infectieuses et Tropicales, Toulouse, France.

*Corresponding author. Email: morgane.bomsel@inserm.fr

Fig. 1. Detection of HIV in platelets from HIV-infected individuals on ART. (A) Number of HIV long terminal repeat (LTR) copies per million platelets in platelet-rich plasma samples from ART-treated HIV-infected individuals with viral loads either below the LOD or detectable at the date of sampling. Platelet-rich plasma from healthy donors was used as a negative control. Platelet samples in which HIV was detected are shown in orange, and samples negative for HIV are shown in gray. The number of different individuals tested (*n*) is shown below the graph. Data are the result of seven independent experiments. Boxplots represent medians with 25th and 75th percentiles and with minimum/maximum values indicated by whiskers (Mann-Whitney *U* test). (B) Top: HIV RNA⁺/p24-Gag⁺ platelets were measured by FISH–flow cytometry. Bottom left: Boxplot shows percentage of HIV RNA⁺/p24-Gag⁺ platelets from healthy donors or HIV-infected individuals on ART detected by FISH–flow cytometry and expressed as a percentage of total platelets in the platelet-rich plasma samples. Normalized percentage values are indicated in italics on the right-hand axis. The quantification threshold (orange dashed line) was established on the basis of healthy donor samples. Samples from HIV-infected individuals on ART were grouped according to the absence (gray, negative) or presence (orange, positive) of HIV in platelets (*P* < 0.001). The number of different individuals tested (*n*) is shown below the graph. Bottom right: Boxplot shows percentages converted into HIV RNA⁺/p24-Gag⁺ platelets per million platelets after data normalization and after subtracting the maximum value obtained from healthy donor control samples. The number of different individuals tested (*n*) is shown below the graph. Results are from seven independent experiments and are expressed as boxplots generated separately for negative and positive groups. Boxplots represent medians with 25th and 75th percentiles and with minimum/maximum values indicated by whiskers (Mann-Whitney *U* test). (C) Representative confocal microscopy images (top panels) show platelets from HIV-infected individuals on ART immunostained for CD41 (green) and p24-Gag (magenta). Images reconstructed in three dimensions are shown in the bottom panels. White arrowheads indicate HIV contained within platelets. Representative images are shown for platelets from 11 different HIV-infected individuals on ART. Scale bars, 1 μm. (D) Representative transmission electron micrograph of an HIV-containing platelet. A viral particle in a small vacuolar compartment is indicated by the magenta box, which is shown at a higher magnification in the image inset. The electron micrograph is representative of samples from five different HIV-infected individuals on ART with viral suppression. (E) Immunogold labeling (10 nm) of p24-Gag in cryosections was performed before electron microscopy to confirm the presence of HIV within a platelet compartment (pink arrowhead). Representative image of 10 different images obtained from two different HIV-infected individuals on ART with viral suppression. αG, α-granule; V, vacuole. Scale bars, 0.5 μm, 100 nm, or 50 nm. (F) p24-Gag immunofluorescence intensities for platelets from healthy donors or HIV-infected individuals on ART detected by flow cytometry. Results are from seven independent experiments and are expressed as boxplots generated separately for negative and positive groups. Boxplots represent median with 25th and 75th percentiles and with minimum/maximum values indicated by whiskers (Student's *t* test). (G) Image shows green fluorescent protein–positive (GFP⁺) reporter T cells (green) after interaction with platelet-rich plasma from an HIV-infected individual on ART. Nuclei are labeled with 4',6'-diamidino-2-phenylindole (DAPI) (blue); the fluorescence signal (green) was merged with phase contrast (white arrowheads). Scale bar, 10 μm. Boxplot shows the quantification of infectious units per million platelets in platelet-rich plasma samples from HIV-infected individuals on ART who either displayed viremia below LOD or had detectable viral load at the date of sampling. Samples lacking infectious virus are in gray (negative), and those with infectious virus are in orange (positive). The number of different individuals tested (*n*) is shown below the graph. Results are from eight independent experiments and are expressed as boxplots generated separately for negative and positive groups. Boxplots represent medians with 25th and 75th percentiles and with minimum/maximum values indicated by whiskers (Mann-Whitney *U* test). ns, not significant.



p24-Gag by immunofluorescence. Both types of labeling were quantified simultaneously by flow cytometry using a single-cell approach referred to as FISH–flow cytometry (Fig. 1B and fig. S2, A to C) (16). HIV RNA⁺/p24-Gag⁺ FISH–flow cytometry can detect the very low number of latent HIV reservoir cells in HIV-infected individuals on ART, which comprise around 1 infected cell per million CD4⁺ T cells (16–18). We found that platelets from HIV-infected individuals on ART that were positive for HIV RNA and p24-Gag comprised 0.1% (CI, 0.047 to 0.15%) of total platelets in the blood of these individuals (Fig. 1B, left). When stratified according to either undetectable (below LOD) or detectable viral load at the date of sampling, HIV-infected individuals on ART did not differ in the number of HIV RNA⁺/p24-Gag⁺ platelets per 10⁶ platelets, which was 1186.99 (CI, 631 to 1600) and 825.8 (CI, 387 to 2676), respectively ($P > 0.05$) (Fig. 1B, right). The HIV RNA⁺/p24-Gag⁺ signal detected in platelets did not originate from HIV-infected CD4⁺ T cells (fig. S1D), as T cells obtained from ART-treated HIV-infected individuals did not transcribe HIV RNA in quantities that could be detected by FISH–flow cytometry in the absence of activation by mitogens (17).

HIV resides in an internal compartment of platelets

HIV was found inside platelets from HIV-infected individuals on ART as shown by p24-Gag immunolocalization using confocal microscopy (Fig. 1C and fig. S3, A and B) and electron microscopy (Fig. 1, D and E, and fig. S3, C and D), in parallel with flow cytometry (Fig. 1F and fig. S2, A, B, and D). At the confocal microscopy level, HIV appeared to be exclusively confined within closed vacuoles (Fig. 1C; p24-Gag detection indicated by arrowheads), as we have previously reported *in vitro* (5, 10), and did not seem to be associated with the platelet surface. Furthermore, at the ultrastructural level, morphological (Fig. 1D and fig. S3C) and immunogold detection of HIV (Fig. 1E, p24-Gag detection indicated by arrowhead, and fig. S3D) was restricted to vesicles that were distinct from both the platelet surface and its connected canalicular system, suggesting that HIV was not in contact with the external environment (8) or α -granules.

To further validate our microscopy-based immunostaining approaches, p24-Gag⁺ immunostaining was evaluated by flow cytometry. Differences in p24-Gag⁺ mean fluorescence intensity were observed for platelets from HIV-infected individuals on ART with (orange bars) or without (gray bars) HIV (Fig. 1F and fig. S2, A, B, and D). The HIV p24-Gag protein was detected in platelets from a subset of ART-treated HIV-infected individuals who either were viremic (8 of 25) or had a viral load below the LOD at the date of sampling (17 of 30).

HIV harbored in platelets is replication competent

We next investigated the replication competence of HIV localized in platelets from HIV-infected individuals on ART using a CD4⁺-CCR5⁺CXCR4⁺ reporter cell line (19, 20) (Fig. 1G). These experiments revealed that in ART-treated HIV-infected individuals with either undetectable (below LOD) or detectable viral load at the date of sampling, a subgroup (Fig. 1G, orange) had platelets with similar amounts of infectious viral particles: 2053 infectious units (IU)/10⁶ platelets (CI, 1195 to 6013; 11 of 23 individuals) and 1353 IU/10⁶ platelets (CI, 533 to 4671; 5 of 14 individuals), respectively (Fig. 1G). Among HIV-infected individuals on ART with infectious HIV in platelets and displaying a viral load below LOD at the date of sampling (indicated by crosses in table S3), 72% (8 of 11 tested) were

consistently virally suppressed for more than 1 year with a median of 30 (CI, 20 to 50) months before sampling (table S3). This suggested that there was no contamination with residual infectious cell-free virus from blood in the reporter cell assay. Furthermore, in a subset of HIV-infected individuals on ART who were virally suppressed below LOD at the date of sampling, no infectious virus was detected in platelet-poor plasma in the reporter cell assay (fig. S4).

Megakaryocytes from HIV-infected individuals on ART contain HIV

We next investigated the potential origin of platelets containing replication-competent HIV. Bone marrow megakaryocyte progenitors from HIV-infected individuals on ART with sustained viral suppression were recently shown to contain replication-competent viral DNA (21), and megakaryocytes, the precursor cells of platelets, from untreated HIV-infected individuals were shown to harbor HIV RNA (14). HIV-1 RNA and HIV virions contained in megakaryocytes could potentially be sequestered by platelets during thrombopoiesis (11, 14, 21). We detected HIV DNA (fig. S5, A to C) and HIV RNA (fig. S5F) in bone marrow from an HIV-infected individual on ART by *in situ* hybridization in cells morphologically identified as megakaryocytes. In addition, HIV-integrated proviral DNA was detected in megakaryocytes purified from bone marrow samples from 82% (9 of 11) of HIV-infected individuals on ART with viral suppression (table S4 and fig. S5, D and E), with an estimate of 74.7 (CI, 39 to 140.6) HIV DNA integrated copies per million megakaryocytes (fig. S5, D and E). In platelet-rich plasma samples from the four of these HIV-infected individuals on ART with viral suppression we could analyze, platelets containing HIV RNA and HIV p24-Gag protein were detected (fig. S5G).

To confirm that HIV harbored in platelets was not blood borne, phylogenetic analyses were performed after deep sequencing of HIV *env* V3 sequences in plasma samples from HIV-infected individuals before and after viral suppression. Plasma samples were obtained before viral suppression and were compared to peripheral blood mononuclear cells (PBMCs) and platelet samples after up to 69 months of viral suppression by ART. These phylogenetic analyses demonstrated that after viral suppression, platelet-associated HIV originated from a different compartment than did PBMC-associated HIV provirus or HIV in plasma before ART suppression (fig. S6A). In addition, translated sequences revealed a shift in HIV tropism from CCR5 variants in plasma before ART treatment to CXCR4 variants in PBMCs and platelets after viral suppression by ART. The independent grouping of platelet-derived CXCR4 variants (fig. S6, A and B) in the phylogenetic analysis demonstrated that HIV in platelets did not originate from a latent reservoir established before ART or from the CD4⁺ T cell latent reservoir (22, 23). More longitudinal, in-depth phylogenetic studies on HIV genome sequences obtained from platelets, bone marrow, and CD4⁺ T cells of HIV-infected individuals before and after viral suppression will be required to confirm this finding.

HIV harbored in platelets can be transferred to macrophages *in vitro*

At the end of their short life span, platelets are ultimately phagocytosed by mononuclear phagocytic cells residing mainly in the liver and spleen (24). Tissue macrophages are central to this process by engulfing senescent and apoptotic platelets via integrins including α_{IIb}/β_3 and scavenger receptors (24–27). HIV harbored in platelets could be transferred to tissue macrophages through this process of

platelet elimination. Therefore, we next investigated whether HIV-containing platelets could be phagocytosed by macrophages in vitro (Fig. 2, fig. S7, and movie S1). HIV-containing platelets from HIV-infected individuals on ART with viral load consistently below LOD for 52.5 (CI, 12 to 75) months were found to adhere to and, in turn, be phagocytosed by macrophages in vitro (Fig. 2, A and B, and movie S1). This resulted in integration of HIV proviral DNA into the genome of macrophages with 48.25 (CI, 5.24 to 183.9) proviral HIV DNA copies per million macrophages (Fig. 2C). Infection appeared to be productive as these HIV-infected macrophages, in turn, produced infectious HIV virions (Fig. 2D). HIV proviral DNA integration and infectious virus production in vitro could be inhibited by preventing platelet-macrophage interactions using abciximab, a platelet-specific anti-integrin $\alpha_{IIb}\beta_3$ Fab (Fig. 2, C and D, and fig. S7, B to D).

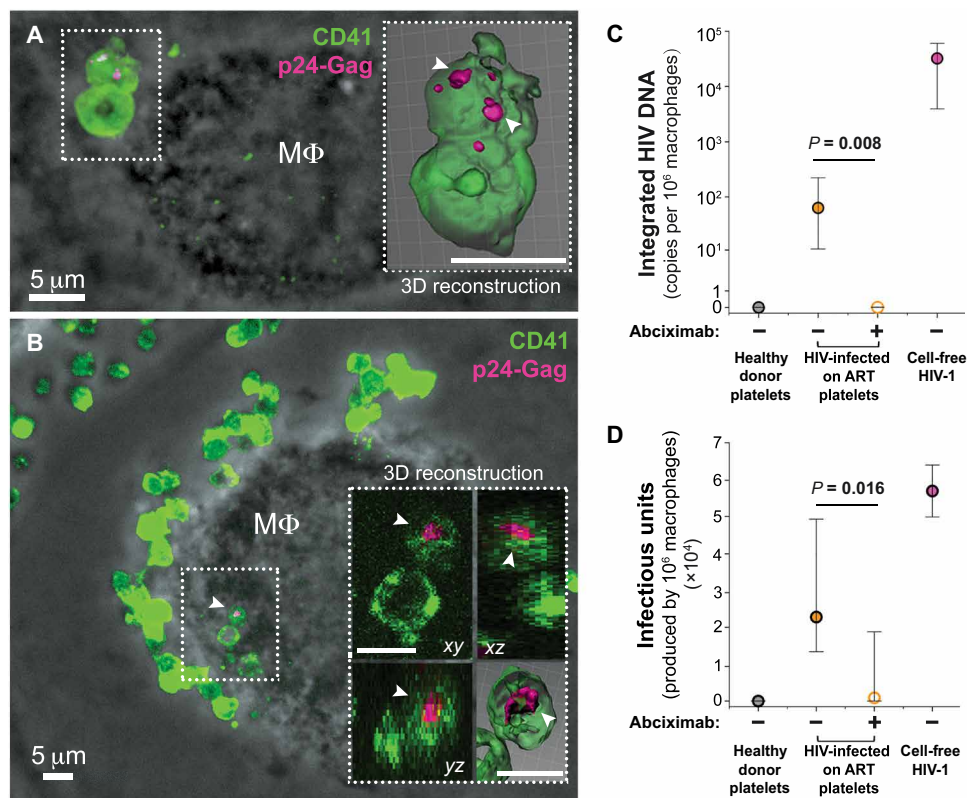


Fig. 2. Transfer of HIV from platelets to macrophages in vitro. (A and B) Representative confocal microscopy images of HIV-containing platelets interacting with macrophages (M Φ) in vitro after immunostaining for CD41 (green) and p24-Gag (pink); image is merged with phase-contrast image. White arrowheads show labeled virus within platelets. Image insets show three-dimensional reconstructions or projections in xy, yz, and xz dimensions for HIV-containing platelets. Images are representative of five different individuals. Scale bars, 5 μ m (main and inset figures). (C) Number of integrated copies of HIV DNA per 10^6 macrophages after 7 days of coculture with platelets from HIV-infected individuals on ART with viral suppression in the presence (solid orange circle) or absence (empty orange circle) of abciximab. Culture with cell-free HIV-1 was used as a positive control (magenta circle), and healthy donor platelets were used as a negative control (gray circle). (D) Infectious units produced per 10^6 macrophages after 7 days of coculture with platelets from HIV-infected individuals on ART with viral suppression in the presence (solid orange circle) or absence (empty orange circle) of abciximab. Culture with cell-free HIV-1 was used as a positive control (magenta circle), and healthy donor platelets were used as a negative control (gray circle). Results for (C) and (D) are presented as medians (circles) with 95% CIs (whiskers). Data represent three independent experiments with samples from five different HIV-infected individuals on ART. Mann-Whitney *U* test was applied for paired experimental data for platelets from HIV-infected individuals on ART, treated or not treated with abciximab in vitro.

HIV-infected individuals on ART with platelets containing HIV have low CD4⁺ T cell counts

Next, we compared clinical characteristics at the date of sampling between HIV-infected individuals on ART who did (orange bars) or who did not (gray bars) have HIV-containing platelets (table S2 and Fig. 3A). HIV-infected individuals on ART with HIV-containing platelets had a low CD4⁺ T cell count (<350/ μ l) that was threefold less compared to HIV-infected individuals on ART without HIV-containing platelets (Fig. 3A). In contrast, the presence of HIV-containing platelets was not associated with total lymphocyte counts or platelet counts, age, years since diagnosis, years on ART (fig. S8, A to C), or the type of ART regimen (table S5). We performed a multivariate analysis of the clinical characteristics of HIV-infected individuals with or without HIV in platelets at the date of sampling. Principal component analysis (PCA) showed separate clusters for

blood samples with or without HIV-containing platelets (Fig. 3B). This distribution was mainly driven by principal component (dimension) 2, where CD4⁺ T cell count was the strongest contributor (fig. S8D) and inversely correlated with the presence of HIV in platelets (Fig. 3B). Furthermore, a multinomial logistic regression indicated that among clinical characteristics, excluding nadir due to collinearity, CD4⁺ T cell count was the only predictive value for the presence of HIV in platelets ($P = 0.007$).

HIV-infected individuals on ART with platelets containing HIV show immunological failure

To address the potential clinical implications of platelets containing HIV, a subset of 35 HIV-infected individuals on ART analyzed above was selected (Table 1). Selection was based on two criteria, namely, HIV detection in platelets using at least two different techniques (tables S2) and unambiguous clinical data available for 1 year before the date of sampling. In these selected HIV-infected individuals on ART, the historical CD4⁺ T cell nadir, a clinical characteristic critical for immune recovery (28), was significantly lower (<200 cells/ μ l) in those with HIV-containing platelets compared to those without HIV-containing platelets ($P = 0.006$, Fig. 4A). A sustained low CD4⁺ T cell count (<350 cells/ μ l), irrespective of viral suppression, persisted in HIV-infected individuals on ART with HIV-containing platelets. In contrast, HIV-infected individuals on ART lacking HIV in platelets had a CD4⁺ T cell count above this threshold, especially if they were aviremic. This was shown by analysis of mean CD4⁺ T cell counts at the date of sampling and

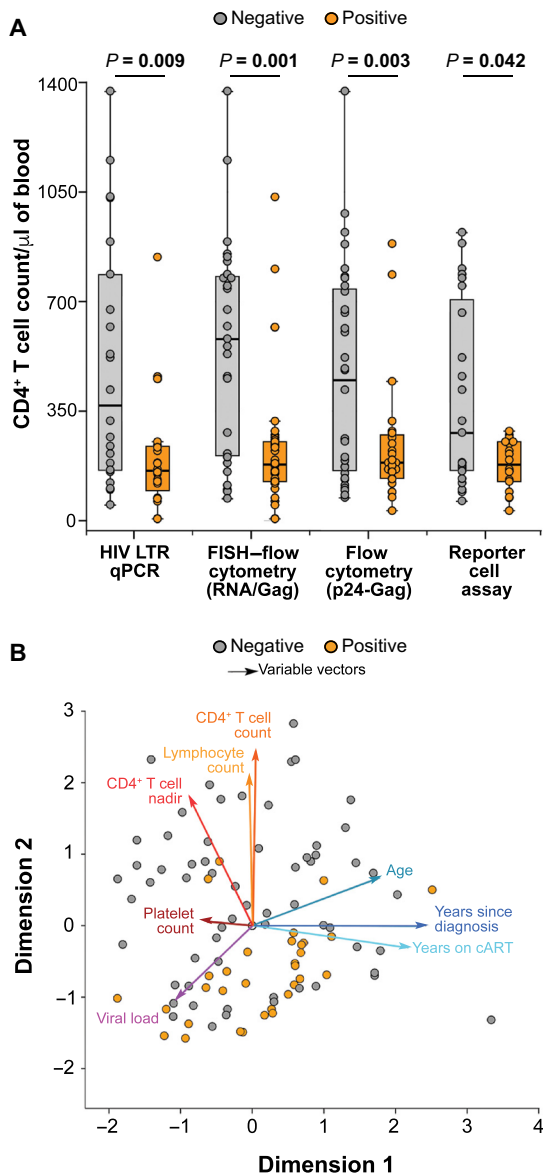


Fig. 3. Platelets containing HIV correlate with low CD4⁺ T cell counts. (A) Comparison of CD4⁺ T cell counts at the date of sampling for HIV-infected individuals on ART whose platelets either contained (positive, orange) or did not contain (negative, gray) HIV. HIV was detected by HIV LTR qPCR, FISH flow cytometry (HIV RNA⁺/p24-Gag⁺), p24-Gag flow cytometry, and a reporter T cell assay in seven, five, seven, and eight independent experiments, respectively. HIV-infected individuals on ART with HIV-containing platelets (orange) showed lower CD4⁺ T cell counts (<350/μl) than did those with platelets lacking HIV (gray). Results are shown as boxplots generated separately for positive and negative groups. The Mann-Whitney *U* test was used to compare negative (gray) and positive (orange) groups for each HIV detection technique. (B) PCA of samples from HIV-infected individuals on ART categorized according to the presence (positive, orange) or absence (negative, gray) of HIV in platelets. These data and the clinical characteristics for each HIV-infected individual at the date of sampling are represented as variable vectors (arrows).

during a retrospective and prospective 18-month period before and after sampling (Fig. 4B). These results indicated that the presence of HIV harbored in platelets correlated with immunological failure, which was defined as HIV-infected individuals on ART whose CD4⁺ T cell counts remained <350 cells/μl for more than one year (29).

We found that 80% of the HIV-infected individuals on ART with HIV-containing platelets (Fig. 4C, orange bars) were in immunological failure compared to only 15% of HIV-infected individuals on ART without HIV-containing platelets (Fig. 4C, gray bars). HIV-infected individuals on ART with HIV-containing platelets had a >20-fold higher chance of failing to recover CD4⁺ T cell counts to above 350 cells/μl, compared to those without HIV in their platelets (odds ratio, 22.6; CI, 3.8 to 132.1; *P* = 0.0005). The likelihood of immunological failure for HIV-infected individuals on ART with viral suppression and HIV-containing platelets was higher (odds ratio, 56; CI, 4.3 to 719.2; *P* = 0.002) compared to those who were viremic at the date of sampling or displayed less than 12 months of continuous viral suppression (odds ratio, 6; CI, 0.3 to 101.5; *P* = 0.21) (Table 1 and table S6).

DISCUSSION

We have shown here that platelets from HIV-infected individuals on ART with sustained low CD4⁺ T cell counts harbor replication-competent HIV and do so despite viral suppression below LOD. Our results show that in platelets, HIV is confined to an intracellular compartment analogous to the virus-containing compartments typically formed in HIV-infected myeloid cells in vitro (30) and in vivo (31, 32). These compartments are functionally distinct from the cell endosomal system, providing a shelter for the virus against the direct action of neutralizing antibodies, cytoplasmic innate immunity sensors, and the late endosomal/lysosomal degradative environment (30). Accordingly, platelets harboring HIV in these privileged compartments could preserve virus integrity throughout their 8- to 10-day life span.

The HIV in platelets that we report could have originated from direct endocytosis of HIV in the circulation of viremic patients by platelets (7, 10). However, the presence of intact, replication-competent virus in platelets from individuals on ART with viral loads below LOD for long periods suggests that platelets may associate with HIV in an active viral replication niche. HIV-infected megakaryocytes that we found in HIV-infected individuals on ART with low CD4⁺ T cell counts potentially could be the source of HIV-containing platelets.

Platelets are short-lived, anuclear blood components lacking the nuclear machinery to meet the recent criteria used to define HIV latent reservoirs (23). These criteria include display of integrated proviral DNA and rebound of virus production upon interruption of ART. Instead, platelets and perhaps other blood cells (33, 34) may participate in HIV transmission and persistence by sheltering the virus from the immune response. The T cell latent reservoir is long-lived and harbors integrated HIV DNA. We suggest that platelets harboring HIV can carry HIV RNA and transport replication-competent virus. Platelets would thus form a transient shelter for HIV in the blood of some HIV-infected individuals on ART and could promote infection by delivering virus to target cells such as macrophages as we have shown here in vitro. Furthermore, our study suggests that HIV may associate with platelets during thrombopoiesis in the HIV-infected bone marrow megakaryocytes of HIV-infected individuals virally suppressed by ART with low CD4⁺ T cell counts.

A potential platelet-mediated pathway for viral dissemination during ART may correlate with sustained immunological failure, although the causative nature of this correlation remains to be established. The poor immunological recovery observed in ART-treated

Table 1. HIV-infected individuals selected for retrospective and prospective analysis of immunological status, viremia, and viral suppression. Patients were classified as positive or negative for the presence of HIV in platelets according to at least two different techniques. Only HIV-infected individuals for whom clinical data were available 18 months before the date of sampling were included in the analysis. The period of viral suppression in months before the date of sampling is indicated. Competent immunological status was defined as >350 CD4⁺ T cells/ μ l of blood for two or more consecutive measurements over 1 year including date of sampling for detecting HIV in platelets. Immunological failure was defined as <350 CD4⁺ T cells/ μ l blood for two or more consecutive measurements over 1 year including date of sampling for detecting HIV in platelets. Controlled viremia was defined as <1.60 HIV RNA log₁₀ copies/ml of plasma for at least 1 year before sampling. Uncontrolled viremia was defined as >1.60 HIV RNA log₁₀ copies/ml of plasma at the date of sampling or less than 12 months of continuous viral suppression.

	Individual number	Immunological status	Viremia	Months suppressed before sampling	
Individuals negative for HIV in platelets	39	Competent	Controlled	17	
	32	Competent	Controlled	18	
	75	Competent	Controlled	31	
	54	Competent	Controlled	18	
	52	Competent	Controlled	12	
	11	Competent	Controlled	18	
	51	Competent	Controlled	18	
	16	Competent	Controlled	12	
	15	Competent	Controlled	13	
	61	Competent	Controlled	13	
	66	Competent	Controlled	47	
	67	Competent	Controlled	31	
	4	Competent	Controlled	78	
	56	Competent	Controlled	62	
	53	In failure	Controlled	22	
	59	In failure	Controlled	18	
		Median months under controlled viremia (CI)			18 (15–31)
	Individuals positive for HIV in platelets	7	In failure	Uncontrolled	<12
60		Competent	Uncontrolled	<12	
24		Competent	Uncontrolled	<12	
46		Competent	Uncontrolled	<12	
9		In failure	Controlled	24	
27		In failure	Controlled	38	
48		In failure	Controlled	19	
6		In failure	Controlled	20	
49		In failure	Controlled	50	
64		In failure	Controlled	52	
79		In failure	Controlled	14	
80		In failure	Controlled	62	
37		Competent	Controlled	13	
		Median months under controlled viremia (CI)			24 (14–52)
		74	Competent	Uncontrolled	<12
	25	Competent	Uncontrolled	<12	
	18	In failure	Uncontrolled	<12	
	78	In failure	Uncontrolled	<12	
	40	In failure	Uncontrolled	<12	
	41	In failure	Uncontrolled	<12	

Downloaded from <http://stm.sciencemag.org/> by 20339660 on March 19, 2020

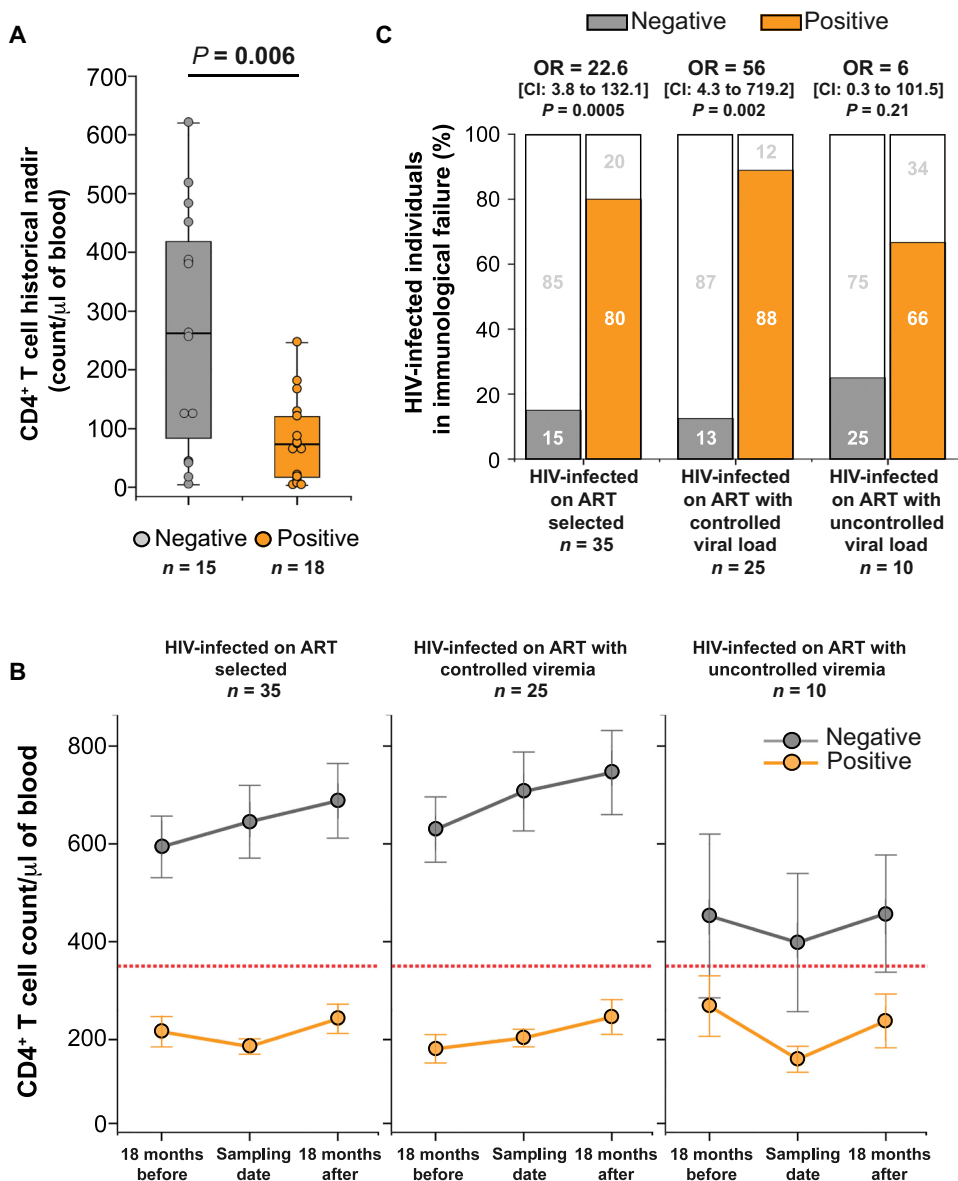


Fig. 4. Platelets containing HIV correlate with poor immunological recovery. (A) CD4⁺ T cell counts (historical nadir) for HIV-infected individuals on ART whose platelets either did (orange, positive) or did not (gray, negative) contain HIV. HIV-infected individuals on ART with HIV-containing platelets had a lower mean CD4⁺ T cell count nadir (<200 cells/μl) compared to the negative group ($P = 0.006$, Mann-Whitney *U* test). The number of individuals (*n*) is shown below the graph. (B) Mean CD4⁺ T cell counts for HIV-infected individuals on ART who were positive (orange line) or negative (gray line) for the presence of HIV in platelets. Data are shown for the time period of 18 months before and 18 months after the date of sampling. Analysis was first performed for a subgroup of 35 HIV-infected individuals on ART who were selected irrespective of viremia (left). This group was then further divided into 25 HIV-infected individuals on ART with controlled viremia (>1 year with viral load consistently below LOD; middle) and 10 HIV-infected individuals on ART with uncontrolled viremia (with a detectable viral load at the date of sampling or less than 12 months of continuous viral suppression; right). Red dotted line indicates a CD4⁺ T cell count threshold of 350 cells/μl. (C) Percentage of HIV-infected individuals on ART in immunological failure (<350 CD4⁺ T cells/μl after at least 1 year of follow-up including the date of sampling) grouped according to the presence (positive, orange) or absence (negative, gray) of HIV in platelets. OR, odds ratio; Fisher's exact test.

HIV-infected individuals may be driven by persistent inflammation associated with T cell immune dysfunction (35–37). Residual inflammation markers in blood, such as d-dimers and interleukin-6

(IL-6) detected in plasma, do not correlate with immunological failure (38) and thus are unlikely to have an impact on the association of HIV with platelets. Inflammation-driven T cell dysfunction could result from the low residual production of HIV by latent reservoirs such as tissue macrophages (31, 39). Further studies are necessary to elucidate the molecular and cellular mechanisms connecting immunological failure to platelets containing HIV.

Twenty percent to 30% of HIV-infected individuals are unable to reconstitute a competent immune system despite adherence to ART and a viral load below LOD (29, 35, 40, 41); no therapeutic strategy is available to improve their immune recovery (41, 42). Systematic clinical studies will be required to demonstrate the potential predictive value of detecting HIV-containing platelets in individuals in immunological failure for the purpose of anticipating appropriate therapeutic interventions. Our results suggest that abciximab, an antiplatelet agent already in clinical use, could block viral dissemination to macrophages by HIV-containing platelets.

Our study has a number of limitations. Further studies are needed to elucidate how HIV shelters in the platelets of HIV-infected individuals on ART despite viral suppression and the association of HIV-containing platelets with CD4⁺ T cell recovery failure. Although our study analyzed samples from 80 HIV-infected individuals on ART, limited sample amounts did not allow testing of every sample with all four techniques we used for detecting HIV in platelets. Samples from a greater number of HIV-infected individuals on ART and longitudinal samples from the same individuals at 1-year intervals should be studied to confirm our results and to establish functional correlations between the presence of HIV in platelets and immunological failure. The finding of HIV virions identified at the ultrastructural level in some platelets needs to be confirmed by directly correlating p24-Gag immunolabeling detected by confocal microscopy with that identified by electron microscopy. Additional immunolabeling experiments will need to be performed to identify the

compartment in platelets in which HIV resides and if it is similar to the HIV compartment in HIV-infected macrophages (31). The activation status of platelets interacting with macrophages during

HIV transfer remains to be determined as well as whether a specific tissue macrophage subset is selectively targeted. To prove our hypothesis that HIV-infected platelets are derived from HIV-infected megakaryocytes, comparative sequencing of HIV *env* V3 will need to be performed on blood T cells, megakaryocytes, and platelets both before ART and after 1 year on ART with consistent blood viral suppression.

In conclusion, our study found that HIV-containing platelets correlated with poor immunological recovery in HIV-infected individuals on ART and suggests a potential alternative pathway for viral dissemination in which platelets act as transient carriers of HIV.

MATERIALS AND METHODS

Study design

Our study investigated whether replication-competent HIV resided within platelets from HIV-infected individuals on ART. The HIV-infected individuals on ART who participated in this study belonged to a large prospective cohort of HIV-infected individuals of at least 15 years of age from the French Hospital Database on HIV created in 1989. These HIV-infected individuals received care at the Ambroise Paré and Raymond Poincaré Hospitals that are among 70 participating centers in the French Hospital Database on HIV. The only enrollment criterion for the French Hospital Database on HIV was documented HIV-1 or HIV-2 infection. Written informed consent was obtained for all study participants, and data submitted by the participating centers were anonymized and encrypted. The French Hospital Database on HIV was approved by the French national institutional ethics committee (Commission Nationale de l'Informatique et des Libertés) on 27 November 1991. Human samples in this study were used in accordance with the World Medical Association Declaration of Helsinki. Ethical authorization for obtaining postmortem bone marrow samples through whole-body donation from uninfected and ART-treated HIV-infected individuals was provided by the State University of New Jersey and The University of Texas Medical Branch, with Institutional Review Board (IRB) authorization numbers of Pro20140000794/Pro2012001303 and 18-0136/18-0134, respectively.

Platelet-rich plasma samples used in this study were obtained during routine blood testing of 80 HIV-infected individuals on ART from the French Hospital Database on HIV, who received care at the Ambroise Paré and Raymond Poincaré Hospitals. The enrollment criterion for these HIV-infected individuals was that ART had been initiated for at least 1 year before the time of blood sampling. Viremia was regularly tested in human plasma samples using the Abbott RealTime HIV-1 assay on an automated m2000 system. This allowed detection of HIV RNA copies per milliliter of plasma with a range of 1.6 log₁₀ copies (40 copies) to 7 log₁₀ copies. Values below the LOD of 1.6 log₁₀ copies/ml were considered to reflect undetectable viremia. Tables S1 and S2 present the following clinical information for study participants: viral load (log₁₀ HIV copies per milliliter of blood), total lymphocyte counts (10⁶/ml of blood), CD4⁺ T cell counts and historical nadir (cells per microliter of blood), and platelet counts (10⁶/ml of blood). Table S5 shows the ART regimens for study participants.

It should be noted that the HIV-infected individuals on ART in our study were seen in a hospital setting and may not be representative of the HIV-infected population seen in local clinics. Therefore, the immunological nonresponders in the HIV-infected cohort

we analyzed may not be representative of immunological failure in the broader HIV-infected population on ART.

Human peripheral blood and platelet-rich plasma samples from healthy HIV-seronegative donors were obtained from the French blood collection center (Paris, France). Platelet-rich plasma from healthy donors was used as a negative control for all experiments and was processed using the same methods as for platelet-rich plasma from HIV-infected individuals.

Platelet-rich plasma collection

Peripheral blood samples were obtained from donors by venipuncture into plastic tubes containing anticoagulant EDTA. Samples were centrifuged for 10 min at 160g and 22°C for blood fractionation, allowing for clear separation of platelet-rich plasma from whole blood. To avoid potential contamination by rare leukocytes, the upper two-thirds of the platelet-rich plasma fraction were carefully collected and transferred to new plastic tubes as recommended for functional analyses (43). Platelet-poor plasma was obtained after centrifugation of platelet-rich plasma at 1100g, 10 min, room temperature, and collection of supernatants.

Platelet-rich plasma fractions were frozen at -80°C until used in the experiments (44). We verified by flow cytometry that (i) viable CD41⁺ platelets represent >70% of total events recorded in platelet-rich plasma, (ii) >90% of CD41⁺ platelets conserved CD42b⁺ membrane staining after thawing, and (iii) thawing does not increase the number of activated platelets characterized by CD62P⁺ immunostaining, with platelet-rich plasma samples displaying 49.2 and 51% of activated platelets (CD41⁺CD62P⁺) before and after thawing, respectively.

Quantitative PCR

qPCR of HIV-1 long terminal repeat (LTR) RNA sequences was performed from platelet pellets obtained after centrifugation of 500 μl of platelet-rich plasma at 1100g, 10 min, at room temperature. Platelet RNA was obtained as described (45) and processed for qPCR TaqMan assay using LTR-specific primer (Vi03453409_s1, Thermo Fisher Scientific Inc.) labeled with a FAM-MGB probe on an Applied Biosystems TaqMan RNA-to-Ct 1-Step Kit protocol (Thermo Fisher Scientific Inc.). RNA from platelet-rich plasma samples was eluted into 15 μl of nuclease-free water, and 5 μl of this eluate was used per qPCR reaction. Platelet-rich plasma RNA samples display an average A260/280 ratio of 1.82 (CI, 1.65 to 2.01), indicating good RNA quality (high quality = ~2 A260/280 ratio according to technical standards). The mean amount of RNA applied per reaction was 63.39 ng (CI, 42.5 to 85.2), which fits into the range of specific detection of the qPCR reagents. Reaction and data acquisition were performed using a LightCycler 480 II (Roche). The number of HIV LTR copies per million platelets was calculated on the basis of platelet-rich plasma platelet counts and qPCR crossing point (Cp) values obtained from a standard curve using a full-length molecular clone of HIV-1 pNL4-3 strain.

Contamination of platelet-rich plasma samples with lymphocytes was assessed by detection of the lymphocyte-specific CD3δ transcript (46) in platelet-rich plasma by qPCR TaqMan assay using CD3δ primer (Hs00174158_m1, Thermo Fisher Scientific Inc.) labeled with FAM-MGB probe on an Applied Biosystems TaqMan RNA-to-Ct 1-Step Kit protocol (Thermo Fisher Scientific Inc.). The number of lymphocytes was calculated on the basis of Cp values obtained from a standard curve using serial dilutions of RNA obtained from known amounts of CD4⁺ T cells.

Flow cytometry after FISH (FISH–flow cytometry)

Paraformaldehyde (4%, v/v, final concentration) was added to 25 μ l of platelet-rich plasma to fix samples, and then platelets were centrifuged at 1100g, 10 min, 22°C, and washed twice in phosphate-buffered saline without $\text{Ca}^{+2}/\text{Mg}^{+2}$. Platelets were then processed for FISH using Cy5-labeled single-molecule FISH probe set for HIV Gag mRNA (HIV-1 vector pNL4-3 GenBank AF324493.2) designed by Stellaris Probe Designer program (<http://www.singlemoleculefish.com>) as we described (47). Probe set is detailed in table S7. Before hybridization, platelets were immunostained with anti-p24 antibody (1:20, KC57 clone, Beckman Coulter Inc.) coupled to fluorescein isothiocyanate (FITC) and anti-CD41/CD61 antibody coupled to phycoerythrin (PE) (1:20, A2A9/6 clone, BioLegend Inc.).

Flow cytometry analyses of platelets processed for FISH (FISH–flow cytometry) were performed under the Guava easyCyte high-throughput system version 6HT2L (Merck Millipore, Merck, KGaA) set to very low flow rate (0.12 μ l/s) and laser gains of 3.5 (GRN-B laser line), 4.3 (YEL-B laser line), and 7.6 (RED-R laser line) in a range of 1 to 1024 units.

The gating strategy to retrieve HIV RNA⁺/p24-Gag⁺ double-positive platelets (fig. S2, A to C) was established in InCyte (Merck Millipore, Merck, KGaA) software consisting in (i) gating the population of single platelets based on forward and side scatter (in log/log scale, forward scatter (FSC) threshold value = 100), (ii) then gating on CD41⁺ events after applying a threshold based on isotype controls, and (iii) calculating CD41⁺ events according to p24 immunostaining and HIV RNA probe hybridization as described (16, 47). Data normalization was performed by subtracting the maximum percentage acquired in $n = 12$ healthy donor samples from the percentages acquired in patient samples per experiment.

FISH–flow cytometry method was also applied as described (17) for detection of HIV RNA⁺/p24-Gag⁺ PBMCs, isolated from blood buffy coats of cART-treated or chronically infected nontreated HIV-infected patients after Ficoll-Hypaque density gradient centrifugation.

Retrospective and prospective analysis of clinical parameters

We categorized ART-treated HIV-infected individuals in two groups according to the presence (positive) or absence (negative) of HIV in platelets. Classification of these individuals as positive or negative was based on similar results obtained in at least two different techniques used for detection of HIV-containing platelets. CD4⁺ T cell historical nadir, age, years since HIV diagnosis, and years since treatment of patients from the positive and negative groups were compared using statistical methods as described below. From this group of patients classified as positive or negative for HIV in platelets, we selected those 35 individuals for which we could collect longitudinal CD4⁺ T cell count and viral load measurements (Table 1). Clinical parameters of these 35 individuals with consistent detection of HIV in platelets were used for retrospective and prospective analyses presented in Fig. 4.

The retrospective and prospective analyses of patient clinical information refer to a period of several months around the date of sampling. When indicated, patients were categorized in controlled viral load group (patients presenting HIV RNA copies per milliliter of plasma always below LOD for at least 1 year before sampling) or noncontrolled viral load group (patients presenting $>1.60 \log_{10}$ copies of HIV RNA per milliliter of plasma at date of sampling or displaying less than 12 months of continuous suppression). Regarding im-

munological status, patients were categorized as immunologically competent when CD4⁺ T cell count was >350 cells/ μ l for two or more consecutive measurements, or in immunological failure when CD4⁺ T cells per microliter was constantly <350 cells/ μ l for all blood sample collected for at least 1 year including the date of sampling for HIV in platelets. We obtained, for each selected patient, a mean CD4⁺ T cell number for counts registered 18 months before sampling (retrospective count) and for 18 months after sampling (prospective count). Figure 4B shows the mean retrospective CD4⁺ T cell count, the mean CD4⁺ T cell count at sampling date, and the mean prospective CD4⁺ T cell count of patients in which CD4⁺ T cell count was surveyed.

Statistical analysis

In all HIV detection assays performed, blood and platelet-rich plasma samples were stratified into two groups (positive or negative) according to the presence or absence of HIV in platelets. Median numbers of HIV-containing platelets per milliliter of blood were calculated exclusively from samples of the positive group. Results are expressed as median, followed by the 95% CI. Boxplots represent median (central line in the box) with 25th and 75th percentiles (box edges) and with minimum/maximum values (upper and lower whiskers).

All statistical analyses were performed using IBM SPSS Statistics software (IBM). Pairwise comparisons of normal distributions were performed using a Student's t test. Pairwise and multiple comparisons of non-normal distributions were performed using the non-parametric tests Mann-Whitney U and Kruskal-Wallis, respectively. Clinical characteristics of HIV-infected individuals at the date of sampling were examined by multivariate analysis using PCA, a data reduction technique that simultaneously quantifies categorical variables while reducing the dimensionality of the data. Results are presented as a two-dimensional PCA plot (biplot), a graphical display that illustrates the relationships among the components, original variables, and observations (48). Clinical information obtained at the date of sampling was normalized to remove bias from the analysis. In the biplot, clinical characteristics are shown as variable vectors (component loading). Samples (objects in the biplot) were labeled according to experimental detection (positive) or lack of detection (negative) of HIV in platelets.

Repetition of parameter values from clinical histories due to multiple samplings (e.g., CD4⁺ T cell nadir) did not interfere with the PCA performed, because random selection of one sample per HIV-infected individual before running the PCA did not change the results. Multinomial logistic regression was performed using detection of HIV in platelets as a dependent variable and clinical parameters at the date of sampling as covariates but excluding CD4⁺ T cell historical nadir due to collinearity with CD4⁺ T cell counts (Pearson's coefficient = 0.635, $P < 0.001$). Fisher's exact test was used for odds ratio and risk estimates. $P < 0.05$ was considered significant.

SUPPLEMENTARY MATERIALS

stm.sciencemag.org/cgi/content/full/12/535/eaat6263/DC1

Material and Methods

Fig. S1. Platelet-rich plasma preparations from HIV-infected individuals were not contaminated by HIV-infected CD4⁺ T cells.

Fig. S2. Flow cytometry gating strategy for the detection of HIV in platelets from HIV-infected individuals on ART.

Fig. S3. HIV-containing platelets detected by electron and confocal microscopy.

Fig. S4. Infection of macrophages by HIV in platelets is due to direct interactions and not residual cell-free viruses present in platelet-rich plasma.

Fig. S5. HIV-1 integrated proviral DNA in megakaryocytes from HIV-infected individuals on ART with viral suppression.

Fig. S6. Deep sequencing and phylogenetic analysis of HIV *env* V3 segments before and after viral suppression in the same HIV-infected individuals on ART.

Fig. S7. Interaction between platelets and macrophages is blocked by the anti-integrin α IIb/3 Fab abciximab.

Fig. S8. Detection of HIV-containing platelets does not correlate with other clinical characteristics.

Table S1. Clinical information on HIV-infected individuals on ART analyzed for HIV in platelets.

Table S2. Clinical information on each HIV-infected individual on ART analyzed for HIV in platelets.

Table S3. Available viral load measurements for HIV-infected individuals on ART positive for HIV in platelets and with a viral load below the LOD at the date of sampling.

Table S4. Clinical information for each HIV-infected individual on ART analyzed for HIV in megakaryocytes.

Table S5. ART regimens for HIV-infected individuals classified as positive or negative for the presence of HIV in platelets.

Table S6. CD4⁺ T cell counts and viral load measurements for HIV-infected individuals on ART with controlled viremia and positive for HIV in platelets.

Table S7. List of Gag mRNA probe sequences used for FISH–flow cytometry.

Data file S1. Individual-level data for Figs. 1, 2, and 4 and figs. S1, S4, and S7.

Movie S1. Laser scanning confocal microscopy image of an HIV-containing platelet being engulfed by a macrophage.

References (49–68)

[View/request a protocol for this paper from Bio-protocol.](#)

REFERENCES AND NOTES

- J. W. Semple, J. E. Italiano Jr., J. Freedman, Platelets and the immune continuum. *Nat. Rev. Immunol.* **11**, 264–274 (2011).
- O. Garraud, F. Cognasse, Are platelets cells? And if yes, are they immune cells? *Front. Immunol.* **6**, 70 (2015).
- A. Assinger, Platelets and infection - an emerging role of platelets in viral infection. *Front. Immunol.* **5**, 649 (2014).
- J. R. Ariede, M. I. Pardini, G. F. Silva, R. M. Grotto, Platelets can be a biological compartment for the hepatitis C virus. *Braz. J. Microbiol.* **46**, 627–629 (2015).
- S. Boukour, J. M. Massé, L. Bénit, A. Dubart-Kupferschmitt, E. M. Cramer, Lentivirus degradation and DC-SIGN expression by human platelets and megakaryocytes. *J. Thromb. Haemost.* **4**, 426–435 (2006).
- A. Chabert, H. Hamzeh-Cognasse, B. Pozzetto, F. Cognasse, M. Schattner, R. M. Gomez, O. Garraud, Human platelets and their capacity of binding viruses: Meaning and challenges? *BMC Immunol.* **16**, 26 (2015).
- C. Chaipan, E. J. Soilleux, P. Simpson, H. Hofmann, T. Gramberg, A. Marzi, M. Geier, E. A. Stewart, J. Eisemann, A. Steinkasserer, K. Suzuki-Inoue, G. L. Fuller, A. C. Pearce, S. P. Watson, J. A. Hoxie, F. Baribaud, S. Pöhlmann, DC-SIGN and CLEC-2 mediate human immunodeficiency virus type 1 capture by platelets. *J. Virol.* **80**, 8951–8960 (2006).
- C. Flaujac, S. Boukour, E. Cramer-Bordé, Platelets and viruses: An ambivalent relationship. *Cell. Mol. Life Sci.* **67**, 545–556 (2010).
- A. Y. Simon, M. R. Sutherland, E. L. Prydzial, Dengue virus binding and replication by platelets. *Blood* **126**, 378–385 (2015).
- T. Yousefian, A. Drouin, J. M. Masse, J. Guichard, E. M. Cramer, Host defense role of platelets: Engulfment of HIV and *Staphylococcus aureus* occurs in a specific subcellular compartment and is enhanced by platelet activation. *Blood* **99**, 4021–4029 (2002).
- D. Zucker-Franklin, S. Seremetis, Z. Y. Zheng, Internalization of human immunodeficiency virus type I and other retroviruses by megakaryocytes and platelets. *Blood* **75**, 1920–1923 (1990).
- T. H. Lee, R. R. Stromberg, J. W. Heitman, L. Sawyer, C. V. Hanson, M. P. Busch, Distribution of HIV type 1 (HIV-1) in blood components: Detection and significance of high levels of HIV-1 associated with platelets. *Transfusion* **38**, 580–588 (1998).
- T. H. Lee, R. R. Stromberg, D. Henrard, M. P. Busch, Effect of platelet-associated virus on assays of HIV-1 in plasma. *Science* **262**, 1585–1586 (1993).
- D. Zucker-Franklin, Y. Z. Cao, Megakaryocytes of human immunodeficiency virus-infected individuals express viral RNA. *Proc. Natl. Acad. Sci. U.S.A.* **86**, 5595–5599 (1989).
- S. G. Deeks, S. R. Lewin, A. L. Ross, J. Ananworanich, M. Benkirane, P. Cannon, N. Chomont, D. Douek, J. D. Lifson, Y.-R. Lo, D. Kuritzkes, D. Margolis, J. Mellors, D. Persaud, J. D. Tucker, F. Barre-Sinoussi, International AIDS Society Towards a Cure Working Group, G. Alter, J. Auerbach, B. Autran, D. H. Barouch, G. Behrens, M. Cavazzana, Z. Chen, É. A. Cohen, G. M. Corbelli, S. Eholié, N. Eyal, S. Fidler, L. Garcia, C. Grossman, G. Henderson, T. J. Henrich, R. Jefferys, H.-P. Kiem, J. M. Cune, K. Moodley, P. A. Newman, M. Nijhuis, M. S. Nsubuga, M. Ott, S. Palmer, D. Richman, A. Saez-Cirion, M. Sharp, J. Siliciano, G. Silvestri, J. Singh, B. Spire, J. Taylor, M. Tolstrup, S. Valente, J. van Lunzen, R. Walensky, I. Wilson, J. Zack, International AIDS society global scientific strategy: Towards an HIV cure 2016. *Nat. Med.* **22**, 839–850 (2016).
- A. E. Baxter, J. Niessl, R. Fromentin, J. Richard, F. Porichis, M. Massanella, N. Brassard, N. Alshafi, J. P. Routy, A. Finzi, N. Chomont, D. E. Kaufmann, Multiparametric characterization of rare HIV-infected cells using an RNA-flow FISH technique. *Nat. Protoc.* **12**, 2029–2049 (2017).
- A. E. Baxter, J. Niessl, R. Fromentin, J. Richard, F. Porichis, R. Charlebois, M. Massanella, N. Brassard, N. Alshafi, G. G. Delgado, J. P. Routy, B. D. Walker, A. Finzi, N. Chomont, D. E. Kaufmann, Single-cell characterization of viral translation-competent reservoirs in HIV-infected individuals. *Cell Host Microbe* **20**, 368–380 (2016).
- J. Grau-Exposito, C. Serra-Peinado, L. Miguel, J. Navarro, A. Curran, J. Burgos, I. Ocaña, E. Ribera, A. Torrella, B. Planas, R. Badía, J. Castellví, V. Falcó, M. Crespo, M. J. Buzon, A novel single-cell fish-flow assay identifies effector memory CD4⁺ T cells as a major niche for HIV-1 transcription in HIV-infected patients. *MBio* **8**, e00876-17 (2017).
- C. Hess, T. Klimkait, L. Schlapbach, V. Del Zenero, S. Sadallah, E. Horakova, G. Balestra, V. Werder, C. Schaefer, M. Battegay, J. A. Schifferli, Association of a pool of HIV-1 with erythrocytes in vivo: A cohort study. *Lancet* **359**, 2230–2234 (2002).
- A. Sanyal, R. B. Mailliard, C. R. Rinaldo, D. Ratner, M. Ding, Y. Chen, J. M. Zerbato, N. S. Giacobbi, N. J. Venkatachari, B. K. Patterson, A. Chargin, N. Sluis-Cremer, P. Gupta, Novel assay reveals a large, inducible, replication-competent HIV-1 reservoir in resting CD4⁺ T cells. *Nat. Med.* **23**, 885–889 (2017).
- N. T. Sebastian, T. D. Zaikos, V. Terry, F. Taschuk, L. A. McNamara, A. Onafuwa-Nuga, R. Yucha, R. A. J. Signer, J. Riddell IV, D. Bixby, N. Markowitz, S. J. Morrison, K. L. Collins, CD4 is expressed on a heterogeneous subset of hematopoietic progenitors, which persistently harbor CXCR4 and CCR5-tropic HIV proviral genomes in vivo. *PLOS Pathog.* **13**, e1006509 (2017).
- J. B. Dinosa, S. Y. Kim, A. M. Wiegand, S. E. Palmer, S. J. Gange, L. Cranmer, A. O'Shea, M. Callender, A. Spivak, T. Brennan, M. F. Kearney, M. A. Proschan, J. M. Mican, C. A. Rehm, J. M. Coffin, J. W. Mellors, R. F. Siliciano, F. Maldarelli, Treatment intensification does not reduce residual HIV-1 viremia in patients on highly active antiretroviral therapy. *Proc. Natl. Acad. Sci. U.S.A.* **106**, 9403–9408 (2009).
- E. Eisele, R. F. Siliciano, Redefining the viral reservoirs that prevent HIV-1 eradication. *Immunity* **37**, 377–388 (2012).
- P. J. Ballem, A. Belzberg, D. V. Devine, D. Lyster, B. Spruston, H. Chambers, P. Doubroff, K. Mikulash, Kinetic studies of the mechanism of thrombocytopenia in patients with human immunodeficiency virus infection. *N. Engl. J. Med.* **327**, 1779–1784 (1992).
- J. E. Italiano Jr., J. Hartwig, Production and destruction of platelets, in *The Non-Thrombotic Role of Platelets in Health and Disease*, S. W. Kerrigan, Ed. (IntechOpen, 2015).
- R. Grozovsky, S. Giannini, H. Falet, K. M. Hoffmeister, Molecular mechanisms regulating platelet clearance and thrombopoietin production. *ISBT Sci. Ser.* **10**, 309–316 (2015).
- R. Grozovsky, K. M. Hoffmeister, H. Falet, Novel clearance mechanisms of platelets. *Curr. Opin. Hematol.* **17**, 585–589 (2010).
- R. D'Amico, Y. Yang, D. Mildvan, S. R. Evans, C. T. Schnitzlein-Bick, R. Hafner, N. Webb, M. Basar, R. Zackin, M. A. Jacobson, Lower CD4⁺ T lymphocyte nadirs may indicate limited immune reconstitution in HIV-1 infected individuals on potent antiretroviral therapy: Analysis of immunophenotypic marker results of AACTG 5067. *J. Clin. Immunol.* **25**, 106–115 (2005).
- C. F. Kelley, C. M. Kitchen, P. W. Hunt, B. Rodriguez, F. M. Hecht, M. Kitahata, H. M. Crane, J. Willig, M. Mugavero, M. Saag, J. N. Martin, S. G. Deeks, Incomplete peripheral CD4⁺ cell count restoration in HIV-infected patients receiving long-term antiretroviral treatment. *Clin. Infect. Dis.* **48**, 787–794 (2009).
- V. Rodrigues, N. Ruffin, M. San-Roman, P. Benaroch, Myeloid cell interaction with HIV: A complex relationship. *Front. Immunol.* **8**, 1698 (2017).
- Y. Ganor, F. Real, A. Sennepin, C. A. Dutertre, L. Prevedel, L. Xu, D. Tudor, B. Charmeteau, A. Couedel-Courteille, S. Marion, A. R. Zenak, J. P. Jourdain, Z. Zhou, A. Schmitt, C. Capron, E. A. Eugenin, R. Cheynier, M. Revol, S. Cristofari, A. Hosmalin, M. Bomsel, HIV-1 reservoirs in urethral macrophages of patients under suppressive antiretroviral therapy. *Nat. Microbiol.* **4**, 633–644 (2019).
- J. M. Orenstein, Replication of HIV-1 in vivo and in vitro. *Ultrastruct. Pathol.* **31**, 151–167 (2007).
- W. He, S. Neil, H. Kulkarni, E. Wright, B. K. Agan, V. C. Marconi, M. J. Dolan, R. A. Weiss, S. K. Ahuja, Duffy antigen receptor for chemokines mediates trans-infection of HIV-1 from red blood cells to target cells and affects HIV-AIDS susceptibility. *Cell Host Microbe* **4**, 52–62 (2008).
- H. Kulkarni, V. C. Marconi, W. He, M. L. Landrum, J. F. Okulicz, J. Delmar, D. Kazandjian, J. Castiblanco, S. S. Ahuja, E. J. Wright, R. A. Weiss, R. A. Clark, M. J. Dolan, S. K. Ahuja, The Duffy-null state is associated with a survival advantage in leukopenic HIV-infected persons of African ancestry. *Blood* **114**, 2783–2792 (2009).
- G. Cenderello, A. De Maria, Discordant responses to cART in HIV-1 patients in the era of high potency antiretroviral drugs: Clinical evaluation, classification, management prospects. *Expert Rev. Anti-Infect. Ther.* **14**, 29–40 (2016).

36. S. G. Deeks, HIV infection, inflammation, immunosenescence, and aging. *Annu. Rev. Med.* **62**, 141–155 (2011).
37. W. Lu, V. Mehraj, K. Vyboh, W. Cao, T. Li, J. P. Routy, CD4:CD8 ratio as a frontier marker for clinical outcome, immune dysfunction and viral reservoir size in virologically suppressed HIV-positive patients. *J. Int. AIDS Soc.* **18**, 20052 (2015).
38. M. M. Lederman, L. Calabrese, N. T. Funderburg, B. Clagett, K. Medvik, H. Bonilla, B. Gripshover, R. A. Salata, A. Taege, M. Lisgaris, G. A. McComsey, E. Kirchner, J. Baum, C. Shive, R. Asaad, R. C. Kalayjian, S. F. Sieg, B. Rodriguez, Immunologic failure despite suppressive antiretroviral therapy is related to activation and turnover of memory CD4 cells. *J. Infect. Dis.* **204**, 1217–1226 (2011).
39. J. B. Honeycutt, W. O. Thayer, C. E. Baker, R. M. Ribeiro, S. M. Lada, Y. Cao, R. A. Cleary, M. G. Hudgens, D. D. Richman, J. V. Garcia, HIV persistence in tissue macrophages of humanized myeloid-only mice during antiretroviral therapy. *Nat. Med.* **23**, 638–643 (2017).
40. G. R. Kaufmann, L. Perrin, G. Pantaleo, M. Opravil, H. Furrer, A. Telenti, B. Hirschel, B. Ledergerber, P. Vernazza, E. Bernasconi, M. Rickenbach, M. Egger, M. Battegay; Swiss HIV Cohort Study Group, CD4 T-lymphocyte recovery in individuals with advanced HIV-1 infection receiving potent antiretroviral therapy for 4 years: The Swiss HIV cohort study. *Arch. Intern. Med.* **163**, 2187–2195 (2003).
41. M. Marziali, W. De Santis, R. Carello, W. Leti, A. Esposito, A. Isgrò, C. Fimiani, M. C. Sirianni, I. Mezzaroma, F. Aiuti, T-cell homeostasis alteration in HIV-1 infected subjects with low CD4 T-cell count despite undetectable virus load during HAART. *AIDS* **20**, 2033–2041 (2006).
42. W. H. V. Carvalho-Silva, J. L. Andrade-Santos, F. O. Souto, A. V. C. Coelho, S. Crovella, R. L. Guimarães, Immunological recovery failure in cART-treated HIV-positive patients is associated with reduced thymic output and RTE CD4+ T cell death by pyroptosis. *J. Leukoc. Biol.* **107**, 85–94 (2020).
43. P. Harrison, I. Mackie, A. Mumford, C. Briggs, R. Liesner, M. Winter, S. Machin; British Committee for Standards in Haematology, Guidelines for the laboratory investigation of heritable disorders of platelet function. *Br. J. Haematol.* **155**, 30–44 (2011).
44. Y. Kajikawa, T. Morihara, H. Sakamoto, K. Matsuda, Y. Oshima, A. Yoshida, M. Nagae, Y. Arai, M. Kawata, T. Kubo, Platelet-rich plasma enhances the initial mobilization of circulation-derived cells for tendon healing. *J. Cell. Physiol.* **215**, 837–845 (2008).
45. S. Amisten, A rapid and efficient platelet purification protocol for platelet gene expression studies. *Methods Mol. Biol.* **788**, 155–172 (2012).
46. C. Palmer, M. Diehn, A. A. Alizadeh, P. O. Brown, Cell-type specific gene expression profiles of leukocytes in human peripheral blood. *BMC Genomics* **7**, 115 (2006).
47. R. Arrigucci, Y. Bushkin, F. Radford, K. Lakehal, P. Vir, R. Pine, D. Martin, J. Sugarman, Y. Zhao, G. S. Yap, A. A. Lardizabal, S. Tyagi, M. L. Gennaro, FISH-flow, a protocol for the concurrent detection of mRNA and protein in single cells using fluorescence in situ hybridization and flow cytometry. *Nat. Protoc.* **12**, 1245–1260 (2017).
48. K. R. Gabriel, C. L. Odoroff, Biplots in biomedical research. *Stat. Med.* **9**, 469–485 (1990).
49. K. Tenner-Racz, P. Rácz, M. Dietrich, P. Kern, Altered follicular dendritic cells and virus-like particles in AIDS and AIDS-related lymphadenopathy. *Lancet* **1**, 105–106 (1985).
50. K. Tenner-Racz, P. Racz, M. Bofill, A. Schulz-Meyer, M. Dietrich, P. Kern, J. Weber, A. J. Pinching, F. Veronese-Dimarzo, M. Popovic, D. Klatzmann, J. C. Gluckman, G. Janossy, HTLV-III/LAV viral antigens in lymph nodes of homosexual men with persistent generalized lymphadenopathy and AIDS. *Am. J. Pathol.* **123**, 9–15 (1986).
51. A. Le Tourneau, J. Audouin, J. Diebold, C. Marche, V. Tricottet, M. Reynes, LAV-like viral particles in lymph node germinal centers in patients with the persistent lymphadenopathy syndrome and the acquired immunodeficiency syndrome-related complex: An ultrastructural study of 30 cases. *Hum. Pathol.* **17**, 1047–1053 (1986).
52. C. J. O'Hara, J. E. Groopman, M. Federman, The ultrastructural and immunohistochemical demonstration of viral particles in lymph nodes from human immunodeficiency virus-related and non-human immunodeficiency virus-related lymphadenopathy syndromes. *Hum. Pathol.* **19**, 545–549 (1988).
53. A. Morner, A. Björndal, J. Albert, V. N. Kewalramani, D. R. Littman, R. Inoue, R. Thorstensson, E. M. Fenyö, E. Björling, Primary human immunodeficiency virus type 2 (HIV-2) isolates, like HIV-1 isolates, frequently useCCR5 but show promiscuity in coreceptor usage. *J. Virol.* **73**, 2343–2349 (1999).
54. A. M. Janas, L. Wu, HIV-1 interactions with cells: From viral binding to cell-cell transmission. *Curr. Protoc. Cell Biol.* **Chapter 26**, Unit 26.5 (2009).
55. M. K. Liszewski, J. J. Yu, U. O'Doherty, Detecting HIV-1 integration by repetitive-sampling Alu-gag PCR. *Methods* **47**, 254–260 (2009).
56. W. De Spiegelaere, E. Malatinkova, L. Lynch, F. Van Nieuwerburgh, P. Messiaen, U. O'Doherty, L. Vandekerckhove, Quantification of integrated HIV DNA by repetitive-sampling Alu-HIV PCR on the basis of poisson statistics. *Clin. Chem.* **60**, 886–895 (2014).
57. J. J. Yu, T. L. Wu, M. K. Liszewski, J. Dai, W. J. Swiggard, C. Baytop, I. Frank, B. L. Levine, W. Yang, T. Theodosopoulos, U. O'Doherty, A more precise HIV integration assay designed to detect small differences finds lower levels of integrated DNA in HAART treated patients. *Virology* **379**, 78–86 (2008).
58. C. Deleage, S. W. Wietgreffe, G. Del Prete, D. R. Morcock, X. P. Hao, M. Piatak Jr., J. Bess, J. L. Anderson, K. E. Perkey, C. Reilly, J. M. McCune, A. T. Haase, J. D. Lifson, T. W. Schacker, J. D. Estes, Defining HIV and SIV reservoirs in lymphoid tissues. *Pathog. Immun.* **1**, 68–106 (2016).
59. F. Real, A. Sennepin, Y. Ganor, A. Schmitt, M. Bomsel, Live imaging of HIV-1 transfer across T cell virological synapse to epithelial cells that promotes stromal macrophage infection. *Cell Rep.* **23**, 1794–1805 (2018).
60. L. Prevedel, N. Ruel, P. Castellano, C. Smith, S. Malik, C. Villeux, M. Bomsel, S. Morgello, E. A. Eugenin, Identification, localization, and quantification of HIV reservoirs using microscopy. *Curr. Protoc. Cell Biol.* **82**, e64 (2019).
61. V. Henn, J. R. Slupsky, M. Gräfe, I. Anagnostopoulos, R. Förster, G. Müller-Berghaus, R. A. Kroczeck, CD40 ligand on activated platelets triggers an inflammatory reaction of endothelial cells. *Nature* **391**, 591–594 (1998).
62. S. Raymond, N. Jeanne, F. Nicot, C. Lefebvre, R. Carcenac, L. Minier, J. Chiabrando, M. Cazabat, P. Delobel, J. Izopet, Long-term evolution of transmitted CXCR4-using HIV-1 under effective antiretroviral therapy. *AIDS* **33**, 1977–1985 (2019).
63. N. Jeanne, A. Saliou, R. Carcenac, C. Lefebvre, M. Dubois, M. Cazabat, F. Nicot, C. Loiseau, S. Raymond, J. Izopet, P. Delobel, Position-specific automated processing of V3 env ultra-deep pyrosequencing data for predicting HIV-1 tropism. *Sci. Rep.* **5**, 16944 (2015).
64. R. C. Edgar, MUSCLE: Multiple sequence alignment with high accuracy and high throughput. *Nucleic Acids Res.* **32**, 1792–1797 (2004).
65. S. Capella-Gutiérrez, J. M. Silla-Martínez, T. Gabaldón, trimAl: A tool for automated alignment trimming in large-scale phylogenetic analyses. *Bioinformatics* **25**, 1972–1973 (2009).
66. S. Guindon, O. Gascuel, A simple, fast, and accurate algorithm to estimate large phylogenies by maximum likelihood. *Syst. Biol.* **52**, 696–704 (2003).
67. D. Darriba, G. L. Taboada, R. Doallo, D. Posada, jModelTest 2: More models, new heuristics and parallel computing. *Nat. Methods* **9**, 772 (2012).
68. I. Letunic, P. Bork, Interactive tree of life (ITOL) v4: Recent updates and new developments. *Nucleic Acids Res.* **47**, W256–W259 (2019).

Acknowledgments: We thank the HIV-infected individuals who participated in this study, V. Boeva from Institut Cochin for advice on multivariate analysis, and A. Schmitt for help with electron microscopy. **Funding:** This work was supported by Agence Nationale de Recherches sur le Sida et les Hépatites Virales (ANRS #AQ2015-2-17046) and SIDACTION (#15CONV03) to M.B. F.R. is the recipient of a postdoctoral fellowship from SIDACTION and ANRS. L.X. and A.Z. received doctoral fellowships from the Chinese Science Council, and A.S. is an ANRS postdoctoral fellow. **Author contributions:** F.R., E.C.B., and M.B. conceived the experiments. C.C., S.G., E.R., and E.C.B. collected the patient samples and provided clinical information. F.R., C.C., and M.B. performed flow cytometry and confocal microscopy. F.R., G.S., and J.Z. performed reporter T cell assays. F.R., A.S., A.Z., and L.X. performed qPCR experiments. F.R., C.C., J.-M.M., and M.B. performed electron microscopy. F.R., R.A., M.L.G., and M.B. set up FISH and flow cytometry assays. F.R., M.B., E.E., and M.D. designed and performed in situ hybridization experiments on megakaryocytes and platelets in vitro. M.C., P.D., and J.I. performed deep sequencing and phylogenetic analyses of HIV env gene V3 segments. F.R., S.G., E.R., E.C.B., and M.B. performed retrospective and prospective analysis of the clinical status of HIV-infected individuals. F.R., E.C.B., and M.B. wrote the manuscript. **Competing interests:** The authors declare that they have no competing interests. **Data and materials availability:** All data associated with this study are in the paper or the Supplementary Materials. HIV env V3 sequences have been deposited in GenBank with accession numbers MN453286, MN453287, MN453288, MN453288, MN453289, MN453290, MN453291, MN453292, MN453293, MN453294, and MN453295.

Submitted 20 March 2018
Resubmitted 23 July 2019
Accepted 1 October 2019
Published 18 March 2020
10.1126/scitranslmed.aat6263

Citation: F. Real, C. Capron, A. Sennepin, R. Arrigucci, A. Zhu, G. Sannier, J. Zheng, L. Xu, J.-M. Massé, S. Greffe, M. Cazabat, M. Donoso, P. Delobel, J. Izopet, E. Eugenin, M. L. Gennaro, E. Rouveix, E. Cramer Bordé, M. Bomsel, Platelets from HIV-infected individuals on antiretroviral drug therapy with poor CD4⁺ T cell recovery can harbor replication-competent HIV despite viral suppression. *Sci. Transl. Med.* **12**, eaat6263 (2020).

Platelets from HIV-infected individuals on antiretroviral drug therapy with poor CD4⁺ T cell recovery can harbor replication-competent HIV despite viral suppression

Fernando Real, Claude Capron, Alexis Sennepin, Riccardo Arrigucci, Aiwei Zhu, G r my Sannier, Jonathan Zheng, Lin Xu, Jean-Marc Mass , S gol ne Greffe, Michelle Cazabat, Maribel Donoso, Pierre Delobel, Jacques Izopet, Eliseo Eugenin, Maria Laura Gennaro, Elisabeth Rouveix, Elisabeth Cramer Bord  and Morgane Bomsel

Sci Transl Med 12, eaat6263.
DOI: 10.1126/scitranslmed.aat6263

Hidden in plain sight

Human platelets carry out several immune functions as well as hemostasis and interact with infectious pathogens including HIV in vitro. Real *et al.* now report that platelets from HIV-infected individuals can harbor replication-competent HIV, despite successful viral suppression by antiretroviral drug therapy (ART). Moreover, in their study, >80% of virally suppressed HIV-infected individuals with platelets containing HIV showed poor restoration of immune status even 1 year after ART treatment initiation. Platelets carrying HIV may provide an alternative pathway for HIV dissemination in HIV-infected individuals on ART with viral suppression and poor CD4⁺ T cell recovery.

ARTICLE TOOLS

<http://stm.sciencemag.org/content/12/535/eaat6263>

SUPPLEMENTARY MATERIALS

<http://stm.sciencemag.org/content/suppl/2020/03/16/12.535.eaat6263.DC1>

RELATED CONTENT

<http://stm.sciencemag.org/content/scitransmed/12/533/eaav3491.full>
<http://stm.sciencemag.org/content/scitransmed/11/509/eaax3447.full>
<http://stm.sciencemag.org/content/scitransmed/11/499/eaap8758.full>
<http://stm.sciencemag.org/content/scitransmed/11/504/eaav5685.full>

REFERENCES

This article cites 67 articles, 11 of which you can access for free
<http://stm.sciencemag.org/content/12/535/eaat6263#BIBL>

PERMISSIONS

<http://www.sciencemag.org/help/reprints-and-permissions>

Use of this article is subject to the [Terms of Service](#)

Science Translational Medicine (ISSN 1946-6242) is published by the American Association for the Advancement of Science, 1200 New York Avenue NW, Washington, DC 20005. The title *Science Translational Medicine* is a registered trademark of AAAS.

Copyright   2020 The Authors, some rights reserved; exclusive licensee American Association for the Advancement of Science. No claim to original U.S. Government Works

HIV

Platelets from HIV-infected individuals on antiretroviral drug therapy with poor CD4⁺ T cell recovery can harbor replication-competent HIV despite viral suppression

Fernando Real^{1,2,3}, Claude Capron⁴, Alexis Sennepin^{1,2,3}, Riccardo Arrigucci⁵, Aiwei Zhu^{1,2,3}, G  r  my Sannier^{1,2,3}, Jonathan Zheng^{1,2,3}, Lin Xu^{1,2,3}, Jean-Marc Mass  ^{2,3,6}, S  gol  ne Greffe⁷, Michelle Cazabat⁸, Maribel Donoso⁹, Pierre Delobel^{10,11,12}, Jacques Izopet^{8,10,11}, Eliseo Eugenin⁹, Maria Laura Gennaro⁵, Elisabeth Rouveix⁷, Elisabeth Cramer Bord  ^{1,2,4}, Morgane Bomsel^{1,2,3*}

In addition to hemostasis, human platelets have several immune functions and interact with infectious pathogens including HIV *in vitro*. Here, we report that platelets from HIV-infected individuals on combined antiretroviral drug therapy (ART) with low blood CD4⁺ T cell counts (<350 cells/ μ l) contained replication-competent HIV despite viral suppression. *In vitro*, human platelets harboring HIV propagated the virus to macrophages, a process that could be prevented with the biologic abciximab, an anti-integrin α IIb/ β 3 Fab. Furthermore, in our cohort, 88% of HIV-infected individuals on ART with viral suppression and with platelets containing HIV were poor immunological responders with CD4⁺ T cell counts remaining below <350 cells/ μ l for more than one year. Our study suggests that platelets may be transient carriers of HIV and may provide an alternative pathway for HIV dissemination in HIV-infected individuals on ART with viral suppression and poor CD4⁺ T cell recovery.

INTRODUCTION

The main function of human platelets is in hemostasis, but they also contribute to immunological responses (1) and can engulf viral and nonviral infectious pathogens (2). *In vitro*, platelets directly interact with and internalize HIV, dengue virus, hepatitis C virus, influenza virus, bacteria such as *Staphylococcus aureus*, and other pathogens (3–11). We and others have shown *in vitro* a direct interaction of HIV with platelets and with megakaryocytes, which are platelet precursor cells (5, 7, 10–13). These experimental studies required large quantities of laboratory-adapted cell-free HIV to interact with platelets and megakaryocytes, thus compromising biological relevance (7, 10). Early *in vivo* studies detected HIV RNA without investigation of replication-competent virions in human platelets (12, 13) and in megakaryocytes (14) from untreated HIV-infected individuals. However, evidence for platelets containing infectious HIV *in vivo*, especially in HIV-infected individuals on combined antiretroviral drug therapy (ART), remains elusive.

Here, we investigated the occurrence of replication-competent HIV in platelets from HIV-infected individuals on ART with viral suppression and analyzed whether a correlation existed with their clinical status.

RESULTS

Platelets from HIV-infected individuals on ART harbor HIV

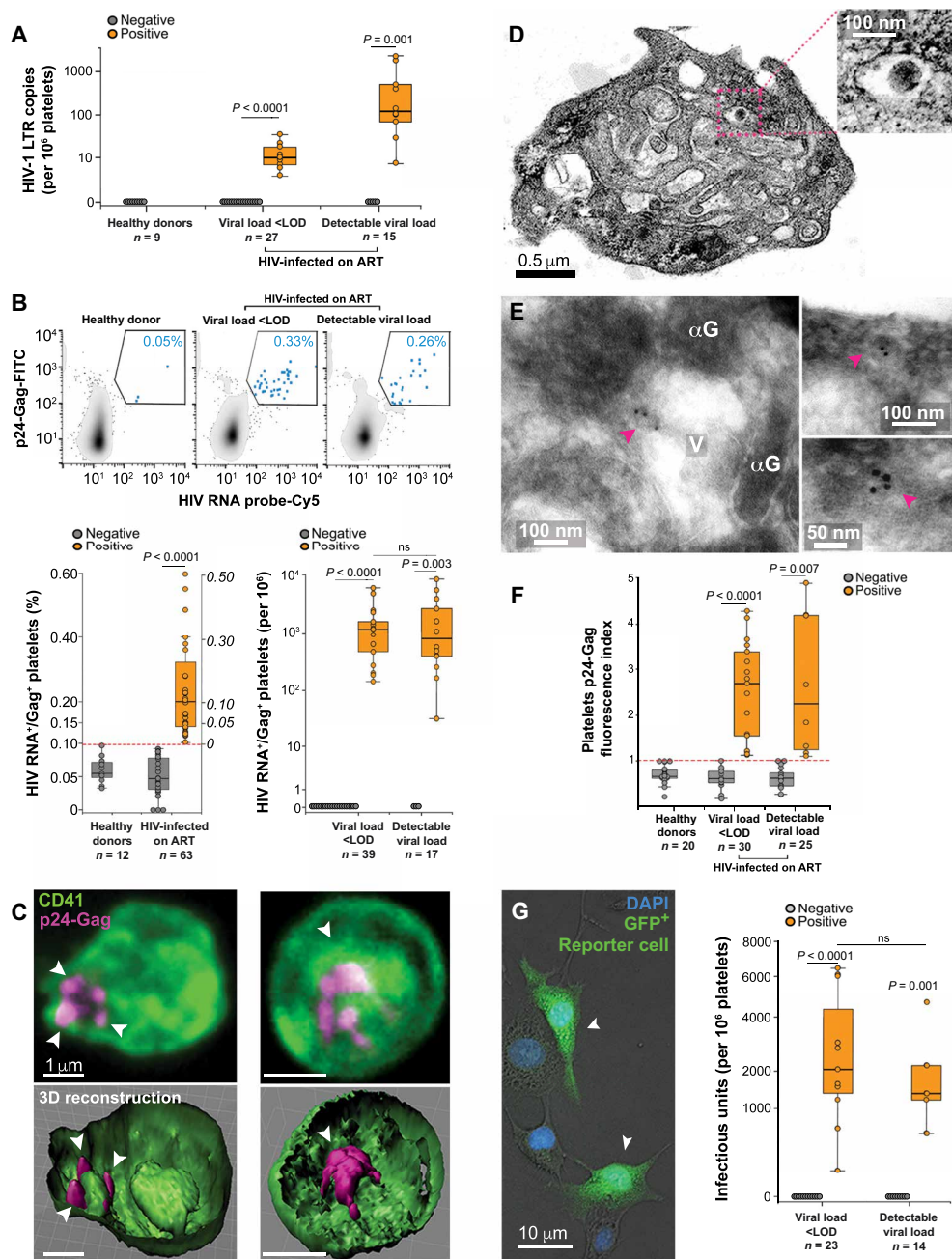
We isolated platelets from HIV-infected individuals on ART (tables S1 and S2), who had either a detectable viral load ($n = 15$) or undetectable virus ($n = 27$) that was below the limit of detection (LOD) of 1.6 log₁₀ HIV RNA copies/ml, and we used quantitative real-time polymerase chain reaction (qPCR) to establish whether the isolated platelets contained HIV. In a subgroup of ART-treated HIV-infected individuals with undetectable blood viral load (10 of 27), platelets were found to contain on average 9.92 HIV RNA copies per million platelets with a confidence interval (CI) of 6.5 to 17.8 (Fig. 1A). A subgroup of ART-treated HIV-infected individuals with detectable viremia (10 of 15) had on average 122.3 HIV RNA copies per million platelets (CI, 65 to 1111) (Fig. 1A). Longitudinal clinical data obtained from these HIV-infected individuals on ART with undetectable viral load at the date of sampling (indicated by an asterisk in table S3) showed that the viral load for six of nine individuals consistently remained below the LOD for more than 1 year (median, 26 months; CI, 14 to 74 months) before the date of sampling (table S3). This finding suggested that circulating HIV had not attached nonspecifically to platelets in the circulation. Furthermore, potential contamination by HIV-infected cells present in the blood of these individuals was evaluated by flow cytometry. Analyses of platelet-rich plasma samples from all assessed HIV-infected individuals on ART detected less than one lymphocyte per sample corresponding to 2.16 CD3⁺ T cells per million platelets (CI, 1.4 to 2.7) (fig. S1, A to C). The likelihood of platelet contamination by HIV-infected T cells was low given that in HIV-infected individuals on ART with undetectable viral load, HIV-infected T cells represented 0.01 to 0.1% of total blood CD4⁺ T cells with 100 to 1000 HIV DNA copies per million CD4⁺ T cells (15).

To identify not only cytosolic HIV RNA but also intact viral particles in platelets, detection of HIV RNA by fluorescence *in situ* hybridization (FISH) was combined with detection of viral protein

¹Mucosal Entry of HIV and Mucosal Immunity, Institut Cochin, Universit   de Paris, Paris, France. ²INSERM U1016, Paris, France. ³CNRS UMR8104, Paris, France. ⁴H  pital Ambroise Par  , Boulogne-Billancourt, France. ⁵Public Health Research Institute, New Jersey Medical School, Rutgers, The State University of New Jersey, Newark, NJ, USA. ⁶Electron Microscopy Platform, Institut Cochin, Universit   de Paris, Paris, France. ⁷Department of Internal Medicine, H  pital Ambroise Par  , Boulogne, France. ⁸CHU de Toulouse, H  pital Purpan, Laboratoire de Virologie, Toulouse, France. ⁹Department of Neuroscience, Cell Biology, and Anatomy, University of Texas Medical Branch (UTMB), Galveston, TX, USA. ¹⁰INSERM U1043, Toulouse, France. ¹¹Universit   Toulouse III Paul-Sabatier, Facult   de M  decine Toulouse-Purpan, Toulouse, France. ¹²CHU de Toulouse, H  pital Purpan, Service des Maladies Infectieuses et Tropicales, Toulouse, France.

*Corresponding author. Email: morgane.bomsel@inserm.fr

Fig. 1. Detection of HIV in platelets from HIV-infected individuals on ART. (A) Number of HIV long terminal repeat (LTR) copies per million platelets in platelet-rich plasma samples from ART-treated HIV-infected individuals with viral loads either below the LOD or detectable at the date of sampling. Platelet-rich plasma from healthy donors was used as a negative control. Platelet samples in which HIV was detected are shown in orange, and samples negative for HIV are shown in gray. The number of different individuals tested (*n*) is shown below the graph. Data are the result of seven independent experiments. Boxplots represent medians with 25th and 75th percentiles and with minimum/maximum values indicated by whiskers (Mann-Whitney *U* test). (B) Top: HIV RNA⁺/p24-Gag⁺ platelets were measured by FISH–flow cytometry. Bottom left: Boxplot shows percentage of HIV RNA⁺/p24-Gag⁺ platelets from healthy donors or HIV-infected individuals on ART detected by FISH–flow cytometry and expressed as a percentage of total platelets in the platelet-rich plasma samples. Normalized percentage values are indicated in italics on the right-hand axis. The quantification threshold (orange dashed line) was established on the basis of healthy donor samples. Samples from HIV-infected individuals on ART were grouped according to the absence (gray, negative) or presence (orange, positive) of HIV in platelets (*P* < 0.001). The number of different individuals tested (*n*) is shown below the graph. Bottom right: Boxplot shows percentages converted into HIV RNA⁺/p24-Gag⁺ platelets per million platelets after data normalization and after subtracting the maximum value obtained from healthy donor control samples. The number of different individuals tested (*n*) is shown below the graph. Results are from seven independent experiments and are expressed as boxplots generated separately for negative and positive groups. Boxplots represent medians with 25th and 75th percentiles and with minimum/maximum values indicated by whiskers (Mann-Whitney *U* test). (C) Representative confocal microscopy images (top panels) show platelets from HIV-infected individuals on ART immunostained for CD41 (green) and p24-Gag (magenta). Images reconstructed in three dimensions are shown in the bottom panels. White arrowheads indicate HIV contained within platelets. Representative images are shown for platelets from 11 different HIV-infected individuals on ART. Scale bars, 1 μm. (D) Representative transmission electron micrograph of an HIV-containing platelet. A viral particle in a small vacuolar compartment is indicated by the magenta box, which is shown at a higher magnification in the image inset. The electron micrograph is representative of samples from five different HIV-infected individuals on ART with viral suppression. (E) Immunogold labeling (10 nm) of p24-Gag in cryosections was performed before electron microscopy to confirm the presence of HIV within a platelet compartment (pink arrowhead). Representative image of 10 different images obtained from two different HIV-infected individuals on ART with viral suppression. αG, α-granule; V, vacuole. Scale bars, 0.5 μm, 100 nm, or 50 nm. (F) p24-Gag immunofluorescence intensities for platelets from healthy donors or HIV-infected individuals on ART detected by flow cytometry. Results are from seven independent experiments and are expressed as boxplots generated separately for negative and positive groups. Boxplots represent median with 25th and 75th percentiles and with minimum/maximum values indicated by whiskers (Student's *t* test). (G) Image shows green fluorescent protein–positive (GFP⁺) reporter T cells (green) after interaction with platelet-rich plasma from an HIV-infected individual on ART. Nuclei are labeled with 4',6'-diamidino-2-phenylindole (DAPI) (blue); the fluorescence signal (green) was merged with phase contrast (white arrowheads). Scale bar, 10 μm. Boxplot shows the quantification of infectious units per million platelets in platelet-rich plasma samples from HIV-infected individuals on ART who either displayed viremia below LOD or had detectable viral load at the date of sampling. Samples lacking infectious virus are in gray (negative), and those with infectious virus are in orange (positive). The number of different individuals tested (*n*) is shown below the graph. Results are from eight independent experiments and are expressed as boxplots generated separately for negative and positive groups. Boxplots represent medians with 25th and 75th percentiles and with minimum/maximum values indicated by whiskers (Mann-Whitney *U* test). ns, not significant.



p24-Gag by immunofluorescence. Both types of labeling were quantified simultaneously by flow cytometry using a single-cell approach referred to as FISH–flow cytometry (Fig. 1B and fig. S2, A to C) (16). HIV RNA⁺/p24-Gag⁺ FISH–flow cytometry can detect the very low number of latent HIV reservoir cells in HIV-infected individuals on ART, which comprise around 1 infected cell per million CD4⁺ T cells (16–18). We found that platelets from HIV-infected individuals on ART that were positive for HIV RNA and p24-Gag comprised 0.1% (CI, 0.047 to 0.15%) of total platelets in the blood of these individuals (Fig. 1B, left). When stratified according to either undetectable (below LOD) or detectable viral load at the date of sampling, HIV-infected individuals on ART did not differ in the number of HIV RNA⁺/p24-Gag⁺ platelets per 10⁶ platelets, which was 1186.99 (CI, 631 to 1600) and 825.8 (CI, 387 to 2676), respectively ($P > 0.05$) (Fig. 1B, right). The HIV RNA⁺/p24-Gag⁺ signal detected in platelets did not originate from HIV-infected CD4⁺ T cells (fig. S1D), as T cells obtained from ART-treated HIV-infected individuals did not transcribe HIV RNA in quantities that could be detected by FISH–flow cytometry in the absence of activation by mitogens (17).

HIV resides in an internal compartment of platelets

HIV was found inside platelets from HIV-infected individuals on ART as shown by p24-Gag immunolocalization using confocal microscopy (Fig. 1C and fig. S3, A and B) and electron microscopy (Fig. 1, D and E, and fig. S3, C and D), in parallel with flow cytometry (Fig. 1F and fig. S2, A, B, and D). At the confocal microscopy level, HIV appeared to be exclusively confined within closed vacuoles (Fig. 1C; p24-Gag detection indicated by arrowheads), as we have previously reported *in vitro* (5, 10), and did not seem to be associated with the platelet surface. Furthermore, at the ultrastructural level, morphological (Fig. 1D and fig. S3C) and immunogold detection of HIV (Fig. 1E, p24-Gag detection indicated by arrowhead, and fig. S3D) was restricted to vesicles that were distinct from both the platelet surface and its connected canalicular system, suggesting that HIV was not in contact with the external environment (8) or α -granules.

To further validate our microscopy-based immunostaining approaches, p24-Gag⁺ immunostaining was evaluated by flow cytometry. Differences in p24-Gag⁺ mean fluorescence intensity were observed for platelets from HIV-infected individuals on ART with (orange bars) or without (gray bars) HIV (Fig. 1F and fig. S2, A, B, and D). The HIV p24-Gag protein was detected in platelets from a subset of ART-treated HIV-infected individuals who either were viremic (8 of 25) or had a viral load below the LOD at the date of sampling (17 of 30).

HIV harbored in platelets is replication competent

We next investigated the replication competence of HIV localized in platelets from HIV-infected individuals on ART using a CD4⁺-CCR5⁺CXCR4⁺ reporter cell line (19, 20) (Fig. 1G). These experiments revealed that in ART-treated HIV-infected individuals with either undetectable (below LOD) or detectable viral load at the date of sampling, a subgroup (Fig. 1G, orange) had platelets with similar amounts of infectious viral particles: 2053 infectious units (IU)/10⁶ platelets (CI, 1195 to 6013; 11 of 23 individuals) and 1353 IU/10⁶ platelets (CI, 533 to 4671; 5 of 14 individuals), respectively (Fig. 1G). Among HIV-infected individuals on ART with infectious HIV in platelets and displaying a viral load below LOD at the date of sampling (indicated by crosses in table S3), 72% (8 of 11 tested) were

consistently virally suppressed for more than 1 year with a median of 30 (CI, 20 to 50) months before sampling (table S3). This suggested that there was no contamination with residual infectious cell-free virus from blood in the reporter cell assay. Furthermore, in a subset of HIV-infected individuals on ART who were virally suppressed below LOD at the date of sampling, no infectious virus was detected in platelet-poor plasma in the reporter cell assay (fig. S4).

Megakaryocytes from HIV-infected individuals on ART contain HIV

We next investigated the potential origin of platelets containing replication-competent HIV. Bone marrow megakaryocyte progenitors from HIV-infected individuals on ART with sustained viral suppression were recently shown to contain replication-competent viral DNA (21), and megakaryocytes, the precursor cells of platelets, from untreated HIV-infected individuals were shown to harbor HIV RNA (14). HIV-1 RNA and HIV virions contained in megakaryocytes could potentially be sequestered by platelets during thrombopoiesis (11, 14, 21). We detected HIV DNA (fig. S5, A to C) and HIV RNA (fig. S5F) in bone marrow from an HIV-infected individual on ART by *in situ* hybridization in cells morphologically identified as megakaryocytes. In addition, HIV-integrated proviral DNA was detected in megakaryocytes purified from bone marrow samples from 82% (9 of 11) of HIV-infected individuals on ART with viral suppression (table S4 and fig. S5, D and E), with an estimate of 74.7 (CI, 39 to 140.6) HIV DNA integrated copies per million megakaryocytes (fig. S5, D and E). In platelet-rich plasma samples from the four of these HIV-infected individuals on ART with viral suppression we could analyze, platelets containing HIV RNA and HIV p24-Gag protein were detected (fig. S5G).

To confirm that HIV harbored in platelets was not blood borne, phylogenetic analyses were performed after deep sequencing of HIV *env* V3 sequences in plasma samples from HIV-infected individuals before and after viral suppression. Plasma samples were obtained before viral suppression and were compared to peripheral blood mononuclear cells (PBMCs) and platelet samples after up to 69 months of viral suppression by ART. These phylogenetic analyses demonstrated that after viral suppression, platelet-associated HIV originated from a different compartment than did PBMC-associated HIV provirus or HIV in plasma before ART suppression (fig. S6A). In addition, translated sequences revealed a shift in HIV tropism from CCR5 variants in plasma before ART treatment to CXCR4 variants in PBMCs and platelets after viral suppression by ART. The independent grouping of platelet-derived CXCR4 variants (fig. S6, A and B) in the phylogenetic analysis demonstrated that HIV in platelets did not originate from a latent reservoir established before ART or from the CD4⁺ T cell latent reservoir (22, 23). More longitudinal, in-depth phylogenetic studies on HIV genome sequences obtained from platelets, bone marrow, and CD4⁺ T cells of HIV-infected individuals before and after viral suppression will be required to confirm this finding.

HIV harbored in platelets can be transferred to macrophages *in vitro*

At the end of their short life span, platelets are ultimately phagocytosed by mononuclear phagocytic cells residing mainly in the liver and spleen (24). Tissue macrophages are central to this process by engulfing senescent and apoptotic platelets via integrins including α_{IIb}/β_3 and scavenger receptors (24–27). HIV harbored in platelets could be transferred to tissue macrophages through this process of

platelet elimination. Therefore, we next investigated whether HIV-containing platelets could be phagocytosed by macrophages in vitro (Fig. 2, fig. S7, and movie S1). HIV-containing platelets from HIV-infected individuals on ART with viral load consistently below LOD for 52.5 (CI, 12 to 75) months were found to adhere to and, in turn, be phagocytosed by macrophages in vitro (Fig. 2, A and B, and movie S1). This resulted in integration of HIV proviral DNA into the genome of macrophages with 48.25 (CI, 5.24 to 183.9) proviral HIV DNA copies per million macrophages (Fig. 2C). Infection appeared to be productive as these HIV-infected macrophages, in turn, produced infectious HIV virions (Fig. 2D). HIV proviral DNA integration and infectious virus production in vitro could be inhibited by preventing platelet-macrophage interactions using abciximab, a platelet-specific anti-integrin $\alpha_{IIb}\beta_3$ Fab (Fig. 2, C and D, and fig. S7, B to D).

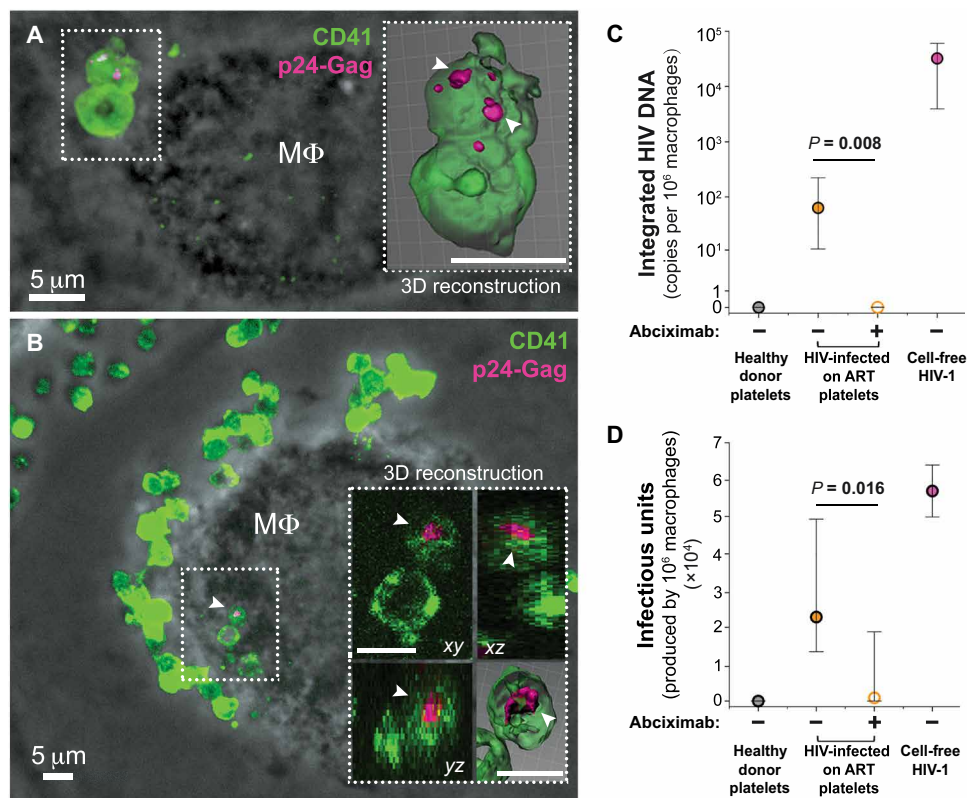


Fig. 2. Transfer of HIV from platelets to macrophages in vitro. (A and B) Representative confocal microscopy images of HIV-containing platelets interacting with macrophages (M Φ) in vitro after immunostaining for CD41 (green) and p24-Gag (pink); image is merged with phase-contrast image. White arrowheads show labeled virus within platelets. Image insets show three-dimensional reconstructions or projections in xy, yz, and xz dimensions for HIV-containing platelets. Images are representative of five different individuals. Scale bars, 5 μ m (main and inset figures). (C) Number of integrated copies of HIV DNA per 10^6 macrophages after 7 days of coculture with platelets from HIV-infected individuals on ART with viral suppression in the presence (solid orange circle) or absence (empty orange circle) of abciximab. Culture with cell-free HIV-1 was used as a positive control (magenta circle), and healthy donor platelets were used as a negative control (gray circle). (D) Infectious units produced per 10^6 macrophages after 7 days of coculture with platelets from HIV-infected individuals on ART with viral suppression in the presence (solid orange circle) or absence (empty orange circle) of abciximab. Culture with cell-free HIV-1 was used as a positive control (magenta circle), and healthy donor platelets were used as a negative control (gray circle). Results for (C) and (D) are presented as medians (circles) with 95% CIs (whiskers). Data represent three independent experiments with samples from five different HIV-infected individuals on ART. Mann-Whitney *U* test was applied for paired experimental data for platelets from HIV-infected individuals on ART, treated or not treated with abciximab in vitro.

HIV-infected individuals on ART with platelets containing HIV have low CD4⁺ T cell counts

Next, we compared clinical characteristics at the date of sampling between HIV-infected individuals on ART who did (orange bars) or who did not (gray bars) have HIV-containing platelets (table S2 and Fig. 3A). HIV-infected individuals on ART with HIV-containing platelets had a low CD4⁺ T cell count (<350/ μ l) that was threefold less compared to HIV-infected individuals on ART without HIV-containing platelets (Fig. 3A). In contrast, the presence of HIV-containing platelets was not associated with total lymphocyte counts or platelet counts, age, years since diagnosis, years on ART (fig. S8, A to C), or the type of ART regimen (table S5). We performed a multivariate analysis of the clinical characteristics of HIV-infected individuals with or without HIV in platelets at the date of sampling. Principal component analysis (PCA) showed separate clusters for

blood samples with or without HIV-containing platelets (Fig. 3B). This distribution was mainly driven by principal component (dimension) 2, where CD4⁺ T cell count was the strongest contributor (fig. S8D) and inversely correlated with the presence of HIV in platelets (Fig. 3B). Furthermore, a multinomial logistic regression indicated that among clinical characteristics, excluding nadir due to collinearity, CD4⁺ T cell count was the only predictive value for the presence of HIV in platelets ($P = 0.007$).

HIV-infected individuals on ART with platelets containing HIV show immunological failure

To address the potential clinical implications of platelets containing HIV, a subset of 35 HIV-infected individuals on ART analyzed above was selected (Table 1). Selection was based on two criteria, namely, HIV detection in platelets using at least two different techniques (tables S2) and unambiguous clinical data available for 1 year before the date of sampling. In these selected HIV-infected individuals on ART, the historical CD4⁺ T cell nadir, a clinical characteristic critical for immune recovery (28), was significantly lower (<200 cells/ μ l) in those with HIV-containing platelets compared to those without HIV-containing platelets ($P = 0.006$, Fig. 4A). A sustained low CD4⁺ T cell count (<350 cells/ μ l), irrespective of viral suppression, persisted in HIV-infected individuals on ART with HIV-containing platelets. In contrast, HIV-infected individuals on ART lacking HIV in platelets had a CD4⁺ T cell count above this threshold, especially if they were aviremic. This was shown by analysis of mean CD4⁺ T cell counts at the date of sampling and

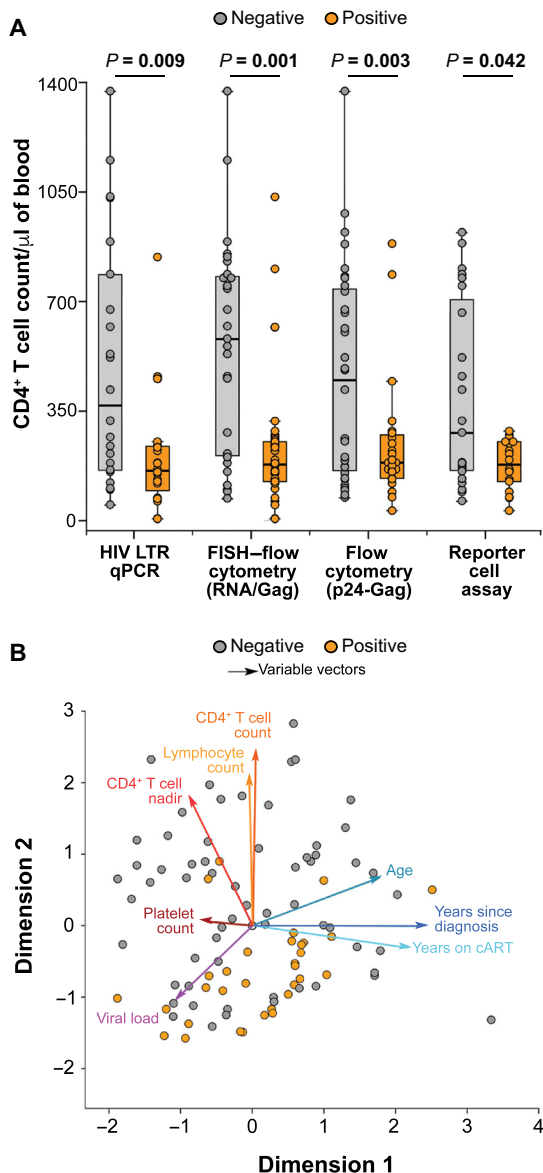


Fig. 3. Platelets containing HIV correlate with low CD4⁺ T cell counts. (A) Comparison of CD4⁺ T cell counts at the date of sampling for HIV-infected individuals on ART whose platelets either contained (positive, orange) or did not contain (negative, gray) HIV. HIV was detected by HIV LTR qPCR, FISH flow cytometry (HIV RNA⁺/p24-Gag⁺), p24-Gag flow cytometry, and a reporter T cell assay in seven, five, seven, and eight independent experiments, respectively. HIV-infected individuals on ART with HIV-containing platelets (orange) showed lower CD4⁺ T cell counts (<350/μl) than did those with platelets lacking HIV (gray). Results are shown as boxplots generated separately for positive and negative groups. The Mann-Whitney *U* test was used to compare negative (gray) and positive (orange) groups for each HIV detection technique. (B) PCA of samples from HIV-infected individuals on ART categorized according to the presence (positive, orange) or absence (negative, gray) of HIV in platelets. These data and the clinical characteristics for each HIV-infected individual at the date of sampling are represented as variable vectors (arrows).

during a retrospective and prospective 18-month period before and after sampling (Fig. 4B). These results indicated that the presence of HIV harbored in platelets correlated with immunological failure, which was defined as HIV-infected individuals on ART whose CD4⁺ T cell counts remained <350 cells/μl for more than one year (29).

We found that 80% of the HIV-infected individuals on ART with HIV-containing platelets (Fig. 4C, orange bars) were in immunological failure compared to only 15% of HIV-infected individuals on ART without HIV-containing platelets (Fig. 4C, gray bars). HIV-infected individuals on ART with HIV-containing platelets had a >20-fold higher chance of failing to recover CD4⁺ T cell counts to above 350 cells/μl, compared to those without HIV in their platelets (odds ratio, 22.6; CI, 3.8 to 132.1; *P* = 0.0005). The likelihood of immunological failure for HIV-infected individuals on ART with viral suppression and HIV-containing platelets was higher (odds ratio, 56; CI, 4.3 to 719.2; *P* = 0.002) compared to those who were viremic at the date of sampling or displayed less than 12 months of continuous viral suppression (odds ratio, 6; CI, 0.3 to 101.5; *P* = 0.21) (Table 1 and table S6).

DISCUSSION

We have shown here that platelets from HIV-infected individuals on ART with sustained low CD4⁺ T cell counts harbor replication-competent HIV and do so despite viral suppression below LOD. Our results show that in platelets, HIV is confined to an intracellular compartment analogous to the virus-containing compartments typically formed in HIV-infected myeloid cells *in vitro* (30) and *in vivo* (31, 32). These compartments are functionally distinct from the cell endosomal system, providing a shelter for the virus against the direct action of neutralizing antibodies, cytoplasmic innate immunity sensors, and the late endosomal/lysosomal degradative environment (30). Accordingly, platelets harboring HIV in these privileged compartments could preserve virus integrity throughout their 8- to 10-day life span.

The HIV in platelets that we report could have originated from direct endocytosis of HIV in the circulation of viremic patients by platelets (7, 10). However, the presence of intact, replication-competent virus in platelets from individuals on ART with viral loads below LOD for long periods suggests that platelets may associate with HIV in an active viral replication niche. HIV-infected megakaryocytes that we found in HIV-infected individuals on ART with low CD4⁺ T cell counts potentially could be the source of HIV-containing platelets.

Platelets are short-lived, anuclear blood components lacking the nuclear machinery to meet the recent criteria used to define HIV latent reservoirs (23). These criteria include display of integrated proviral DNA and rebound of virus production upon interruption of ART. Instead, platelets and perhaps other blood cells (33, 34) may participate in HIV transmission and persistence by sheltering the virus from the immune response. The T cell latent reservoir is long-lived and harbors integrated HIV DNA. We suggest that platelets harboring HIV can carry HIV RNA and transport replication-competent virus. Platelets would thus form a transient shelter for HIV in the blood of some HIV-infected individuals on ART and could promote infection by delivering virus to target cells such as macrophages as we have shown here *in vitro*. Furthermore, our study suggests that HIV may associate with platelets during thrombopoiesis in the HIV-infected bone marrow megakaryocytes of HIV-infected individuals virally suppressed by ART with low CD4⁺ T cell counts.

A potential platelet-mediated pathway for viral dissemination during ART may correlate with sustained immunological failure, although the causative nature of this correlation remains to be established. The poor immunological recovery observed in ART-treated

Table 1. HIV-infected individuals selected for retrospective and prospective analysis of immunological status, viremia, and viral suppression. Patients were classified as positive or negative for the presence of HIV in platelets according to at least two different techniques. Only HIV-infected individuals for whom clinical data were available 18 months before the date of sampling were included in the analysis. The period of viral suppression in months before the date of sampling is indicated. Competent immunological status was defined as >350 CD4⁺ T cells/ μ l of blood for two or more consecutive measurements over 1 year including date of sampling for detecting HIV in platelets. Immunological failure was defined as <350 CD4⁺ T cells/ μ l blood for two or more consecutive measurements over 1 year including date of sampling for detecting HIV in platelets. Controlled viremia was defined as <1.60 HIV RNA log₁₀ copies/ml of plasma for at least 1 year before sampling. Uncontrolled viremia was defined as >1.60 HIV RNA log₁₀ copies/ml of plasma at the date of sampling or less than 12 months of continuous viral suppression.

	Individual number	Immunological status	Viremia	Months suppressed before sampling	
Individuals negative for HIV in platelets	39	Competent	Controlled	17	
	32	Competent	Controlled	18	
	75	Competent	Controlled	31	
	54	Competent	Controlled	18	
	52	Competent	Controlled	12	
	11	Competent	Controlled	18	
	51	Competent	Controlled	18	
	16	Competent	Controlled	12	
	15	Competent	Controlled	13	
	61	Competent	Controlled	13	
	66	Competent	Controlled	47	
	67	Competent	Controlled	31	
	4	Competent	Controlled	78	
	56	Competent	Controlled	62	
	53	In failure	Controlled	22	
	59	In failure	Controlled	18	
		Median months under controlled viremia (CI)			18 (15–31)
	Individuals positive for HIV in platelets	7	In failure	Uncontrolled	<12
60		Competent	Uncontrolled	<12	
24		Competent	Uncontrolled	<12	
46		Competent	Uncontrolled	<12	
9		In failure	Controlled	24	
27		In failure	Controlled	38	
48		In failure	Controlled	19	
6		In failure	Controlled	20	
49		In failure	Controlled	50	
64		In failure	Controlled	52	
79		In failure	Controlled	14	
80		In failure	Controlled	62	
37		Competent	Controlled	13	
		Median months under controlled viremia (CI)			24 (14–52)
		74	Competent	Uncontrolled	<12
	25	Competent	Uncontrolled	<12	
	18	In failure	Uncontrolled	<12	
	78	In failure	Uncontrolled	<12	
	40	In failure	Uncontrolled	<12	
	41	In failure	Uncontrolled	<12	

Downloaded from <http://stm.sciencemag.org/> by 20339660 on March 19, 2020

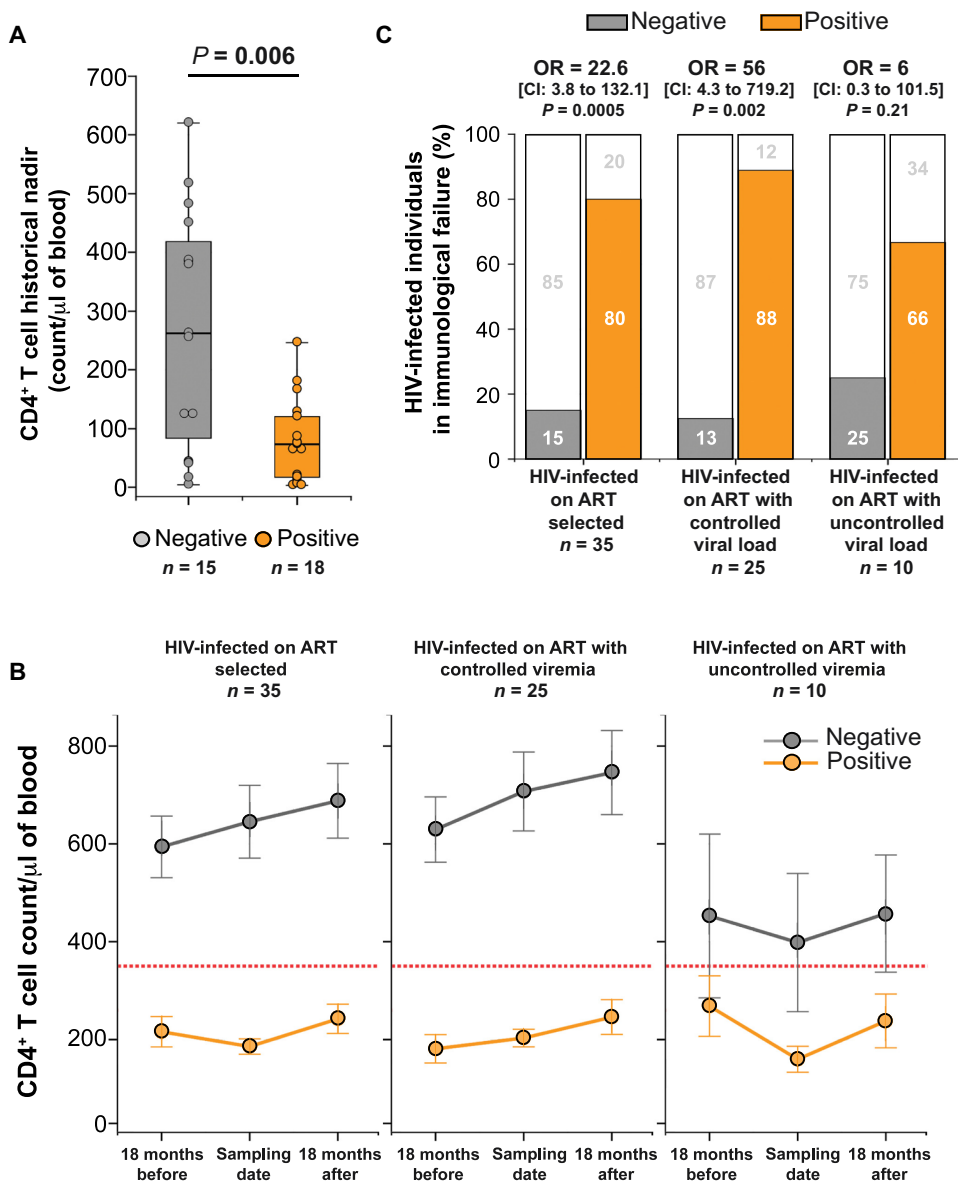


Fig. 4. Platelets containing HIV correlate with poor immunological recovery. (A) CD4⁺ T cell counts (historical nadir) for HIV-infected individuals on ART whose platelets either did (orange, positive) or did not (gray, negative) contain HIV. HIV-infected individuals on ART with HIV-containing platelets had a lower mean CD4⁺ T cell count nadir (<200 cells/μl) compared to the negative group ($P = 0.006$, Mann-Whitney *U* test). The number of individuals (*n*) is shown below the graph. (B) Mean CD4⁺ T cell counts for HIV-infected individuals on ART who were positive (orange line) or negative (gray line) for the presence of HIV in platelets. Data are shown for the time period of 18 months before and 18 months after the date of sampling. Analysis was first performed for a subgroup of 35 HIV-infected individuals on ART who were selected irrespective of viremia (left). This group was then further divided into 25 HIV-infected individuals on ART with controlled viremia (>1 year with viral load consistently below LOD; middle) and 10 HIV-infected individuals on ART with uncontrolled viremia (with a detectable viral load at the date of sampling or less than 12 months of continuous viral suppression; right). Red dotted line indicates a CD4⁺ T cell count threshold of 350 cells/μl. (C) Percentage of HIV-infected individuals on ART in immunological failure (<350 CD4⁺ T cells/μl after at least 1 year of follow-up including the date of sampling) grouped according to the presence (positive, orange) or absence (negative, gray) of HIV in platelets. OR, odds ratio; Fisher's exact test.

HIV-infected individuals may be driven by persistent inflammation associated with T cell immune dysfunction (35–37). Residual inflammation markers in blood, such as d-dimers and interleukin-6

(IL-6) detected in plasma, do not correlate with immunological failure (38) and thus are unlikely to have an impact on the association of HIV with platelets. Inflammation-driven T cell dysfunction could result from the low residual production of HIV by latent reservoirs such as tissue macrophages (31, 39). Further studies are necessary to elucidate the molecular and cellular mechanisms connecting immunological failure to platelets containing HIV.

Twenty percent to 30% of HIV-infected individuals are unable to reconstitute a competent immune system despite adherence to ART and a viral load below LOD (29, 35, 40, 41); no therapeutic strategy is available to improve their immune recovery (41, 42). Systematic clinical studies will be required to demonstrate the potential predictive value of detecting HIV-containing platelets in individuals in immunological failure for the purpose of anticipating appropriate therapeutic interventions. Our results suggest that abciximab, an antiplatelet agent already in clinical use, could block viral dissemination to macrophages by HIV-containing platelets.

Our study has a number of limitations. Further studies are needed to elucidate how HIV shelters in the platelets of HIV-infected individuals on ART despite viral suppression and the association of HIV-containing platelets with CD4⁺ T cell recovery failure. Although our study analyzed samples from 80 HIV-infected individuals on ART, limited sample amounts did not allow testing of every sample with all four techniques we used for detecting HIV in platelets. Samples from a greater number of HIV-infected individuals on ART and longitudinal samples from the same individuals at 1-year intervals should be studied to confirm our results and to establish functional correlations between the presence of HIV in platelets and immunological failure. The finding of HIV virions identified at the ultrastructural level in some platelets needs to be confirmed by directly correlating p24-Gag immunolabeling detected by confocal microscopy with that identified by electron microscopy. Additional immunolabeling experiments will need to be performed to identify the

compartment in platelets in which HIV resides and if it is similar to the HIV compartment in HIV-infected macrophages (31). The activation status of platelets interacting with macrophages during

HIV transfer remains to be determined as well as whether a specific tissue macrophage subset is selectively targeted. To prove our hypothesis that HIV-infected platelets are derived from HIV-infected megakaryocytes, comparative sequencing of HIV *env* V3 will need to be performed on blood T cells, megakaryocytes, and platelets both before ART and after 1 year on ART with consistent blood viral suppression.

In conclusion, our study found that HIV-containing platelets correlated with poor immunological recovery in HIV-infected individuals on ART and suggests a potential alternative pathway for viral dissemination in which platelets act as transient carriers of HIV.

MATERIALS AND METHODS

Study design

Our study investigated whether replication-competent HIV resided within platelets from HIV-infected individuals on ART. The HIV-infected individuals on ART who participated in this study belonged to a large prospective cohort of HIV-infected individuals of at least 15 years of age from the French Hospital Database on HIV created in 1989. These HIV-infected individuals received care at the Ambroise Paré and Raymond Poincaré Hospitals that are among 70 participating centers in the French Hospital Database on HIV. The only enrollment criterion for the French Hospital Database on HIV was documented HIV-1 or HIV-2 infection. Written informed consent was obtained for all study participants, and data submitted by the participating centers were anonymized and encrypted. The French Hospital Database on HIV was approved by the French national institutional ethics committee (Commission Nationale de l'Informatique et des Libertés) on 27 November 1991. Human samples in this study were used in accordance with the World Medical Association Declaration of Helsinki. Ethical authorization for obtaining postmortem bone marrow samples through whole-body donation from uninfected and ART-treated HIV-infected individuals was provided by the State University of New Jersey and The University of Texas Medical Branch, with Institutional Review Board (IRB) authorization numbers of Pro20140000794/Pro2012001303 and 18-0136/18-0134, respectively.

Platelet-rich plasma samples used in this study were obtained during routine blood testing of 80 HIV-infected individuals on ART from the French Hospital Database on HIV, who received care at the Ambroise Paré and Raymond Poincaré Hospitals. The enrollment criterion for these HIV-infected individuals was that ART had been initiated for at least 1 year before the time of blood sampling. Viremia was regularly tested in human plasma samples using the Abbott RealTime HIV-1 assay on an automated m2000 system. This allowed detection of HIV RNA copies per milliliter of plasma with a range of 1.6 log₁₀ copies (40 copies) to 7 log₁₀ copies. Values below the LOD of 1.6 log₁₀ copies/ml were considered to reflect undetectable viremia. Tables S1 and S2 present the following clinical information for study participants: viral load (log₁₀ HIV copies per milliliter of blood), total lymphocyte counts (10⁶/ml of blood), CD4⁺ T cell counts and historical nadir (cells per microliter of blood), and platelet counts (10⁶/ml of blood). Table S5 shows the ART regimens for study participants.

It should be noted that the HIV-infected individuals on ART in our study were seen in a hospital setting and may not be representative of the HIV-infected population seen in local clinics. Therefore, the immunological nonresponders in the HIV-infected cohort

we analyzed may not be representative of immunological failure in the broader HIV-infected population on ART.

Human peripheral blood and platelet-rich plasma samples from healthy HIV-seronegative donors were obtained from the French blood collection center (Paris, France). Platelet-rich plasma from healthy donors was used as a negative control for all experiments and was processed using the same methods as for platelet-rich plasma from HIV-infected individuals.

Platelet-rich plasma collection

Peripheral blood samples were obtained from donors by venipuncture into plastic tubes containing anticoagulant EDTA. Samples were centrifuged for 10 min at 160g and 22°C for blood fractionation, allowing for clear separation of platelet-rich plasma from whole blood. To avoid potential contamination by rare leukocytes, the upper two-thirds of the platelet-rich plasma fraction were carefully collected and transferred to new plastic tubes as recommended for functional analyses (43). Platelet-poor plasma was obtained after centrifugation of platelet-rich plasma at 1100g, 10 min, room temperature, and collection of supernatants.

Platelet-rich plasma fractions were frozen at -80°C until used in the experiments (44). We verified by flow cytometry that (i) viable CD41⁺ platelets represent >70% of total events recorded in platelet-rich plasma, (ii) >90% of CD41⁺ platelets conserved CD42b⁺ membrane staining after thawing, and (iii) thawing does not increase the number of activated platelets characterized by CD62P⁺ immunostaining, with platelet-rich plasma samples displaying 49.2 and 51% of activated platelets (CD41⁺CD62P⁺) before and after thawing, respectively.

Quantitative PCR

qPCR of HIV-1 long terminal repeat (LTR) RNA sequences was performed from platelet pellets obtained after centrifugation of 500 μl of platelet-rich plasma at 1100g, 10 min, at room temperature. Platelet RNA was obtained as described (45) and processed for qPCR TaqMan assay using LTR-specific primer (Vi03453409_s1, Thermo Fisher Scientific Inc.) labeled with a FAM-MGB probe on an Applied Biosystems TaqMan RNA-to-Ct 1-Step Kit protocol (Thermo Fisher Scientific Inc.). RNA from platelet-rich plasma samples was eluted into 15 μl of nuclease-free water, and 5 μl of this eluate was used per qPCR reaction. Platelet-rich plasma RNA samples display an average A260/280 ratio of 1.82 (CI, 1.65 to 2.01), indicating good RNA quality (high quality = ~2 A260/280 ratio according to technical standards). The mean amount of RNA applied per reaction was 63.39 ng (CI, 42.5 to 85.2), which fits into the range of specific detection of the qPCR reagents. Reaction and data acquisition were performed using a LightCycler 480 II (Roche). The number of HIV LTR copies per million platelets was calculated on the basis of platelet-rich plasma platelet counts and qPCR crossing point (Cp) values obtained from a standard curve using a full-length molecular clone of HIV-1 pNL4-3 strain.

Contamination of platelet-rich plasma samples with lymphocytes was assessed by detection of the lymphocyte-specific CD3δ transcript (46) in platelet-rich plasma by qPCR TaqMan assay using CD3δ primer (Hs00174158_m1, Thermo Fisher Scientific Inc.) labeled with FAM-MGB probe on an Applied Biosystems TaqMan RNA-to-Ct 1-Step Kit protocol (Thermo Fisher Scientific Inc.). The number of lymphocytes was calculated on the basis of Cp values obtained from a standard curve using serial dilutions of RNA obtained from known amounts of CD4⁺ T cells.

Flow cytometry after FISH (FISH–flow cytometry)

Paraformaldehyde (4%, v/v, final concentration) was added to 25 μ l of platelet-rich plasma to fix samples, and then platelets were centrifuged at 1100g, 10 min, 22°C, and washed twice in phosphate-buffered saline without $\text{Ca}^{+2}/\text{Mg}^{+2}$. Platelets were then processed for FISH using Cy5-labeled single-molecule FISH probe set for HIV Gag mRNA (HIV-1 vector pNL4-3 GenBank AF324493.2) designed by Stellaris Probe Designer program (<http://www.singlemoleculefish.com>) as we described (47). Probe set is detailed in table S7. Before hybridization, platelets were immunostained with anti-p24 antibody (1:20, KC57 clone, Beckman Coulter Inc.) coupled to fluorescein isothiocyanate (FITC) and anti-CD41/CD61 antibody coupled to phycoerythrin (PE) (1:20, A2A9/6 clone, BioLegend Inc.).

Flow cytometry analyses of platelets processed for FISH (FISH–flow cytometry) were performed under the Guava easyCyte high-throughput system version 6HT2L (Merck Millipore, Merck, KGaA) set to very low flow rate (0.12 μ l/s) and laser gains of 3.5 (GRN-B laser line), 4.3 (YEL-B laser line), and 7.6 (RED-R laser line) in a range of 1 to 1024 units.

The gating strategy to retrieve HIV RNA⁺/p24-Gag⁺ double-positive platelets (fig. S2, A to C) was established in InCyte (Merck Millipore, Merck, KGaA) software consisting in (i) gating the population of single platelets based on forward and side scatter (in log/log scale, forward scatter (FSC) threshold value = 100), (ii) then gating on CD41⁺ events after applying a threshold based on isotype controls, and (iii) calculating CD41⁺ events according to p24 immunostaining and HIV RNA probe hybridization as described (16, 47). Data normalization was performed by subtracting the maximum percentage acquired in $n = 12$ healthy donor samples from the percentages acquired in patient samples per experiment.

FISH–flow cytometry method was also applied as described (17) for detection of HIV RNA⁺/p24-Gag⁺ PBMCs, isolated from blood buffy coats of cART-treated or chronically infected nontreated HIV-infected patients after Ficoll-Hypaque density gradient centrifugation.

Retrospective and prospective analysis of clinical parameters

We categorized ART-treated HIV-infected individuals in two groups according to the presence (positive) or absence (negative) of HIV in platelets. Classification of these individuals as positive or negative was based on similar results obtained in at least two different techniques used for detection of HIV-containing platelets. CD4⁺ T cell historical nadir, age, years since HIV diagnosis, and years since treatment of patients from the positive and negative groups were compared using statistical methods as described below. From this group of patients classified as positive or negative for HIV in platelets, we selected those 35 individuals for which we could collect longitudinal CD4⁺ T cell count and viral load measurements (Table 1). Clinical parameters of these 35 individuals with consistent detection of HIV in platelets were used for retrospective and prospective analyses presented in Fig. 4.

The retrospective and prospective analyses of patient clinical information refer to a period of several months around the date of sampling. When indicated, patients were categorized in controlled viral load group (patients presenting HIV RNA copies per milliliter of plasma always below LOD for at least 1 year before sampling) or noncontrolled viral load group (patients presenting $>1.60 \log_{10}$ copies of HIV RNA per milliliter of plasma at date of sampling or displaying less than 12 months of continuous suppression). Regarding im-

munological status, patients were categorized as immunologically competent when CD4⁺ T cell count was >350 cells/ μ l for two or more consecutive measurements, or in immunological failure when CD4⁺ T cells per microliter was constantly <350 cells/ μ l for all blood sample collected for at least 1 year including the date of sampling for HIV in platelets. We obtained, for each selected patient, a mean CD4⁺ T cell number for counts registered 18 months before sampling (retrospective count) and for 18 months after sampling (prospective count). Figure 4B shows the mean retrospective CD4⁺ T cell count, the mean CD4⁺ T cell count at sampling date, and the mean prospective CD4⁺ T cell count of patients in which CD4⁺ T cell count was surveyed.

Statistical analysis

In all HIV detection assays performed, blood and platelet-rich plasma samples were stratified into two groups (positive or negative) according to the presence or absence of HIV in platelets. Median numbers of HIV-containing platelets per milliliter of blood were calculated exclusively from samples of the positive group. Results are expressed as median, followed by the 95% CI. Boxplots represent median (central line in the box) with 25th and 75th percentiles (box edges) and with minimum/maximum values (upper and lower whiskers).

All statistical analyses were performed using IBM SPSS Statistics software (IBM). Pairwise comparisons of normal distributions were performed using a Student's *t* test. Pairwise and multiple comparisons of non-normal distributions were performed using the non-parametric tests Mann-Whitney *U* and Kruskal-Wallis, respectively. Clinical characteristics of HIV-infected individuals at the date of sampling were examined by multivariate analysis using PCA, a data reduction technique that simultaneously quantifies categorical variables while reducing the dimensionality of the data. Results are presented as a two-dimensional PCA plot (biplot), a graphical display that illustrates the relationships among the components, original variables, and observations (48). Clinical information obtained at the date of sampling was normalized to remove bias from the analysis. In the biplot, clinical characteristics are shown as variable vectors (component loading). Samples (objects in the biplot) were labeled according to experimental detection (positive) or lack of detection (negative) of HIV in platelets.

Repetition of parameter values from clinical histories due to multiple samplings (e.g., CD4⁺ T cell nadir) did not interfere with the PCA performed, because random selection of one sample per HIV-infected individual before running the PCA did not change the results. Multinomial logistic regression was performed using detection of HIV in platelets as a dependent variable and clinical parameters at the date of sampling as covariates but excluding CD4⁺ T cell historical nadir due to collinearity with CD4⁺ T cell counts (Pearson's coefficient = 0.635, $P < 0.001$). Fisher's exact test was used for odds ratio and risk estimates. $P < 0.05$ was considered significant.

SUPPLEMENTARY MATERIALS

stm.sciencemag.org/cgi/content/full/12/535/eaat6263/DC1

Material and Methods

Fig. S1. Platelet-rich plasma preparations from HIV-infected individuals were not contaminated by HIV-infected CD4⁺ T cells.

Fig. S2. Flow cytometry gating strategy for the detection of HIV in platelets from HIV-infected individuals on ART.

Fig. S3. HIV-containing platelets detected by electron and confocal microscopy.

Fig. S4. Infection of macrophages by HIV in platelets is due to direct interactions and not residual cell-free viruses present in platelet-rich plasma.

Fig. S5. HIV-1 integrated proviral DNA in megakaryocytes from HIV-infected individuals on ART with viral suppression.

Fig. S6. Deep sequencing and phylogenetic analysis of HIV *env* V3 segments before and after viral suppression in the same HIV-infected individuals on ART.

Fig. S7. Interaction between platelets and macrophages is blocked by the anti-integrin α IIb/3 Fab abciximab.

Fig. S8. Detection of HIV-containing platelets does not correlate with other clinical characteristics.

Table S1. Clinical information on HIV-infected individuals on ART analyzed for HIV in platelets.

Table S2. Clinical information on each HIV-infected individual on ART analyzed for HIV in platelets.

Table S3. Available viral load measurements for HIV-infected individuals on ART positive for HIV in platelets and with a viral load below the LOD at the date of sampling.

Table S4. Clinical information for each HIV-infected individual on ART analyzed for HIV in megakaryocytes.

Table S5. ART regimens for HIV-infected individuals classified as positive or negative for the presence of HIV in platelets.

Table S6. CD4⁺ T cell counts and viral load measurements for HIV-infected individuals on ART with controlled viremia and positive for HIV in platelets.

Table S7. List of Gag mRNA probe sequences used for FISH–flow cytometry.

Data file S1. Individual-level data for Figs. 1, 2, and 4 and figs. S1, S4, and S7.

Movie S1. Laser scanning confocal microscopy image of an HIV-containing platelet being engulfed by a macrophage.

References (49–68)

[View/request a protocol for this paper from Bio-protocol.](#)

REFERENCES AND NOTES

- J. W. Semple, J. E. Italiano Jr., J. Freedman, Platelets and the immune continuum. *Nat. Rev. Immunol.* **11**, 264–274 (2011).
- O. Garraud, F. Cognasse, Are platelets cells? And if yes, are they immune cells? *Front. Immunol.* **6**, 70 (2015).
- A. Assinger, Platelets and infection - an emerging role of platelets in viral infection. *Front. Immunol.* **5**, 649 (2014).
- J. R. Ariede, M. I. Pardini, G. F. Silva, R. M. Grotto, Platelets can be a biological compartment for the hepatitis C virus. *Braz. J. Microbiol.* **46**, 627–629 (2015).
- S. Boukour, J. M. Massé, L. Bénit, A. Dubart-Kupferschmitt, E. M. Cramer, Lentivirus degradation and DC-SIGN expression by human platelets and megakaryocytes. *J. Thromb. Haemost.* **4**, 426–435 (2006).
- A. Chabert, H. Hamzeh-Cognasse, B. Pozzetto, F. Cognasse, M. Schattner, R. M. Gomez, O. Garraud, Human platelets and their capacity of binding viruses: Meaning and challenges? *BMC Immunol.* **16**, 26 (2015).
- C. Chaipan, E. J. Soilleux, P. Simpson, H. Hofmann, T. Gramberg, A. Marzi, M. Geier, E. A. Stewart, J. Eisemann, A. Steinkasserer, K. Suzuki-Inoue, G. L. Fuller, A. C. Pearce, S. P. Watson, J. A. Hoxie, F. Baribaud, S. Pöhlmann, DC-SIGN and CLEC-2 mediate human immunodeficiency virus type 1 capture by platelets. *J. Virol.* **80**, 8951–8960 (2006).
- C. Flaujac, S. Boukour, E. Cramer-Bordé, Platelets and viruses: An ambivalent relationship. *Cell. Mol. Life Sci.* **67**, 545–556 (2010).
- A. Y. Simon, M. R. Sutherland, E. L. Prydzial, Dengue virus binding and replication by platelets. *Blood* **126**, 378–385 (2015).
- T. Yousefian, A. Drouin, J. M. Masse, J. Guichard, E. M. Cramer, Host defense role of platelets: Engulfment of HIV and *Staphylococcus aureus* occurs in a specific subcellular compartment and is enhanced by platelet activation. *Blood* **99**, 4021–4029 (2002).
- D. Zucker-Franklin, S. Seremetis, Z. Y. Zheng, Internalization of human immunodeficiency virus type I and other retroviruses by megakaryocytes and platelets. *Blood* **75**, 1920–1923 (1990).
- T. H. Lee, R. R. Stromberg, J. W. Heitman, L. Sawyer, C. V. Hanson, M. P. Busch, Distribution of HIV type 1 (HIV-1) in blood components: Detection and significance of high levels of HIV-1 associated with platelets. *Transfusion* **38**, 580–588 (1998).
- T. H. Lee, R. R. Stromberg, D. Henrard, M. P. Busch, Effect of platelet-associated virus on assays of HIV-1 in plasma. *Science* **262**, 1585–1586 (1993).
- D. Zucker-Franklin, Y. Z. Cao, Megakaryocytes of human immunodeficiency virus-infected individuals express viral RNA. *Proc. Natl. Acad. Sci. U.S.A.* **86**, 5595–5599 (1989).
- S. G. Deeks, S. R. Lewin, A. L. Ross, J. Ananworanich, M. Benkirane, P. Cannon, N. Chomont, D. Douek, J. D. Lifson, Y.-R. Lo, D. Kuritzkes, D. Margolis, J. Mellors, D. Persaud, J. D. Tucker, F. Barre-Sinoussi, International AIDS Society Towards a Cure Working Group, G. Alter, J. Auerbach, B. Autran, D. H. Barouch, G. Behrens, M. Cavazzana, Z. Chen, É. A. Cohen, G. M. Corbelli, S. Eholié, N. Eyal, S. Fidler, L. Garcia, C. Grossman, G. Henderson, T. J. Henrich, R. Jefferys, H.-P. Kiem, J. M. Cune, K. Moodley, P. A. Newman, M. Nijhuis, M. S. Nsubuga, M. Ott, S. Palmer, D. Richman, A. Saez-Cirion, M. Sharp, J. Siliciano, G. Silvestri, J. Singh, B. Spire, J. Taylor, M. Tolstrup, S. Valente, J. van Lunzen, R. Walensky, I. Wilson, J. Zack, International AIDS society global scientific strategy: Towards an HIV cure 2016. *Nat. Med.* **22**, 839–850 (2016).
- A. E. Baxter, J. Niessl, R. Fromentin, J. Richard, F. Porichis, M. Massanella, N. Brassard, N. Alshafiq, J. P. Routy, A. Finzi, N. Chomont, D. E. Kaufmann, Multiparametric characterization of rare HIV-infected cells using an RNA-flow FISH technique. *Nat. Protoc.* **12**, 2029–2049 (2017).
- A. E. Baxter, J. Niessl, R. Fromentin, J. Richard, F. Porichis, R. Charlebois, M. Massanella, N. Brassard, N. Alshafiq, G. G. Delgado, J. P. Routy, B. D. Walker, A. Finzi, N. Chomont, D. E. Kaufmann, Single-cell characterization of viral translation-competent reservoirs in HIV-infected individuals. *Cell Host Microbe* **20**, 368–380 (2016).
- J. Grau-Exposito, C. Serra-Peinado, L. Miguel, J. Navarro, A. Curran, J. Burgos, I. Ocaña, E. Ribera, A. Torrella, B. Planas, R. Badía, J. Castellví, V. Falcó, M. Crespo, M. J. Buzon, A novel single-cell fish-flow assay identifies effector memory CD4⁺ T cells as a major niche for HIV-1 transcription in HIV-infected patients. *MBio* **8**, e00876-17 (2017).
- C. Hess, T. Klimkait, L. Schlapbach, V. Del Zenero, S. Sadallah, E. Horakova, G. Balestra, V. Werder, C. Schaefer, M. Battegay, J. A. Schifferli, Association of a pool of HIV-1 with erythrocytes in vivo: A cohort study. *Lancet* **359**, 2230–2234 (2002).
- A. Sanyal, R. B. Mailliard, C. R. Rinaldo, D. Ratner, M. Ding, Y. Chen, J. M. Zerbato, N. S. Giacobbi, N. J. Venkatachari, B. K. Patterson, A. Chargin, N. Sluis-Cremer, P. Gupta, Novel assay reveals a large, inducible, replication-competent HIV-1 reservoir in resting CD4⁺ T cells. *Nat. Med.* **23**, 885–889 (2017).
- N. T. Sebastian, T. D. Zaikos, V. Terry, F. Taschuk, L. A. McNamara, A. Onafuwa-Nuga, R. Yucha, R. A. J. Signer, J. Riddell IV, D. Bixby, N. Markowitz, S. J. Morrison, K. L. Collins, CD4 is expressed on a heterogeneous subset of hematopoietic progenitors, which persistently harbor CXCR4 and CCR5-tropic HIV proviral genomes in vivo. *PLOS Pathog.* **13**, e1006509 (2017).
- J. B. Dinosa, S. Y. Kim, A. M. Wiegand, S. E. Palmer, S. J. Gange, L. Cranmer, A. O'Shea, M. Callender, A. Spivak, T. Brennan, M. F. Kearney, M. A. Proschan, J. M. Mican, C. A. Rehm, J. M. Coffin, J. W. Mellors, R. F. Siliciano, F. Maldarelli, Treatment intensification does not reduce residual HIV-1 viremia in patients on highly active antiretroviral therapy. *Proc. Natl. Acad. Sci. U.S.A.* **106**, 9403–9408 (2009).
- E. Eisele, R. F. Siliciano, Redefining the viral reservoirs that prevent HIV-1 eradication. *Immunity* **37**, 377–388 (2012).
- P. J. Ballem, A. Belzberg, D. V. Devine, D. Lyster, B. Spruston, H. Chambers, P. Doubroff, K. Mikulash, Kinetic studies of the mechanism of thrombocytopenia in patients with human immunodeficiency virus infection. *N. Engl. J. Med.* **327**, 1779–1784 (1992).
- J. E. Italiano Jr., J. Hartwig, Production and destruction of platelets, in *The Non-Thrombotic Role of Platelets in Health and Disease*, S. W. Kerrigan, Ed. (IntechOpen, 2015).
- R. Grozovsky, S. Giannini, H. Falet, K. M. Hoffmeister, Molecular mechanisms regulating platelet clearance and thrombopoietin production. *ISBT Sci. Ser.* **10**, 309–316 (2015).
- R. Grozovsky, K. M. Hoffmeister, H. Falet, Novel clearance mechanisms of platelets. *Curr. Opin. Hematol.* **17**, 585–589 (2010).
- R. D'Amico, Y. Yang, D. Mildvan, S. R. Evans, C. T. Schnitzlein-Bick, R. Hafner, N. Webb, M. Basar, R. Zackin, M. A. Jacobson, Lower CD4⁺ T lymphocyte nadirs may indicate limited immune reconstitution in HIV-1 infected individuals on potent antiretroviral therapy: Analysis of immunophenotypic marker results of AACTG 5067. *J. Clin. Immunol.* **25**, 106–115 (2005).
- C. F. Kelley, C. M. Kitchen, P. W. Hunt, B. Rodriguez, F. M. Hecht, M. Kitahata, H. M. Crane, J. Willig, M. Mugavero, M. Saag, J. N. Martin, S. G. Deeks, Incomplete peripheral CD4⁺ cell count restoration in HIV-infected patients receiving long-term antiretroviral treatment. *Clin. Infect. Dis.* **48**, 787–794 (2009).
- V. Rodrigues, N. Ruffin, M. San-Roman, P. Benaroch, Myeloid cell interaction with HIV: A complex relationship. *Front. Immunol.* **8**, 1698 (2017).
- Y. Ganor, F. Real, A. Sennepin, C. A. Dutertre, L. Prevedel, L. Xu, D. Tudor, B. Charmeteau, A. Couedel-Courteille, S. Marion, A. R. Zenak, J. P. Jourdain, Z. Zhou, A. Schmitt, C. Capron, E. A. Eugenin, R. Cheynier, M. Revol, S. Cristofari, A. Hosmalin, M. Bomsel, HIV-1 reservoirs in urethral macrophages of patients under suppressive antiretroviral therapy. *Nat. Microbiol.* **4**, 633–644 (2019).
- J. M. Orenstein, Replication of HIV-1 in vivo and in vitro. *Ultrastruct. Pathol.* **31**, 151–167 (2007).
- W. He, S. Neil, H. Kulkarni, E. Wright, B. K. Agan, V. C. Marconi, M. J. Dolan, R. A. Weiss, S. K. Ahuja, Duffy antigen receptor for chemokines mediates trans-infection of HIV-1 from red blood cells to target cells and affects HIV-AIDS susceptibility. *Cell Host Microbe* **4**, 52–62 (2008).
- H. Kulkarni, V. C. Marconi, W. He, M. L. Landrum, J. F. Okulicz, J. Delmar, D. Kazandjian, J. Castiblanco, S. S. Ahuja, E. J. Wright, R. A. Weiss, R. A. Clark, M. J. Dolan, S. K. Ahuja, The Duffy-null state is associated with a survival advantage in leukopenic HIV-infected persons of African ancestry. *Blood* **114**, 2783–2792 (2009).
- G. Cenderello, A. De Maria, Discordant responses to cART in HIV-1 patients in the era of high potency antiretroviral drugs: Clinical evaluation, classification, management prospects. *Expert Rev. Anti-Infect. Ther.* **14**, 29–40 (2016).

36. S. G. Deeks, HIV infection, inflammation, immunosenescence, and aging. *Annu. Rev. Med.* **62**, 141–155 (2011).
37. W. Lu, V. Mehraj, K. Vyboh, W. Cao, T. Li, J. P. Routy, CD4:CD8 ratio as a frontier marker for clinical outcome, immune dysfunction and viral reservoir size in virologically suppressed HIV-positive patients. *J. Int. AIDS Soc.* **18**, 20052 (2015).
38. M. M. Lederman, L. Calabrese, N. T. Funderburg, B. Clagett, K. Medvik, H. Bonilla, B. Gripshover, R. A. Salata, A. Taege, M. Lisgaris, G. A. McComsey, E. Kirchner, J. Baum, C. Shive, R. Asaad, R. C. Kalayjian, S. F. Sieg, B. Rodriguez, Immunologic failure despite suppressive antiretroviral therapy is related to activation and turnover of memory CD4 cells. *J. Infect. Dis.* **204**, 1217–1226 (2011).
39. J. B. Honeycutt, W. O. Thayer, C. E. Baker, R. M. Ribeiro, S. M. Lada, Y. Cao, R. A. Cleary, M. G. Hudgens, D. D. Richman, J. V. Garcia, HIV persistence in tissue macrophages of humanized myeloid-only mice during antiretroviral therapy. *Nat. Med.* **23**, 638–643 (2017).
40. G. R. Kaufmann, L. Perrin, G. Pantaleo, M. Opravil, H. Furrer, A. Telenti, B. Hirschel, B. Ledergerber, P. Vernazza, E. Bernasconi, M. Rickenbach, M. Egger, M. Battegay; Swiss HIV Cohort Study Group, CD4 T-lymphocyte recovery in individuals with advanced HIV-1 infection receiving potent antiretroviral therapy for 4 years: The Swiss HIV cohort study. *Arch. Intern. Med.* **163**, 2187–2195 (2003).
41. M. Marziali, W. De Santis, R. Carello, W. Leti, A. Esposito, A. Isgrò, C. Fimiani, M. C. Sirianni, I. Mezzaroma, F. Aiuti, T-cell homeostasis alteration in HIV-1 infected subjects with low CD4 T-cell count despite undetectable virus load during HAART. *AIDS* **20**, 2033–2041 (2006).
42. W. H. V. Carvalho-Silva, J. L. Andrade-Santos, F. O. Souto, A. V. C. Coelho, S. Crovella, R. L. Guimarães, Immunological recovery failure in cART-treated HIV-positive patients is associated with reduced thymic output and RTE CD4+ T cell death by pyroptosis. *J. Leukoc. Biol.* **107**, 85–94 (2020).
43. P. Harrison, I. Mackie, A. Mumford, C. Briggs, R. Liesner, M. Winter, S. Machin; British Committee for Standards in Haematology, Guidelines for the laboratory investigation of heritable disorders of platelet function. *Br. J. Haematol.* **155**, 30–44 (2011).
44. Y. Kajikawa, T. Morihara, H. Sakamoto, K. Matsuda, Y. Oshima, A. Yoshida, M. Nagae, Y. Arai, M. Kawata, T. Kubo, Platelet-rich plasma enhances the initial mobilization of circulation-derived cells for tendon healing. *J. Cell. Physiol.* **215**, 837–845 (2008).
45. S. Amisten, A rapid and efficient platelet purification protocol for platelet gene expression studies. *Methods Mol. Biol.* **788**, 155–172 (2012).
46. C. Palmer, M. Diehn, A. A. Alizadeh, P. O. Brown, Cell-type specific gene expression profiles of leukocytes in human peripheral blood. *BMC Genomics* **7**, 115 (2006).
47. R. Arrigucci, Y. Bushkin, F. Radford, K. Lakehal, P. Vir, R. Pine, D. Martin, J. Sugarman, Y. Zhao, G. S. Yap, A. A. Lardizabal, S. Tyagi, M. L. Gennaro, FISH-flow, a protocol for the concurrent detection of mRNA and protein in single cells using fluorescence in situ hybridization and flow cytometry. *Nat. Protoc.* **12**, 1245–1260 (2017).
48. K. R. Gabriel, C. L. Odoroff, Biplots in biomedical research. *Stat. Med.* **9**, 469–485 (1990).
49. K. Tenner-Racz, P. Rácz, M. Dietrich, P. Kern, Altered follicular dendritic cells and virus-like particles in AIDS and AIDS-related lymphadenopathy. *Lancet* **1**, 105–106 (1985).
50. K. Tenner-Racz, P. Rácz, M. Bofill, A. Schulz-Meyer, M. Dietrich, P. Kern, J. Weber, A. J. Pinching, F. Veronese-Dimarzo, M. Popovic, D. Klatzmann, J. C. Gluckman, G. Janossy, HTLV-III/LAV viral antigens in lymph nodes of homosexual men with persistent generalized lymphadenopathy and AIDS. *Am. J. Pathol.* **123**, 9–15 (1986).
51. A. Le Tourneau, J. Audouin, J. Diebold, C. Marche, V. Tricottet, M. Reynes, LAV-like viral particles in lymph node germinal centers in patients with the persistent lymphadenopathy syndrome and the acquired immunodeficiency syndrome-related complex: An ultrastructural study of 30 cases. *Hum. Pathol.* **17**, 1047–1053 (1986).
52. C. J. O'Hara, J. E. Groopman, M. Federman, The ultrastructural and immunohistochemical demonstration of viral particles in lymph nodes from human immunodeficiency virus-related and non-human immunodeficiency virus-related lymphadenopathy syndromes. *Hum. Pathol.* **19**, 545–549 (1988).
53. A. Morner, A. Björndal, J. Albert, V. N. Kewalramani, D. R. Littman, R. Inoue, R. Thorstensson, E. M. Fenyö, E. Björling, Primary human immunodeficiency virus type 2 (HIV-2) isolates, like HIV-1 isolates, frequently useCCR5 but show promiscuity in coreceptor usage. *J. Virol.* **73**, 2343–2349 (1999).
54. A. M. Janas, L. Wu, HIV-1 interactions with cells: From viral binding to cell-cell transmission. *Curr. Protoc. Cell Biol.* **Chapter 26**, Unit 26.5 (2009).
55. M. K. Liszewski, J. J. Yu, U. O'Doherty, Detecting HIV-1 integration by repetitive-sampling Alu-gag PCR. *Methods* **47**, 254–260 (2009).
56. W. De Spiegelaere, E. Malatinkova, L. Lynch, F. Van Nieuwerburgh, P. Messiaen, U. O'Doherty, L. Vandekerckhove, Quantification of integrated HIV DNA by repetitive-sampling Alu-HIV PCR on the basis of poisson statistics. *Clin. Chem.* **60**, 886–895 (2014).
57. J. J. Yu, T. L. Wu, M. K. Liszewski, J. Dai, W. J. Swiggard, C. Baytop, I. Frank, B. L. Levine, W. Yang, T. Theodosopoulos, U. O'Doherty, A more precise HIV integration assay designed to detect small differences finds lower levels of integrated DNA in HAART treated patients. *Virology* **379**, 78–86 (2008).
58. C. Deleage, S. W. Wietgreffe, G. Del Prete, D. R. Morcock, X. P. Hao, M. Piatak Jr., J. Bess, J. L. Anderson, K. E. Perkey, C. Reilly, J. M. McCune, A. T. Haase, J. D. Lifson, T. W. Schacker, J. D. Estes, Defining HIV and SIV reservoirs in lymphoid tissues. *Pathog. Immun.* **1**, 68–106 (2016).
59. F. Real, A. Sennepin, Y. Ganor, A. Schmitt, M. Bomsel, Live imaging of HIV-1 transfer across T cell virological synapse to epithelial cells that promotes stromal macrophage infection. *Cell Rep.* **23**, 1794–1805 (2018).
60. L. Prevedel, N. Ruel, P. Castellano, C. Smith, S. Malik, C. Villeux, M. Bomsel, S. Morgello, E. A. Eugenin, Identification, localization, and quantification of HIV reservoirs using microscopy. *Curr. Protoc. Cell Biol.* **82**, e64 (2019).
61. V. Henn, J. R. Slupsky, M. Gräfe, I. Anagnostopoulos, R. Förster, G. Müller-Berghaus, R. A. Kroccek, CD40 ligand on activated platelets triggers an inflammatory reaction of endothelial cells. *Nature* **391**, 591–594 (1998).
62. S. Raymond, N. Jeanne, F. Nicot, C. Lefebvre, R. Carcenac, L. Minier, J. Chiabrando, M. Cazabat, P. Delobel, J. Izopet, Long-term evolution of transmitted CXCR4-using HIV-1 under effective antiretroviral therapy. *AIDS* **33**, 1977–1985 (2019).
63. N. Jeanne, A. Saliou, R. Carcenac, C. Lefebvre, M. Dubois, M. Cazabat, F. Nicot, C. Loiseau, S. Raymond, J. Izopet, P. Delobel, Position-specific automated processing of V3 env ultra-deep pyrosequencing data for predicting HIV-1 tropism. *Sci. Rep.* **5**, 16944 (2015).
64. R. C. Edgar, MUSCLE: Multiple sequence alignment with high accuracy and high throughput. *Nucleic Acids Res.* **32**, 1792–1797 (2004).
65. S. Capella-Gutiérrez, J. M. Silla-Martínez, T. Gabaldón, trimAl: A tool for automated alignment trimming in large-scale phylogenetic analyses. *Bioinformatics* **25**, 1972–1973 (2009).
66. S. Guindon, O. Gascuel, A simple, fast, and accurate algorithm to estimate large phylogenies by maximum likelihood. *Syst. Biol.* **52**, 696–704 (2003).
67. D. Darriba, G. L. Taboada, R. Doallo, D. Posada, jModelTest 2: More models, new heuristics and parallel computing. *Nat. Methods* **9**, 772 (2012).
68. I. Letunic, P. Bork, Interactive tree of life (ITOL) v4: Recent updates and new developments. *Nucleic Acids Res.* **47**, W256–W259 (2019).

Acknowledgments: We thank the HIV-infected individuals who participated in this study, V. Boeva from Institut Cochin for advice on multivariate analysis, and A. Schmitt for help with electron microscopy. **Funding:** This work was supported by Agence Nationale de Recherches sur le Sida et les Hépatites Virales (ANRS #AQ2015-2-17046) and SIDACTION (#15CONV03) to M.B. F.R. is the recipient of a postdoctoral fellowship from SIDACTION and ANRS. L.X. and A.Z. received doctoral fellowships from the Chinese Science Council, and A.S. is an ANRS postdoctoral fellow. **Author contributions:** F.R., E.C.B., and M.B. conceived the experiments. C.C., S.G., E.R., and E.C.B. collected the patient samples and provided clinical information. F.R., C.C., and M.B. performed flow cytometry and confocal microscopy. F.R., G.S., and J.Z. performed reporter T cell assays. F.R., A.S., A.Z., and L.X. performed qPCR experiments. F.R., C.C., J.-M.M., and M.B. performed electron microscopy. F.R., R.A., M.L.G., and M.B. set up FISH and flow cytometry assays. F.R., M.B., E.E., and M.D. designed and performed in situ hybridization experiments on megakaryocytes and platelets in vitro. M.C., P.D., and J.I. performed deep sequencing and phylogenetic analyses of HIV env gene V3 segments. F.R., S.G., E.R., E.C.B., and M.B. performed retrospective and prospective analysis of the clinical status of HIV-infected individuals. F.R., E.C.B., and M.B. wrote the manuscript. **Competing interests:** The authors declare that they have no competing interests. **Data and materials availability:** All data associated with this study are in the paper or the Supplementary Materials. HIV env V3 sequences have been deposited in GenBank with accession numbers MN453286, MN453287, MN453288, MN453288, MN453289, MN453290, MN453291, MN453292, MN453293, MN453294, and MN453295.

Submitted 20 March 2018
Resubmitted 23 July 2019
Accepted 1 October 2019
Published 18 March 2020
10.1126/scitranslmed.aat6263

Citation: F. Real, C. Capron, A. Sennepin, R. Arrigucci, A. Zhu, G. Sannier, J. Zheng, L. Xu, J.-M. Massé, S. Greffe, M. Cazabat, M. Donoso, P. Delobel, J. Izopet, E. Eugenin, M. L. Gennaro, E. Rouveix, E. Cramer Bordé, M. Bomsel, Platelets from HIV-infected individuals on antiretroviral drug therapy with poor CD4⁺ T cell recovery can harbor replication-competent HIV despite viral suppression. *Sci. Transl. Med.* **12**, eaat6263 (2020).

Platelets from HIV-infected individuals on antiretroviral drug therapy with poor CD4⁺ T cell recovery can harbor replication-competent HIV despite viral suppression

Fernando Real, Claude Capron, Alexis Sennepin, Riccardo Arrigucci, Aiwei Zhu, G r my Sannier, Jonathan Zheng, Lin Xu, Jean-Marc Mass , S gol ne Greffe, Michelle Cazabat, Maribel Donoso, Pierre Delobel, Jacques Izopet, Eliseo Eugenin, Maria Laura Gennaro, Elisabeth Rouveix, Elisabeth Cramer Bord  and Morgane Bomsel

Sci Transl Med 12, eaat6263.
DOI: 10.1126/scitranslmed.aat6263

Hidden in plain sight

Human platelets carry out several immune functions as well as hemostasis and interact with infectious pathogens including HIV in vitro. Real *et al.* now report that platelets from HIV-infected individuals can harbor replication-competent HIV, despite successful viral suppression by antiretroviral drug therapy (ART). Moreover, in their study, >80% of virally suppressed HIV-infected individuals with platelets containing HIV showed poor restoration of immune status even 1 year after ART treatment initiation. Platelets carrying HIV may provide an alternative pathway for HIV dissemination in HIV-infected individuals on ART with viral suppression and poor CD4⁺ T cell recovery.

ARTICLE TOOLS

<http://stm.sciencemag.org/content/12/535/eaat6263>

SUPPLEMENTARY MATERIALS

<http://stm.sciencemag.org/content/suppl/2020/03/16/12.535.eaat6263.DC1>

RELATED CONTENT

<http://stm.sciencemag.org/content/scitransmed/12/533/eaav3491.full>
<http://stm.sciencemag.org/content/scitransmed/11/509/eaax3447.full>
<http://stm.sciencemag.org/content/scitransmed/11/499/eaap8758.full>
<http://stm.sciencemag.org/content/scitransmed/11/504/eaav5685.full>

REFERENCES

This article cites 67 articles, 11 of which you can access for free
<http://stm.sciencemag.org/content/12/535/eaat6263#BIBL>

PERMISSIONS

<http://www.sciencemag.org/help/reprints-and-permissions>

Use of this article is subject to the [Terms of Service](#)

Science Translational Medicine (ISSN 1946-6242) is published by the American Association for the Advancement of Science, 1200 New York Avenue NW, Washington, DC 20005. The title *Science Translational Medicine* is a registered trademark of AAAS.

Copyright   2020 The Authors, some rights reserved; exclusive licensee American Association for the Advancement of Science. No claim to original U.S. Government Works

SUPPLEMENTARY MATERIAL

Flow cytometry of p24-Gag immunostained platelets

HIV-containing platelets were detected by single p24(Gag) immunostaining in a qualitative approach as described below. After fixation of 25 μ l of PRP in 4% paraformaldehyde, samples were incubated for 15 minutes, 22°C, in PBS containing 2% bovine serum albumin (BSA) fraction V (Euromedex, Strasbourg, France) and 0.25% saponin (Sigma-Aldrich Co. LLC.) (blocking/permeabilizing solution), in the presence of Fc Receptor Blocking solution 1:20 v/v (Human TruStain FcX, Biolegend, Inc.). Next, platelets were resuspended in a blocking/permeabilizing solution containing anti-p24 antibody (1:20 v/v, KC57 clone, Beckman Coulter Inc.) coupled to FITC and anti-CD41 antibody coupled to APC (1:20 v/v, HIP8 clone, reactive to the α_{IIb} region of CD41, Biolegend, Inc.), and incubated for 30 minutes at 4°C. Platelets were then washed three times and proceeded to flow cytometry. The same staining protocol was applied for detection of PRP lymphocyte contaminants, using anti-CD45-FITC and anti-CD4-PE antibodies (1:20 v/v each, Beckman Coulter Inc.).

Flow cytometry analyzes of platelets were performed under the Guava easyCyte high-throughput system version 6HT2L set to a very low flow rate (0.12 μ l/s) and laser gains of 18.2 (GRN-B laser line) and 29.3 (RED-R laser line) in a range of 1 to 1024 units.

Immunostained platelets were submitted to flow cytometry analysis under the gating strategy shown in Figure S2A-B and D established in the InCyte software which consists in: i) gating the population of platelets, discarding smaller cell debris and doublets, based on forward and side-scatter (in log/log scale, FSC threshold value=100); ii) gating on CD41⁺ events after applying a threshold based on the fluorescence intensity of PRP samples treated with isotype controls; and iii) gating on CD41⁺/ p24-Gag⁺, setting up a threshold of p24-Gag⁺ events based on fluorescence intensity of p24-Gag in PRP samples from n=20 healthy donors. A fluorescence index was calculated by multiplying percentage by mean fluorescence intensity (MFI) of gated CD41⁺ p24-Gag⁺ events [% x MFI]. Results are expressed as the ratio between the

fluorescence index obtained in HIV-infected patient platelet samples and the maximum fluorescence index obtained using healthy donor platelet samples per experiment ($\text{HIV}^{\text{pos}}[\% \times \text{MFI}] : \text{maximum HIV}^{\text{neg}} [\% \times \text{MFI}]$). Ratio above 1 correspond to patients' samples that contain platelets sheltering HIV.

Laser Scanning Confocal Microscopy

Glass coverslips containing platelet-macrophage cocultures were washed six times to remove fixative and incubated 10 minutes at 22°C, with an autofluorescence quenching solution composed of 75 mM of NH_4Cl and 50 mM glycine in PBS. Next, samples were treated with the blocking/permeabilizing solution for 15 minutes, 22°C, before incubation overnight, at 4°C, with the blocking/permeabilizing solution containing mouse (IgG1) anti-HIV-1 p24-Gag monoclonal antibodies EVA365 and 366 combined (1:1 v/v each, The National Institute for Biological Standards and Control, UK). Secondary immunostaining was performed using anti-mouse IgG-Cy3 (1:100 Jackson ImmunoResearch Inc.) in the blocking/permeabilizing solution for 2 hours, 22°C. Next, samples were treated with rabbit polyclonal anti-CD41 antibodies (5, 10) (1:100 v/v, kindly provided by Dr Michael Berndt (Pahran, Victoria, Australia)) for 2 hours and revealed by an anti-rabbit-FITC antibody (1:100 v/v, Jackson ImmunoResearch Inc.) in the blocking/permeabilizing solution. Nuclei were then stained with 5 $\mu\text{g}/\text{ml}$ 4',6-diamidino-2-phenylindole (DAPI, Sigma-Aldrich Co. LLC.). The same immunostaining protocol was applied to isolated platelets seeded into Poly-L-lysine-coated plates (μ -Slide 18 well, ibidi GmbH), fixed after 15 minutes of adhesion (37°C).

Laser scanning confocal microscopy was performed in a Leica DMI6000 inverted microscope (Leica Microsystems, Wetzlar, Germany) coupled to Melles GRIOT (Idex Corp.) and Cobolt (Cobolt AB, Sweden) lasers, Yokogawa CSU-X1M1 spinning disk head (Yokogawa Electric, Tokyo, Japan), and a CoolSnap HQ² Firewire camera (Photometrics). Images were acquired using a 100 \times objective (N.A.: 1.4). Metamorph 7.7.5 software (Molecular Devices, LLC.) and Imaris software version 8.4.1 (Bitplane AG, Andor Technology) were used for image acquisition and image processing, respectively.

Three-dimensional reconstructions of HIV-containing platelets interacting with macrophages were performed by image segmentation (Imaris Measurement Pro 8.3, Isosurface tools) and visualized by Imaris 3D View mode. Images were also projected in three-dimensions (xy, xz and yz projections) visualized by Imaris Section View mode.

The detection of HIV-containing platelets was performed by image fluorescence thresholding as follows: i) the confocal unit provides images which fluorescence intensity that can be numerically interpreted as arbitrary units per pixel (AU/pixel). The maximum AU/pixel for p24-Gag fluorescence channel acquired within healthy donor platelets was established per experiment as the threshold above which specific p24 signal is detected.

Electron Microscopy

For electron microscopy, platelets were fixed in 1.5% v/v glutaraldehyde solution prior to processing for Epon embedding for standard electron microscopy or alternatively, for cryo-sectioning followed by immunogold p24-Gag labeling using a pool of three monoclonal antibodies against the core protein p24-Gag HIV-1 a generous gift from Dr H. R. Gelderblom (Berlin, Germany), as we previously described (5, 10). Image acquisition was performed at the Electron Microscopy Platform of the Cochin Institute, and at least 20 fields were observed per platelet sample (n=3 independent samples from different individuals). The virions observed in platelets display a remarkable ultrastructure variability (Figure 1D and Figure S3C), as expected from virions detected in ART-treated, virally suppressed HIV-infected human samples, which size ranges from 60 to 120 nm with an electron dense core ranging from 10 to 60 nm (32, 49-51). The p24-Gag immunolabeling method for detection of HIV capsid protein fully validates the detection of HIV by these morphological criteria (Figure 1E and Figure S3D), although at expense of ultrastructural resolution as described (32, 52)

Coculture of macrophages and platelets

Tissue-like macrophages were obtained from peripheral blood mononuclear cells (PBMC) of healthy donors, isolated from buffy coats after Ficoll-Hypaque density gradient centrifugation. CD14⁺ cells from PBMC were obtained by negative selection (STEMCELL Technologies Inc.), seeded at 5×10^5 cells/well in 12-well plates (Corning) or in 24-well plates with 14mm glass coverslips (Menzel-Glaser, Thermo Fisher Scientific, Inc.), and incubated for 6 days at 37°C 5% CO₂ in macrophage complete medium composed of RPMI supplemented with 10% fetal bovine serum (FBS), 2 mM L-glutamine (Gibco, Thermo Fisher Scientific Inc.), 15 mM HEPES (Euromedex, Strasbourg, France), 100 U/ml of penicillin, 100 µg/ml streptomycin (Gibco, Thermo Fisher Scientific Inc.) and macrophage-colony stimulating factor (M-CSF, 25ng/ml, R&D Systems, Inc.). IL-4 and IL-13 (20ng/ml each, R&D Systems, Inc.) were added for 48 hours at day 4 of the incubation period. The tissue-like macrophages obtained are CD68⁺CD14^{low}CD206^{low}IL4-R⁺CD163^{neg}IL1-R^{neg} as assessed by flow cytometry immunophenotyping.

Next, platelets were added directly from the PRP into tissue-like macrophage cultures at a multiplicity of 50 platelets per macrophage. In some experiments, platelets were treated with 10µg/ml of abciximab (Reopro, Janssen-Cilag B.V., Netherlands) for 15 minutes, 37°C, before being added to macrophage cultures. Abciximab was detected on the surface of treated platelets by incubation of anti-human IgG-APC (1:20, Jackson ImmunoResearch Inc.) and analyzed by flow cytometry (Figure S7B). Macrophages cultivated with cell-free R5-tropic HIV-1 (primary isolate 93BR029, NIH Reagents program, US) for 2 hours, in the presence or absence of 10µg/ml of abciximab, were used as positive control for macrophage infection. Abciximab does not interact directly with the virus itself, enclosed into platelet and lacking α_{IIb}/β_3 integrin expression and thus does not interfere in HIV infection of macrophages (Figure S7D).

When using 24-well plates with coverslips, platelets and macrophages were allowed to interact for 2 hours, free platelets were washed out and cells were fixed and processed for confocal microscopy. When using 12-well plates, platelets and macrophages were allowed to interact overnight at 37°C, free platelets

were washed out, macrophage complete medium was replenished, and macrophages were then incubated for additional 7 days for supernatants collection and DNA purification.

Quantification of infectious viruses using GFP-reporter cell assays

Indicator reporter cell assays have been widely used to quantify HIV infectivity with high sensitivity (20) and have provided an estimation of how many infectious particles our platelet preparations contained. Ghost(3)X4/R5 GFP-reporter cells were obtained through the NIH AIDS Reagent Program (53). GFP-reporter cells were seeded in microscopy chamber slides (μ -Slide 8 Well, ibidi, GmbH) at 10^5 cells per well and incubated overnight at 37°C in DMEM, 10% FBS, 2 mM L-glutamine, 15 mM HEPES, 100 U/ml of penicillin, 100 μ g/ml streptomycin (complete medium). Platelet-rich (PRP) or Platelet-poor plasma, tissue-macrophage supernatants or known amounts of cell-free HIV-1 (HIV-1 primary isolate 93BR029, NIH Reagents program, US) (50 μ l/well) were added to GFP-indicator cells complemented with medium supplemented with 20 μ g/ml polybrene in a total volume of 100 μ l/well. After 2 hours at 37°C to favor contact of HIV with indicator cells, 200 μ l/well of complete medium were added and cells were re-cultured overnight, 37°C, washed with PBS to remove non-adhered platelets and re-incubated for additional 24 hours for detectable GFP expression. To improve detection of green fluorescence protein (GFP) expressed by GFP-reporter cells, samples were fixed and treated with blocking/permeabilizing solution for 15 minutes, 22°C, incubated overnight at 4°C with 5 μ g/ml of goat anti-GFP antibody (Abcam plc.) and for 1 hour, 22°C, with anti-goat Cy3 secondary antibody (1:200, Jackson ImmunoResearch Inc.), both antibodies diluted in blocking/permeabilizing solution. GFP-reporter cell nuclei were also stained with DAPI for 15 minutes 22°C before proceed to GFP-reporter cell blind count under epifluorescence microscope.

The following criteria were employed to assess the presence of infectious virus in GFP-reporter cell assays: GFP⁺ reporter cells were scored in the entire cultivation well and the number of GFP⁺ cell nuclei was counted. The counting per well were subtracted by the maximum number of GFP⁺ cells nuclei counted in the negative controls. Using this technique, infectious HIV was detected at viral concentrations as low as 0.1 pg

HIV-1 p24 per 30 μ l sample test corresponding to 3.3 pg/ml p24 using standard curves obtained from blind count of GFP⁺ reporter cells, performed by two different investigators. Infectious units were calculated from GFP-reporter cell assay as previously described (54).

Quantification of HIV DNA integration

Seven days after interaction with HIV-containing platelets, tissue-like macrophage cultures were dried out and stored at -80°C until DNA purification. Tissue-like macrophage DNA was purified using the QIAamp DNA Micro Kit (Qiagen, Les Ulis, France) following manufacturer's instructions. The nested Alu-gag PCR followed by qPCR of the R and U5 regions of HIV long terminal repeat DNA sequences were performed as we and others described earlier (31, 55), allowing for the detection of integrated copies of the virus into tissue-like macrophage genome. The first PCR was performed in a PTC-100 thermocycler (Bio-Rad, Marnes-la-Coquette, France) and the second in a LightCycler 480 II (Roche). The number of HIV integrated copies per 10⁶ tissue-like macrophage was assessed by a standard curve correlating the number of integrated copies found in serial dilutions of HIV-1 infected U937 (U1) cells (known to display 2 integrated copies per cell) and the amount of genomic DNA retrieved by β -globin amplification and quantification.

Bone marrow samples were obtained from femur aspiration after 30 minutes to 6 hours post-mortem. Aspirated cells were maintained in MarrowMax Bone marrow medium (Thermo Fisher Scientific Inc.) until processed for isolation of megakaryocytes (MK) using a CD61-targeted positive selection (MicroBeads, Miltenyi Biotec) following manufacturer's special cell separation protocol for megakaryocytes. Megakaryocytes were processed for Alu-gag PCR and the number of HIV DNA copies per million megakaryocytes (with confidence intervals) was quantified by Poisson statistics as described (55-57). HIV-1 infected OM-10 cells (known to display a single integrated proviral copy of HIV) were used for standard curve determination and positive control.

Morphological detection of HIV DNA/RNA by in situ hybridization

Megakaryocyte infection was evaluated by morphological analysis of bone marrow smears after *in situ* hybridization of HIV DNA or RNA probes using the DNA/RNAscope® Technology (Advanced Cell Diagnostics, Inc.) as we and others described earlier (58, 59) following manufacturer's instructions. Specificity of the HIV DNA or HIV RNA hybridization probes was evaluated by applying the same technique to U1 cells used as positive control and bone marrow from non-infected donors serving as negative control. Megakaryocyte smears were finally counterstained with DAPI prior mounting and observation with the confocal microscopy system described above, allowing megakaryocyte identification by their polylobular nucleus. HIV DNA/RNA probe hybridization was detected by the chromogenic reagent Fast Red, observed by epifluorescence microscopy in the red fluorescence acquisition channel. HIV nef mRNA *in situ* hybridization coupled to p24 detection in platelets was performed as we described (31, 60) using CD154 as platelet marker (61). Platelet purity was 99%, as quantified by DAPI staining.

MiSeq deep sequencing of the HIV-1 V3 env region and phylogenetic analyses

Fresh blood was obtained from ART-treated patients and used to prepare PBMCs and platelets as described above. Plasma from the same patient prior to suppression had been stored at -80°C. Plasma, PBMCs and platelet samples were prepared for sequencing on the Illumina MiSeq as we previously described (62). This method is accredited (ISO 15189 norm). Briefly, the first PCR and the nested PCR resulted in a 406-nucleotide long fragment encompassing the V3 env region. The amplified PCR products were purified using Agencourt Ampure PCR Purification beads (Beckman Coulter, Brea, CA) and quantified using a Quant-iT Picogreen dsDNA Assay Kit (Invitrogen) on a LightCycler 480 (Roche Diagnostics, Meylan, France). PCR amplicons were combined and diluted to obtain a concentration of 30 ng/μL and the Nextera XT DNA Library Preparation kit was used for index amplification. Only sequences with an average phred equivalent quality score of >Q30 were retained.

Miseq gave 5660 reads for plasma, 4135 reads for PBMC, and 5633 reads for platelets. The sequence reads were aligned with the BaL consensus sequence (GenBank accession no. AY426110.1) and processed using an in-house automated data cleaning strategy (63). Non-functional V3 sequences were discarded using biological filters and statistical filters were used to discard sequences with artifactual point mutations. This biological and statistical data cleaning strategy is an integral part of Pyrovir software (PyroVir, IDDN FR. 001.160011.000. S.P.2012.000.31230, Inserm-Transfert) that provides a fast, automated position-specific process for inferring HIV-1 tropism from V3 *env* deep sequencing data with improved detection of minor variants. The threshold for detecting X4 variants is indicated as a function of the number of reads of V3 for each sample. Prediction of correceptor usage combines the 11/25 and net charge rule and are specific for the virus subtype, here HIV-1 subtype B.

A phylogenetic tree was generated as follows: after sequence alignment using MUSCLE software (64) and removal of poorly aligned regions with trimA1 software (65), Maximum-likelihood phylogeny was performed by PhyML software (66) using the HKY85 model with an estimated gamma shape parameter (HKY+G) nucleotide substitution model, inferred by jModeltest2 software (67). 1000 bootstraps were performed to estimate tree topology and the tree was visualized and annotated by iTOL software (68).

SUPPLEMENTARY FIGURES AND TABLES

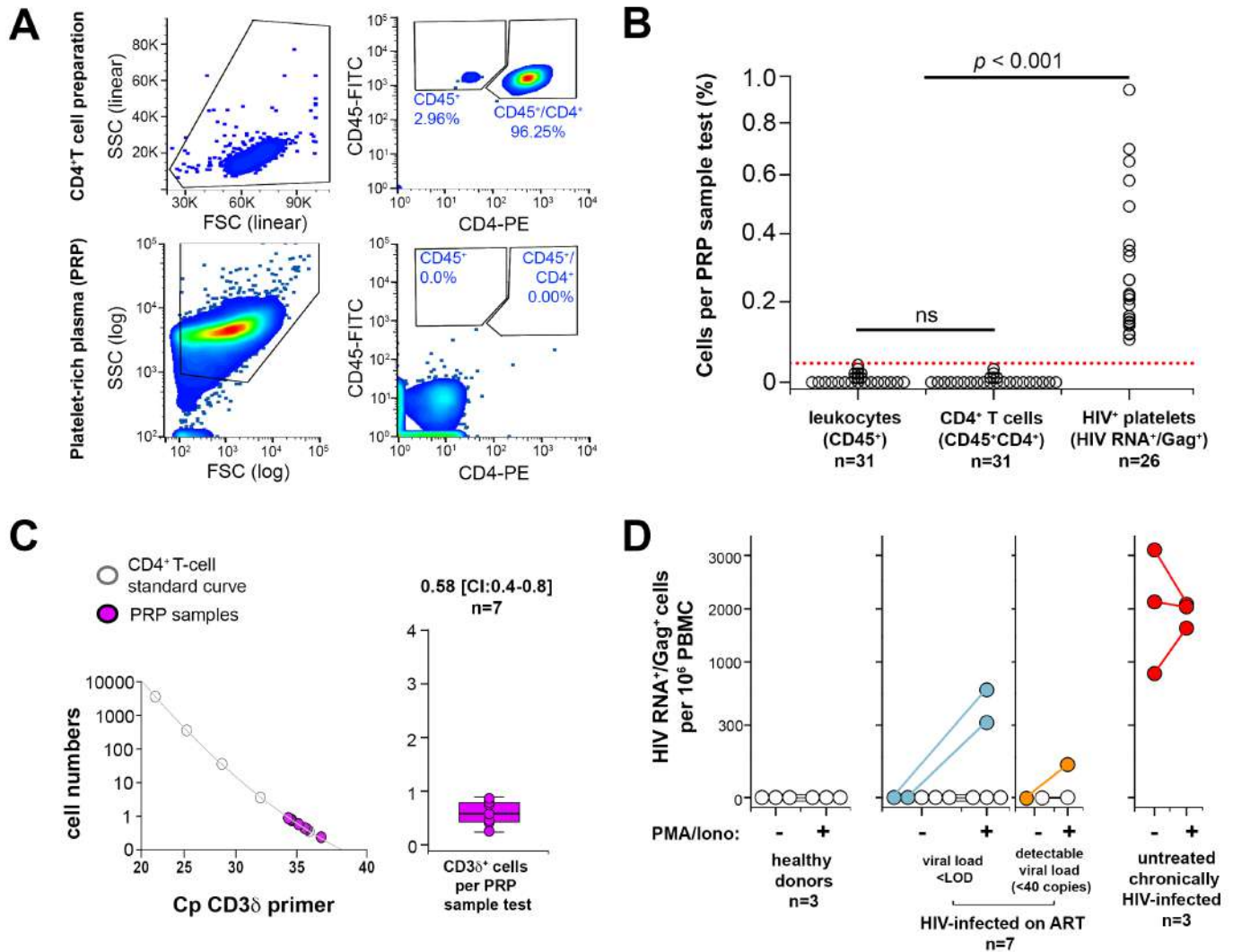


Figure S1: Platelet-rich plasma (PRP) preparations from HIV-infected individuals are not contaminated by HIV-infected CD4⁺ T-cells.

(A) Gating strategy for primary CD4⁺ T cell (positive control, upper row, first gated on leukocyte population based on size) and PRP preparation from HIV-infected patient (lower row, first gated on the whole population based on size) immunostained with CD45-FITC and CD4-PE. Representative plots are shown.

(B) Gated percentages of leukocytes (CD45⁺ events) and CD4⁺ T-cells (CD45⁺CD4⁺ events) among total events recorded in PRP preparations as compared to gated percentages of HIV⁺ platelets detected by FISH-flow (HIV RNA⁺/Gag⁺ events). Dotted red line indicate the threshold for contaminant leukocytes in PRP. The potential contamination of PRP by CD4⁺ T cells appears in the range of 0.01% of recorded events (median

0.0, [CI:0.0-0.01]). Kruskal-Wallis statistical test was used to calculate p values. ns=non-significant with $p>0.05$. n=number of different individuals tested; N=3 independent experiments. (C) Low-level contamination of PRP samples with lymphocytes assessed by qPCR using CD3 δ primer. Left graph: PCR amplification Cp values obtained from a standard curve using serial dilutions of RNA obtained from known amounts of CD4⁺ T cells (grey circles) and Cp values obtained from PRP samples tested (magenta circles). Right graph: Cp values were obtained from PRP samples tested and the median number of lymphocytes per PRP sample test 0.58 [CI:0.4-0.8] was calculated based on the standard curve and presented as a boxplot. n=number of different individuals tested; N=3 independent experiments. (D) HIV RNA fluorescence *in situ* hybridization combined with p24-Gag immunofluorescence detected by flow cytometry (FISH-flow) of PBMC obtained from healthy donors, HIV-infected ART-treated patients and non-treated patients chronically infected with HIV used as positive control. PBMC were stimulated or not with 50 ng/ml phorbol myristate acetate and 0.5 μ g/ml Ionomycin (PMA/Iono) for 12 hours at 37°C 5% CO₂ environment before FISH-flow procedure. n=number of different individuals tested; N=3 independent experiments.

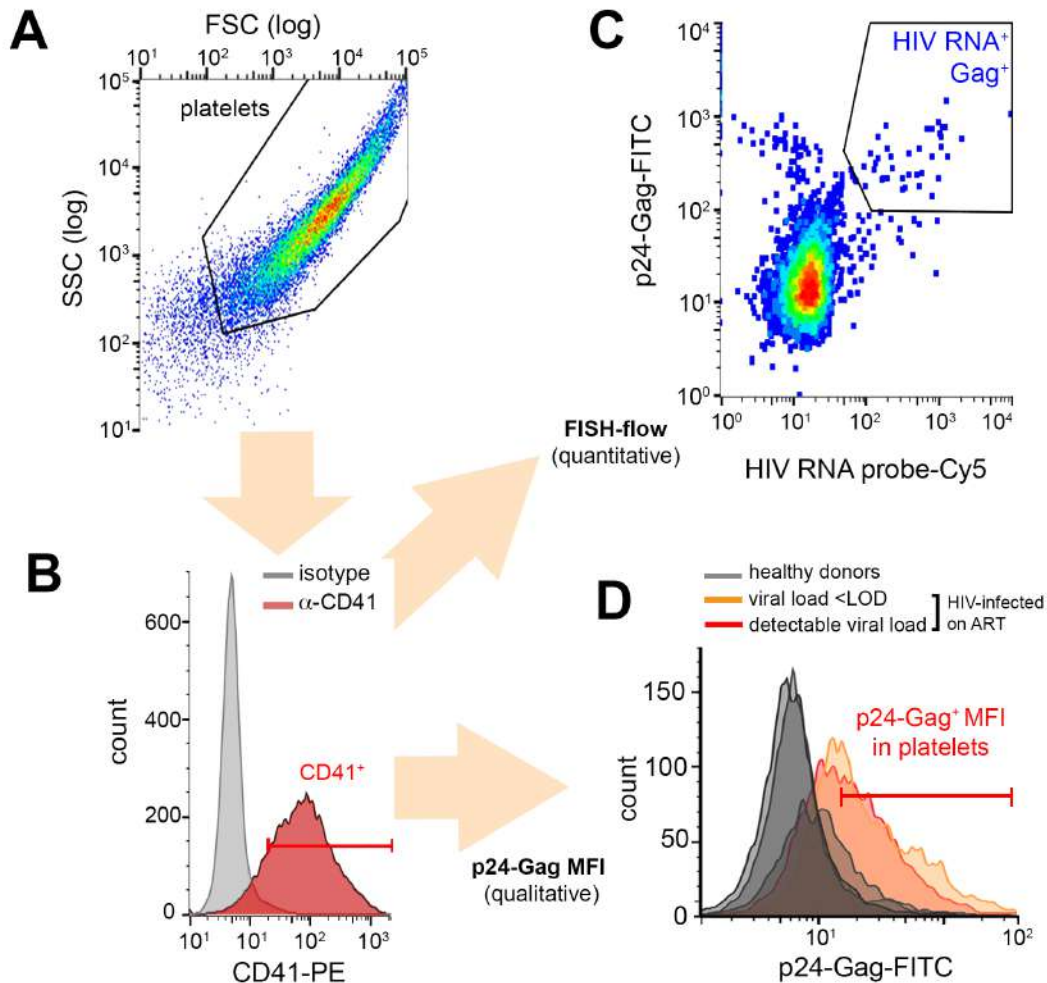


Figure S2: Flow cytometry gating strategy for the detection of HIV in platelets from HIV-infected ART-treated individuals.

Gating strategy for the detection of CD41⁺p24-Gag⁺ platelets in PRP samples: (A) events were gated according to forward and side scatter parameters set to log/log scale; (B) events were then gated according to the presence of the platelet-specific marker CD41 (red histogram); the threshold for CD41⁺ events was defined based on the fluorescence intensity of PRP samples treated with isotype control (grey histogram). C-D) Finally, CD41⁺ events were gated (dot plot, C) according to HIV RNA probe combined with p24-Gag fluorescence in FISH-Flow experiments for combined detection of p24-Gag and HIV RNA. HIV-containing platelets were assessed quantitatively in terms of percentage of gated HIV RNA⁺ p24-Gag⁺ events in a population of CD41⁺ events; or (histograms, D) according to the mean fluorescence intensity (MFI) of anti-p24-Gag mAbs in single p24 immunodetection experiments. Association of HIV with platelets was assessed

qualitatively by measuring p24-Gag MFI of CD41⁺ p24-Gag⁺ gated events. Image is representative of tested samples from 3 different healthy donor samples (gray histograms) and HIV-infected ART-treated patients with undetectable (below limit of detection [$<LOD$], orange histogram) or detected (red histogram) viral load. A fluorescence intensity index was calculated as described in methods session.

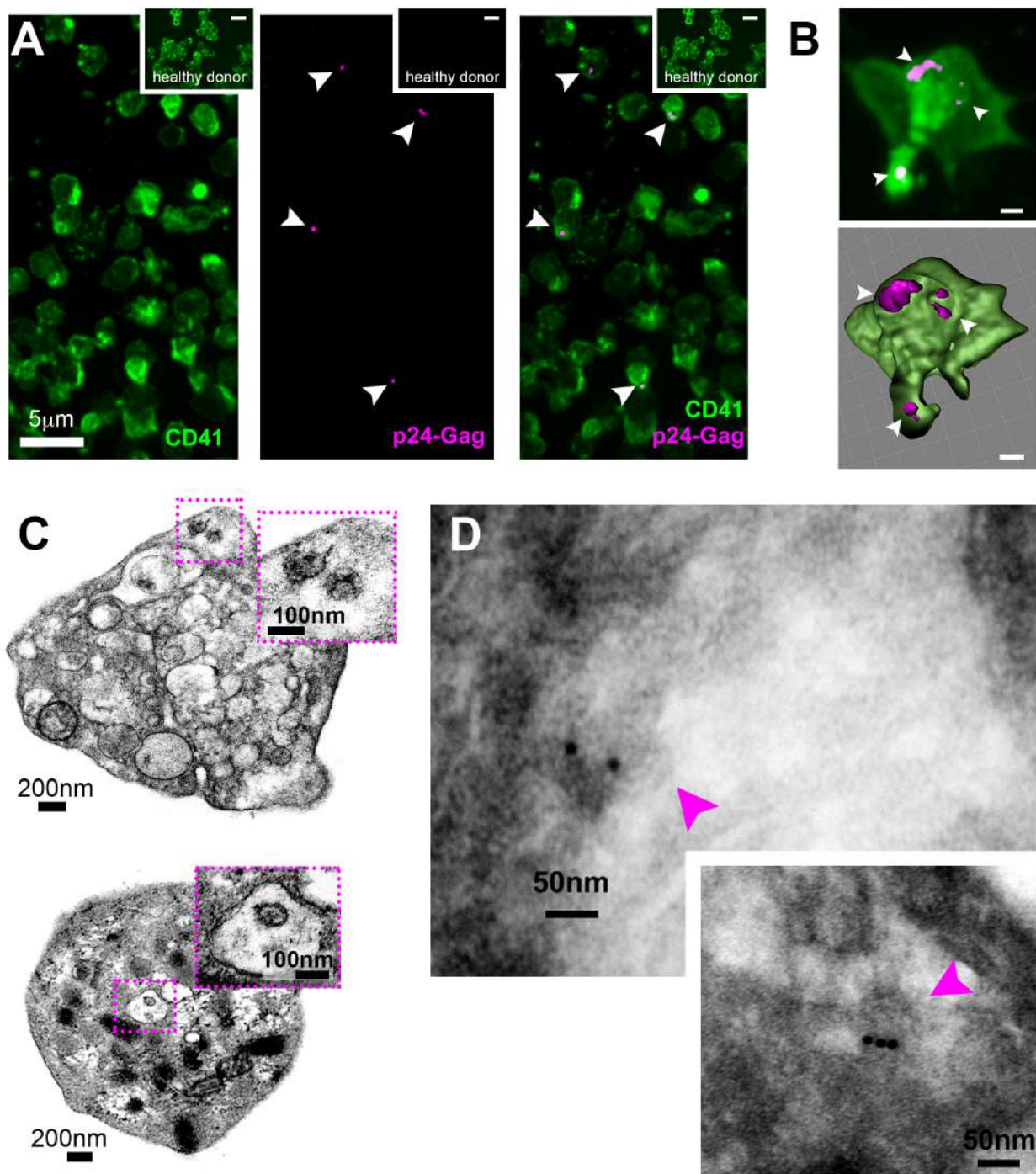


Figure S3: HIV-containing platelets detected by electron and confocal microscopy.

(A) Platelets from HIV-infected ART-treated patient immunostained for CD41 (green) and p24-Gag (magenta), and observed by confocal microscopy. Arrowheads indicate HIV-containing platelets. Healthy donor platelets were used as negative controls (insets). Bar=5 μ m. (B) High-magnification image of HIV-containing platelet immunostained for CD41 and p24-Gag with three-dimensional reconstructions (lower

image) highlights viruses (magenta, arrowheads) contained within platelet (green). Bar= 1 μm . (C) Ultrastructure of HIV contained in platelets from 2 different ART-treated patients: Round-shaped structures ranging from 70-120 nm and an electron-dense core ranging from 20-60 nm are the two main morphological criteria for detection of virus-like particles indicated by dotted magenta box (inset: higher magnification). (D) Presence of HIV within platelets (magenta arrowheads, p24⁺ virions around 100 nm of size) detected by p24-immunogol labeling images in cryosections of HIV-containing platelets from 3 different HIV-infected ART-treated patients.

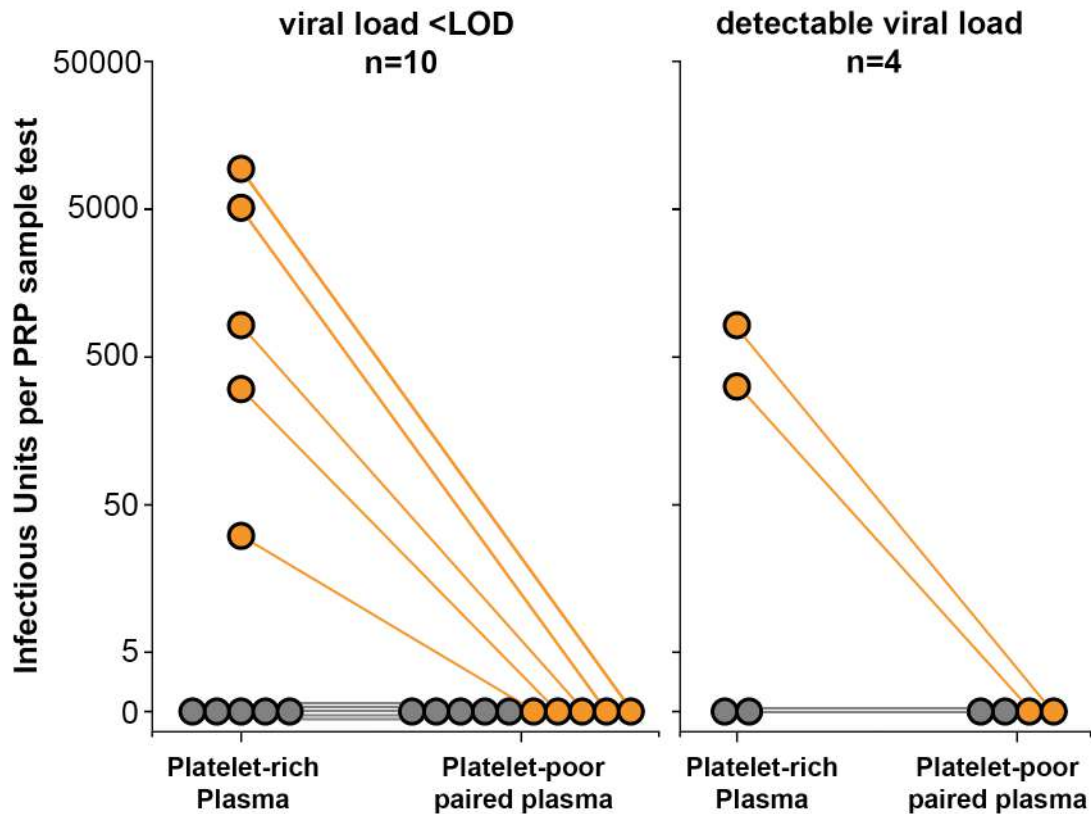


Figure S4: Infection of macrophages by HIV contained in platelets is due to direct interaction between macrophages and platelets and not to residual cell-free viruses present in PRP.

Infectious HIV units could not be detected in plasma depleted in platelets. Platelet-poor plasma was obtained after centrifugation of Platelet-rich plasma (PRP) and collection of the supernatant fraction. Infectious HIV units in PRP from ART-treated patients with undetectable (<LOD) and detectable viral load were quantified by indicator cell assays comparing pairwise full PRP and Platelet-poor plasma. Orange dots indicate samples positive for detection of infectious units in PRP, whereas grey dots indicate samples negative in the test.

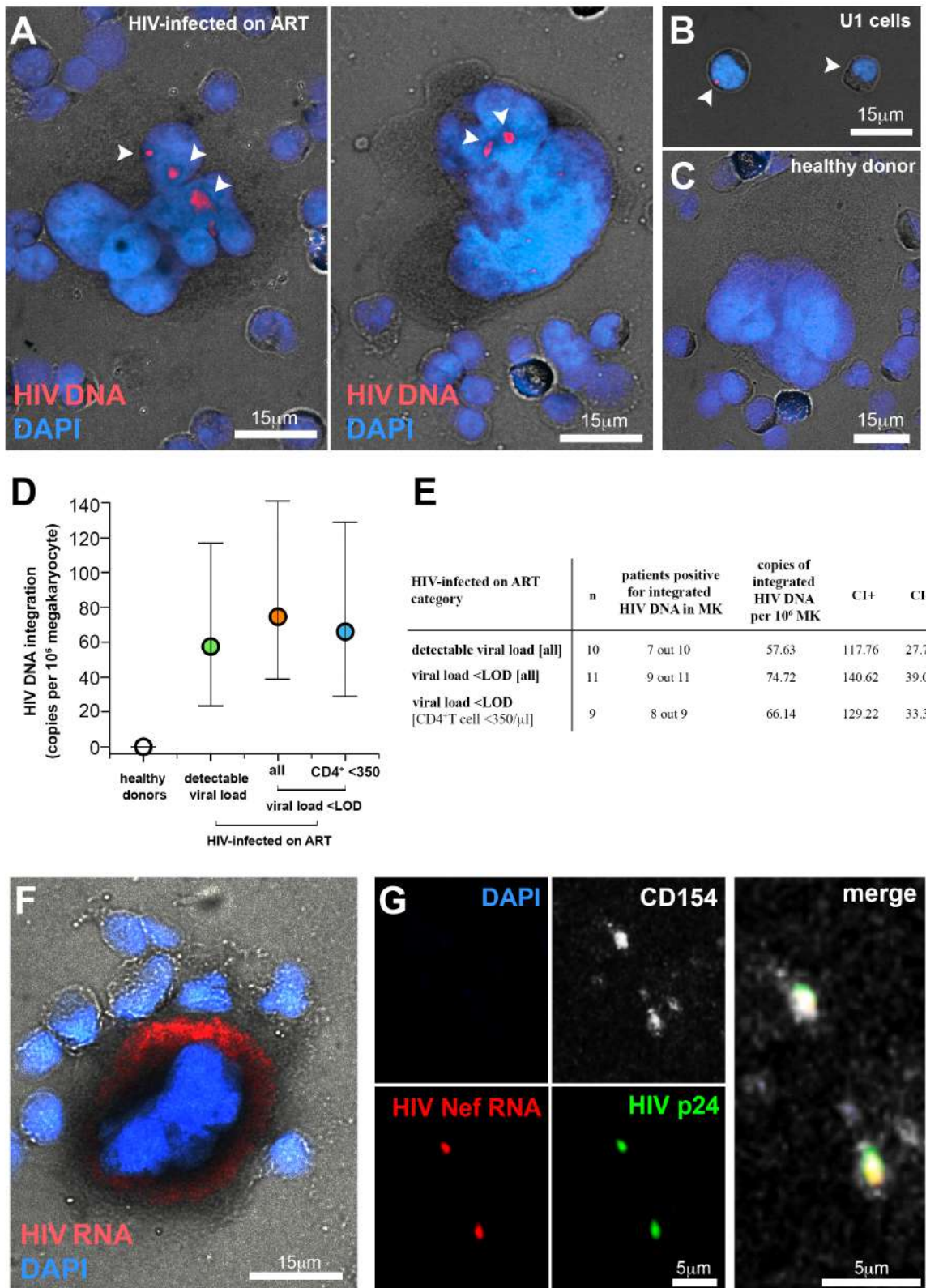


Figure S5: Megakaryocytes (MK) are infected by HIV in HIV-infected individuals on ART with viral suppression. (A) MK from bone marrow smears of a ART-treated patient harboring integrated HIV revealed by Fast Red chromogenic reaction fluorescence (white arrows) colocalized in megakaryocyte nuclei upon

assessment by DNA/RNAscope® Technology (Advanced Cell Diagnostics, Inc.). Megakaryocytes are identified by their specific polylobular nucleus labeled in blue with DAPI (B-C) Specificity of the hybridization using probes for HIV DNA was evaluated by applying the same technique to U1 cells constitutively expressing integrated HIV DNA (B, positive control) and bone marrow from non-infected donor (C, negative control). (D) Number of HIV DNA copies per million megakaryocytes (estimated number with confidence intervals) assessed by Alu-gag PCR and quantified by Poisson statistics as described in Method section, using cell-sorted populations of MK from healthy donors (n=13) and ART-treated patients (n=21). Among the ART-treated patients, data were categorized according to detectable viremia (green dot, n=10, with 7 out of 10 patients positive for integrated HIV DNA in megakaryocytes) and undetectable (<LOD) viremia (orange dot, n=11, with 9 out of 11 patients positive for integrated HIV DNA in megakaryocytes). A subcategory of patients with undetectable viremia and low CD4+ T-cell count (<350 cells/ μ l) is also shown by blue dot. (E) Summary of the results shown in D. n=number of different individuals tested; N=3 independent experiments. (F) Detection of cell-associated HIV RNA in MK from bone marrow smears of the same ART-treated patient shown in (A) by DNA/RNAscope® Technology as above. (G) Fluorescence *in situ* hybridization of HIV RNA (nef, in red) coupled to HIV p24 (Gag, in green) protein in platelets from one of the individual positive for integrated HIV DNA in MK shown in (D). Platelets were detected by CD154 marker (in white). DAPI staining (blue) was performed to rule out any contamination with nucleated cells in the preparation. An image showing merged fluorescent channels indicated colocalization of HIV RNA and proteins within platelets.

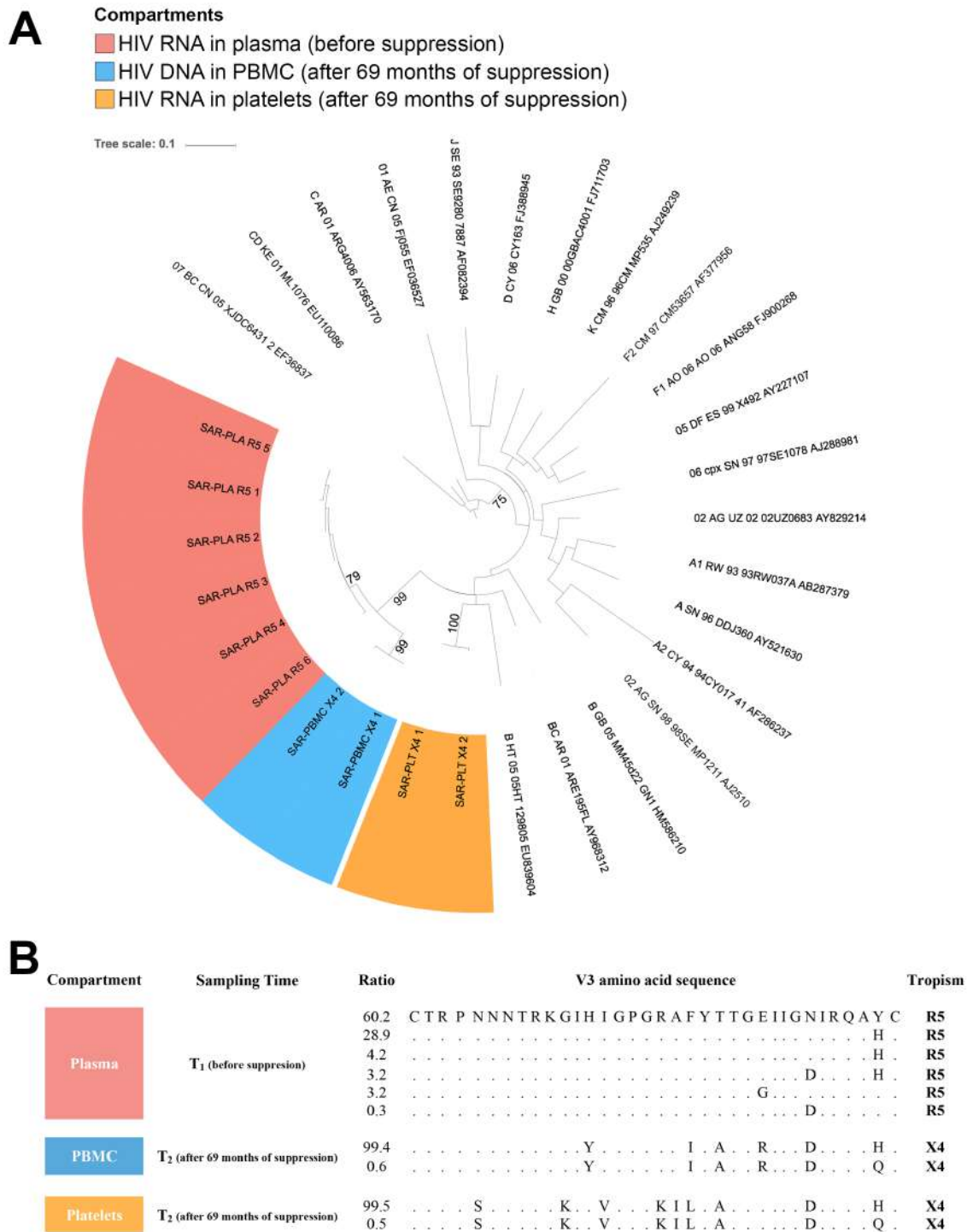


Figure S6: Deep sequencing and phylogenetic analysis of HIV *env* V3 before and after viral suppression in different compartments of the same ART-suppressed HIV-infected individual.

(A) Maximum-likelihood phylogenetic tree of *env* V3 showing the divergence of HIV RNA sequences detected: i) in the plasma before virological suppression (red area), from ii) HIV DNA sequences detected in peripheral blood mononuclear cells (PBMC, blue area) and iii) HIV RNA sequences detected in platelets

(orange area) after 69 months of virological suppression. Reference sequences with their accession number were also included. (B) HIV *env* V3 amino acid sequence alignment of the three compartments. Sampling time is indicated as T₁ (before virological suppression, for plasma sample) and T₂ (for PBMC and platelet samples collected at the same date after 69 months of suppression). The ratio indicates the proportion of the variant in the virus population. *Env* V3 sequences were analyzed for coreceptor usage indicating X4 or R5 tropism.

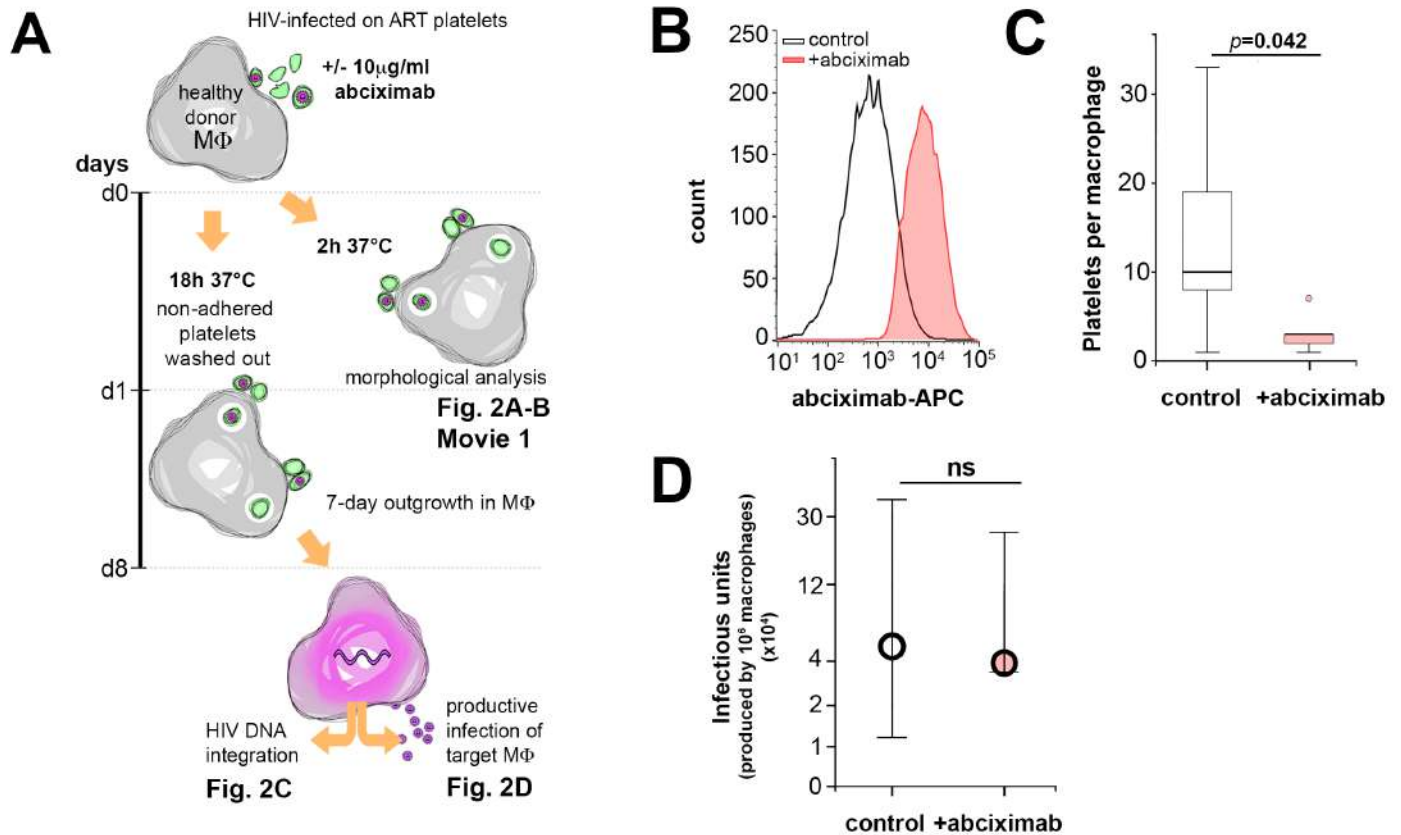


Figure S7: Interaction between platelet and macrophages is blocked by anti-integrin α II/ β 3 Fab abciximab. (A) Scheme of *in vitro* assay to quantify the propagation of infection from HIV-containing platelets to macrophages (M Φ). (B) Representative flow cytometry histogram of platelet samples treated with the platelet activation-blocker abciximab that was detected by anti-human IgG-APC (untreated, control platelets in dark lines; abciximab-treated platelets in red histogram). (C) Quantification of platelets per macrophage interacting *in vitro* assessed by epifluorescence microscopy, in the absence or presence of abciximab. Mann-Whitney U Test, n=3 biological replicates of macrophage samples, N=1. (D) Abciximab does not interfere in HIV infection of macrophages. R5-tropic HIV primary isolate were incubated with macrophages in the presence or absence of 10 μ g/ml of abciximab for 2 hours at 37°C, and recultured with fresh medium. Three days later, macrophage supernatants were collected and the presence of replication-competent virus was assessed by indicator cell assay. Mann-Whitney U Test, n=3 biological replicates of macrophage samples, N=1. ns= non-significant.

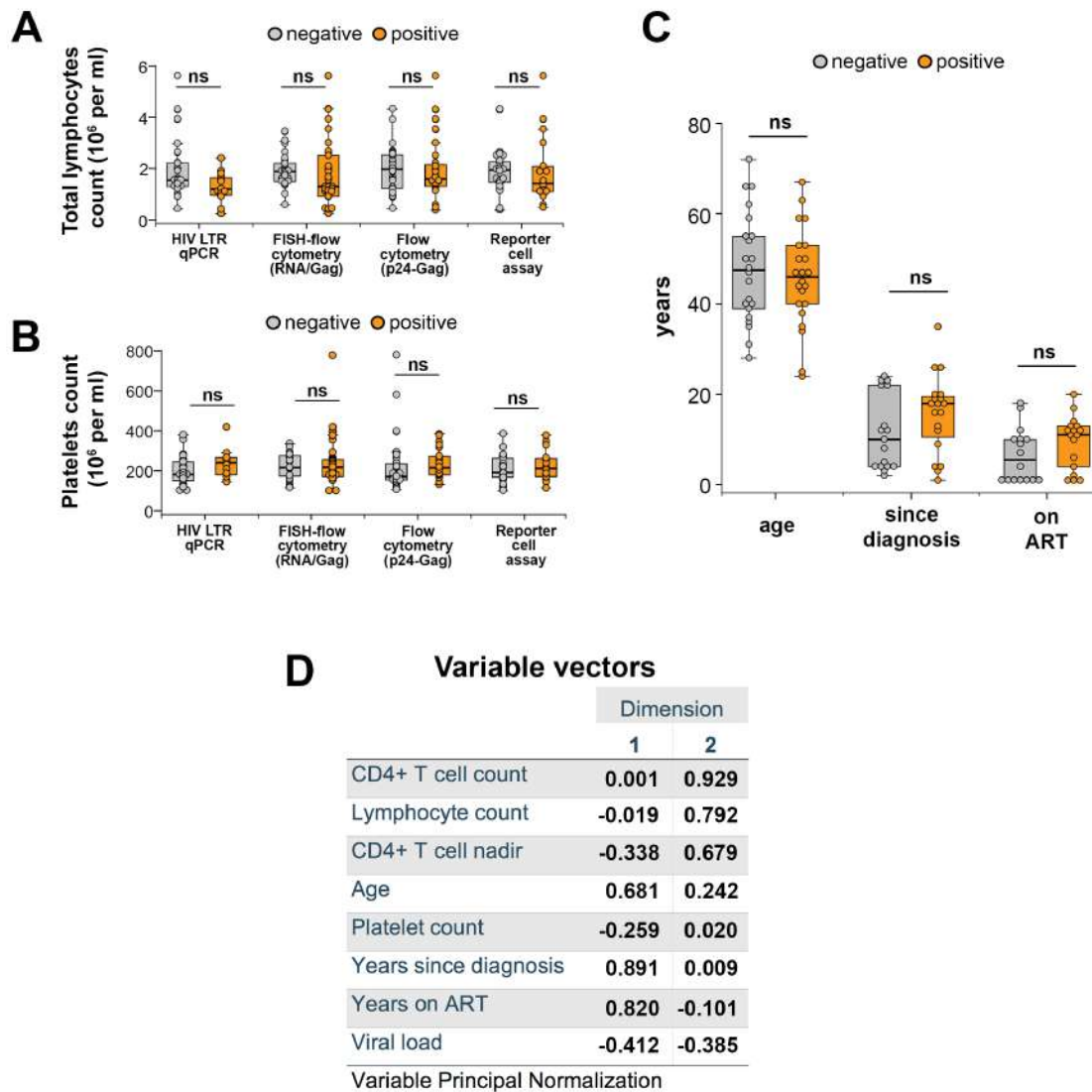


Figure S8: Detection of HIV-containing platelets do not correlate with other clinical parameters.

Comparison of total lymphocyte (A) and platelet count (B) of patients whose platelets contain (orange boxplot, positive) or not (grey boxplot, negative) HIV as assessed by HIV LTR qPCR, FISH-flow cytometry (HIV RNA/Gag), p24-Gag flow cytometry and reporter cell assays. Mann-Whitney statistical test applied to data related to each technique, ns=non-significant with $p>0.05$. (C) Detection of HIV-containing platelets do not correlate as well with patients age, years since HIV infection diagnosis or years under antiretroviral treatment. Mann-Whitney statistical test applied to each clinical parameter, ns=non-significant with $p>0.05$. (D) Values of variable vectors contribution (component loadings) to dimension 1 and 2 of the Principal Component Analysis shown in Figure 3B.

Table S1. Clinical information on HIV-infected individuals on ART analyzed for HIV in platelets

Individuals information	values	min	max
Total of HIV-infected individuals on ART	n=80		
Gender (male/female number)	55/25		
Age (median years [confidence interval 95%])	47 [CI:44-50]	24	80
Time since HIV diagnosis (median years [confidence interval 95%])	13 [CI:10-17]	1	36
Years on ART (median years [confidence interval 95%])	8 [CI:4-10]	1	34
Clinical parameters			
CD4 ⁺ T cell count (median cells per μ l [confidence interval 95%])	258 [CI:192.5-480]	6.5	1371
CD4 ⁺ T cell nadir (median cells per μ l [confidence interval 95%])	115 [CI:64-134]	2	736
Platelet count (median $\times 10^6$ platelets/ml [confidence interval 95%])	217 [CI:186-238.9]	101	778
Total lymphocyte count (median $\times 10^6$ cells/ml [confidence interval 95%])	1.65 [CI:1.5-1.91]	0.25	5.6
HIV viral load copies (\log_{10} copies/ml) ¹	<LOD [CI:<LOD-1.97]	<LOD	5.33
Viremia ² (controlled/uncontrolled number [% controlled viremia])	56/20 (73.6%)		
Immunological status ³ (in failure/competent number [% in failure])	35/40 (46.6%)		

¹<LOD: below the limit of detection of 1.6 \log_{10} copies/ml

²competent immunological status: >350 CD4⁺T-cells per ml for two or more consecutive measurements in blood samplings during at least 1 year including date of sampling for HIV in platelets; immunological status in failure: <350 CD4⁺T-cells per ml in all blood samplings during at least 1 year including date of sampling for HIV in platelets

³controlled viremia: HIV RNA \log_{10} copies/ml plasma always tested <1.60 \log_{10} copies/ml during at least 1 year including date of sampling for HIV in platelets; uncontrolled viremia: HIV RNA \log_{10} copies/ml plasma tested >1.60 \log_{10} copies/ml at date of sampling or displaying less than 12 months of continuous suppression

Supplementary table S1: Clinical information on HIV-infected individuals on ART analyzed for HIV in platelets.

Summary of the clinical information on HIV-infected ART-treated patients from which PRP samples were used in this study. Control of viremia was defined as controlled viremia (HIV RNA \log_{10} copies/ml plasma always tested undetectable for at least 1 year prior sampling for HIV in platelets) or non-controlled viremia (HIV RNA >1.60 \log_{10} copies/ml at date of sampling or displaying less than 12 months of virological suppression). Immunological status was defined as competent immunological status (>350 CD4⁺ T cells per μ l in two or more consecutive measurements during at least 1 year including the date of sampling for HIV in platelets) or immunological status in failure (<350 CD4⁺ T cells per μ l in all blood samplings during at least 1 year including the date of sampling for HIV in platelets).

Table S2. Clinical information on each HIV-infected individual on ART analyzed for HIV in platelets

Individual number	HIV-infected individual history					Clinical parameters at date of sampling for HIV detection in platelets				Techniques employed for detection of HIV in platelets				
	Gender	Age	Years since diagnosis	CD4 ⁺ T cell nadir (cells per µl)	Years on ART	CD4 ⁺ T cell count (per µl)	Viral load (log ₁₀ copies/ml)	Platelets count (x10 ⁹ /ml)	Total lymphocytes count (x10 ⁹ /ml)	HIV-1 LTR qPCR	FISH flow cytometry (RNA/Gag)	Flow cytometry (p24-Gag)	Reporter cell assay	outgrowth in MΦ
1	M	47	4	43	1	91	3.22	191	1.51					
2	F	36	3	380	1	150	2.09	144	1.19					
3	M	43	8	451	3	885	2.15	185	2.50					
4	M	66	22	NA	NA	779	2.35	237	2.36					
5	M	26	6	575	2	460	<LOD	NA	1.90					
6	M	47	19	128	11	580	<LOD	214	3.41					
7	F	50	2	4	1	185	<LOD	238	1.66					
8	M	61	NA	NA	NA	274	<LOD	218	1.88					
9	M	63	35	20	20	98	1.60	280	1.60					
10	M	40	NA	NA	1	851	<LOD	281	3.08					
11	M	62	NA	NA	NA	266	<LOD	181	5.60					
12	F	68	20	NA	10	740	<LOD	292	1.99					
13	M	69	15	210	10	673	<LOD	151	1.55					
14	M	46	NA	NA	NA	827	<LOD	176	2.19					
15	F	40	NA	482	10	601	<LOD	154	2.15					
16	M	45	10	620	10	453	2.34	267	1.80					
17	M	43	36	11	34	920	1.61	186	2.56					
18	M	44	12	NA	10	804	NA	156	2.50					
19	F	49	6	27	2	237	<LOD	NA	0.42					
20	M	44	6	NA	3	241	3.57	249	1.65					
21	F	58	NA	NA	NA	164	2.24	272	0.37					
22	F	68	20	163	8	258	2.24	778	4.32					
23	M	69	23	736	10	556	<LOD	216	1.72					
24	M	37	24	124	10	480	<LOD	125	0.95					
25	F	24	4	246	NA	774	<LOD	336	3.44					
26	M	40	6	12	1	261	2.15	186	0.90					
27	M	59	13	76	11	246	4.52	255	1.27					
28	M	57	13	8	10	62	<LOD	101	1.30					
29	M	46	18	13	10	92	<LOD	262	0.58					
30	F	57	20	62	10	180	<LOD	204	0.70					
31	M	48	5	173	2	445	<LOD	137	1.53					
32	M	39	8	NA	NA	135	<LOD	175	1.72					
33	F	43	NA	64	14	842	<LOD	290	2.40					
34	F	47	16	3	12	613	1.94	279	2.62					
35	F	25	26	13	NA	786	<LOD	275	2.22					
36	M	50	20	64	17	119	4.55	384	1.96					
37	M	34	NA	NA	NA	150	2.42	420	1.66					
38	F	37	11	414	4	171	3.40	167	1.27					
39	F	66	23	40	17	131	3.24	154	1.02					
40	M	40	4	73	4	185	<LOD	168	1.20					
41	F	35	18	75	13	32	<LOD	348	1.51					
42	M	51	NA	459	12	170	1.97	234	2.63					
43	M	34	7	115	6	159	<LOD	240	2.09					
44	M	50	17	2	13	252	<LOD	188	1.10					
45	M	40	19	6	13	618	<LOD	101	1.98					
46	M	50	12	262	9	863	<LOD	NA	1.99					
47	F	33	11	119	10	164	4.54	146	1.53					
48	M	53	3	86	2	73	5.42	171	0.91					
49	M	67	18	NA	12	112	<LOD	293	0.44					
50	F	49	23	19	22	155	4.90	NA	1.20					
51	M	48	12	384	7	731	<LOD	169	2.19					
52	M	31	3	386	1	50	2.47	357	0.89					
53	M	72	5	124	4	96	<LOD	141	1.54					
54	M	35	13	517	1	176	1.74	220	1.13					
55	F	48	12	NA	7	485	3.32	159	1.85					
56	F	54	23	NA	12	120	2.38	NA	0.90					
57	F	44	20	NA	NA	286	<LOD	166	3.53					
58	F	45	15	NA	NA	223	<LOD	212	3.92					
59	F	59	22	16	18	254	<LOD	194	3.30					
60	M	36	4	255	1	156	<LOD	378	3.00					
61	M	28	4	379	1	1030	<LOD	378	2.20					
62	M	41	7	6	4	1030	<LOD	217	1.53					
63	M	80	27	80	7	1371	<LOD	131	2.97					
64	M	53	9	120	6	133	<LOD	132	1.94					
65	M	59	24	123	17	252	<LOD	115	1.88					
66	M	55	NA	NA	NA	774	<LOD	173	2.31					
67	M	55	NA	NA	NA	620	<LOD	252	1.50					
68	M	40	3	134	1	980	2.74	167	2.57					
69	M	57	NA	NA	NA	1034	<LOD	NA	2.60					
70	M	52	NA	40	11	213	<LOD	NA	1.34					
71	F	50	NA	166	1	70	2.86	210	1.50					
72	F	38	2	4	1	155	<LOD	117	1.00					
73	F	47	1	3	1	183	<LOD	118	1.42					
74	M	45	16	NA	12	749	<LOD	263	1.96					
75	M	41	NA	NA	NA	417	1.75	221	2.00					
76	M	59	26	180	NA	161	<LOD	181	1.55					
77	M	40	4	450	1	81	<LOD	105	1.04					
78	F	38	18	17	1	194	<LOD	206	1.14					
79	M	59	NA	NA	NA	191	1.61	158	1.65					
80	M	58	17	22	5	890	<LOD	174	2.63					
81	M	40	4	450	1	531	<LOD	160	1.40					
82	F	38	18	17	1	134	5.33	397	2.67					
83	M	59	NA	NA	NA	157	<LOD	165	0.44					
84	M	52	NA	40	11	882	3.15	239	3.90					
85	F	50	NA	166	1	202	NA	175	2.03					
86	F	38	2	4	1	318	1.68	187	4.30					
87	F	47	1	3	1	102	<LOD	254	1.30					
88	M	45	16	NA	12	7	<LOD	257	0.24					
89	M	41	NA	NA	NA	6	<LOD	NA	0.25					
90	M	59	26	180	NA	119	4.90	232	0.41					
91	M	40	4	450	1	1150	<LOD	245	1.90					
92	M	59	26	180	NA	75	<LOD	330	0.48					
93	M	40	4	450	1	280	<LOD	318	1.60					
94	F	38	18	17	1	125	1.60	266	1.10					
95	M	59	NA	NA	NA	183	<LOD	220	1.30					
96	M	58	17	22	5	234	<LOD	194	1.50					

NA: not available

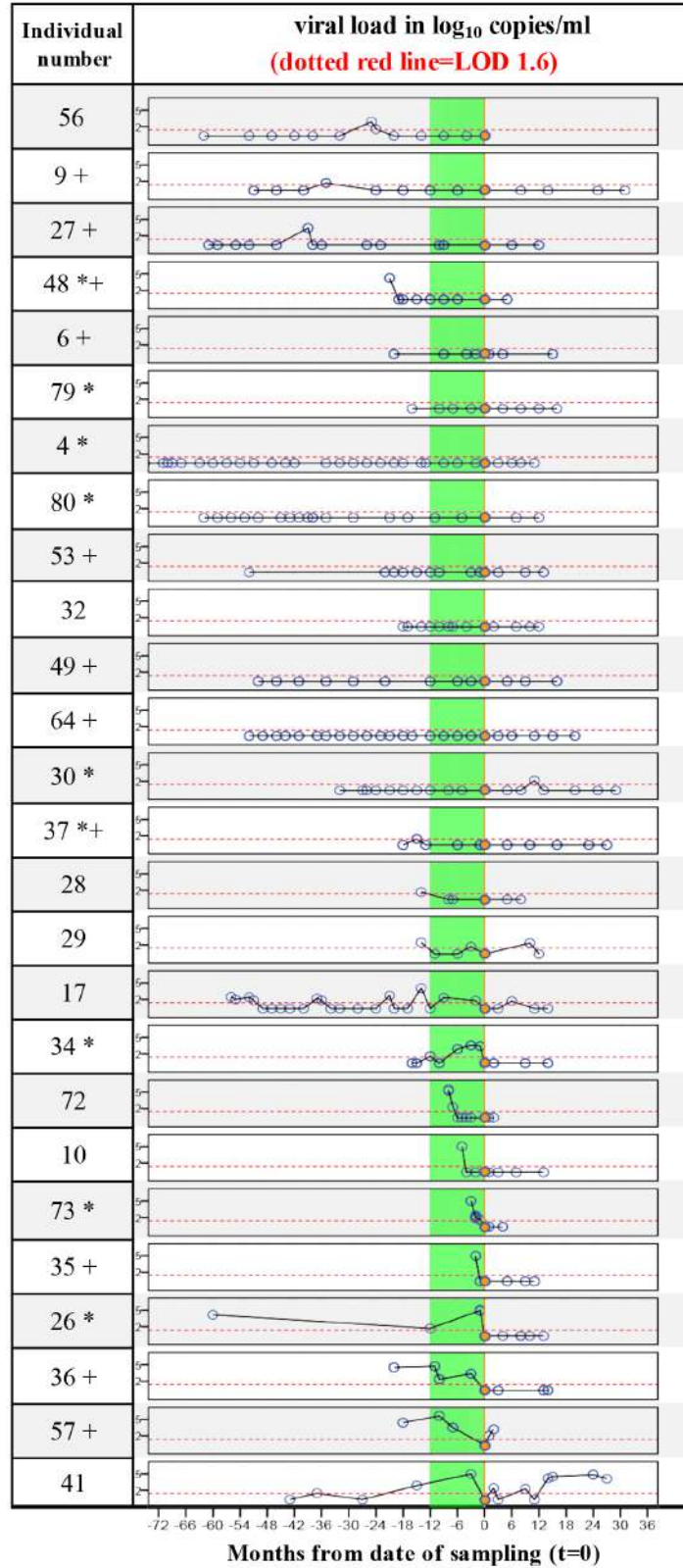
<LOD: below the limit of detection of 1.6 log₁₀ copies/ml

Multiple samplings are listed in the chronological order from earlier (up) to later (down) date of samplings

Supplementary table S2: Clinical information on each HIV-infected individual on ART analyzed for HIV in platelets.

Clinical information from patient clinical history (gender, age, years since HIV diagnosis, CD4⁺ T cell nadir and years under ART) and from the date of PRP sampling (CD4⁺ T cell count, viral load, platelet count and total lymphocytes count) of each HIV-infected ART-treated patient tested for HIV in platelets. Techniques employed for detection of HIV in platelets were quantitative PCR of HIV-LTR copies (qPCR), quantitative HIV RNA/Gag combined detection by flow cytometry (FISH-Flow), semiquantitative p24-Gag fluorescence intensity measures by flow cytometry (FACS), indicator cell assay and outgrowth of platelet-associated HIV in target macrophages. Multiple samplings were separated by 3 [CI: 2-6] months and listed in chronological order.

Table S3. Available viral load measurements for HIV-infected individuals on ART positive for HIV in platelets and with a viral load below the limit of detection (LOD) at the date of sampling



* Patients positive for HIV in platelets as assessed by HIV-1 LTR qPCR

+ Patients positive for infectious HIV in platelets as assessed by reporter cells

Supplementary table S3: Available viral load measurements for HIV-infected individuals on ART positive for HIV in platelets and with a viral load below the limit of detection (LOD) at the date of sampling.

Longitudinal plasma viral load measured around the date of sampling for patients categorized as undetectable VL below LOD at date of sampling and positive for HIV LTR (highlighted by asterisk in the table, Figure 1A), HIV RNA/Gag (Figure 1B and C) and infectious units (highlighted by +, Figure 1E) in platelet samples. Temporal data was normalized by the date of sampling, shown in the graph as time coordinate $t=0$ in x axis. Negative temporal values correspond to measures prior date of sampling, with the 1-year range prior sampling highlighted in green. Viral load in \log_{10} copies/ml is expressed in y axis, and the limit of detection (LOD) of $1.6 \log_{10}$ copies/ml is shown as dotted red line. Altogether, 53.8% of patients positive for HIV in platelets displaying VL $<$ LOD at date of sampling do display long-term (>12 months) virological control prior sampling.

Table S4. Clinical information for each HIV-infected individual on ART analyzed for HIV in megakaryocytes

Individual Number	Gender	Age	Years on ART	CD4⁺ T cell count (per μl)	Viral load (\log_{10} copies/ml)¹
81	F	39	8	265	detectable < 1.6
82	M	39	7	332	detectable < 1.6
83	M	40	7	170	1.7
84	M	47	7	231	1.7
85	M	47	4	164	1.68
86	M	47	22	144	1.96
87	M	41	7	13	1.68
88	F	44	3	68	1.7
89	F	44	5	70	1.68
90	F	45	22	289	1.7
91	M	37	7	20	< LOD
92	M	51	11	431	< LOD
93	F	51	10	407	< LOD
94	F	43	9	58	< LOD
95	M	51	21	126	< LOD
96	F	46	20	158	< LOD
97	F	43	20	115	< LOD
98	F	43	4	75	< LOD
99	M	50	18	139	< LOD
100	M	51	8	172	< LOD
101	M	46	18	250	< LOD

¹<LOD: below the limit of detection of 1.6 \log_{10} copies/ml

Supplementary table S4: Clinical information for each HIV-infected individual on ART analyzed for HIV in megakaryocytes.

Clinical information of HIV-infected ART-treated patients at the date of sampling for HIV in megakaryocytes from bone marrow samples. Information comprises patient clinical history (gender, age, and years under ART) and from the date of sampling (CD4⁺ T-cell count and viral load).

Table S5. ART regimens for HIV-infected individuals classified as positive or negative for the presence of HIV in platelets

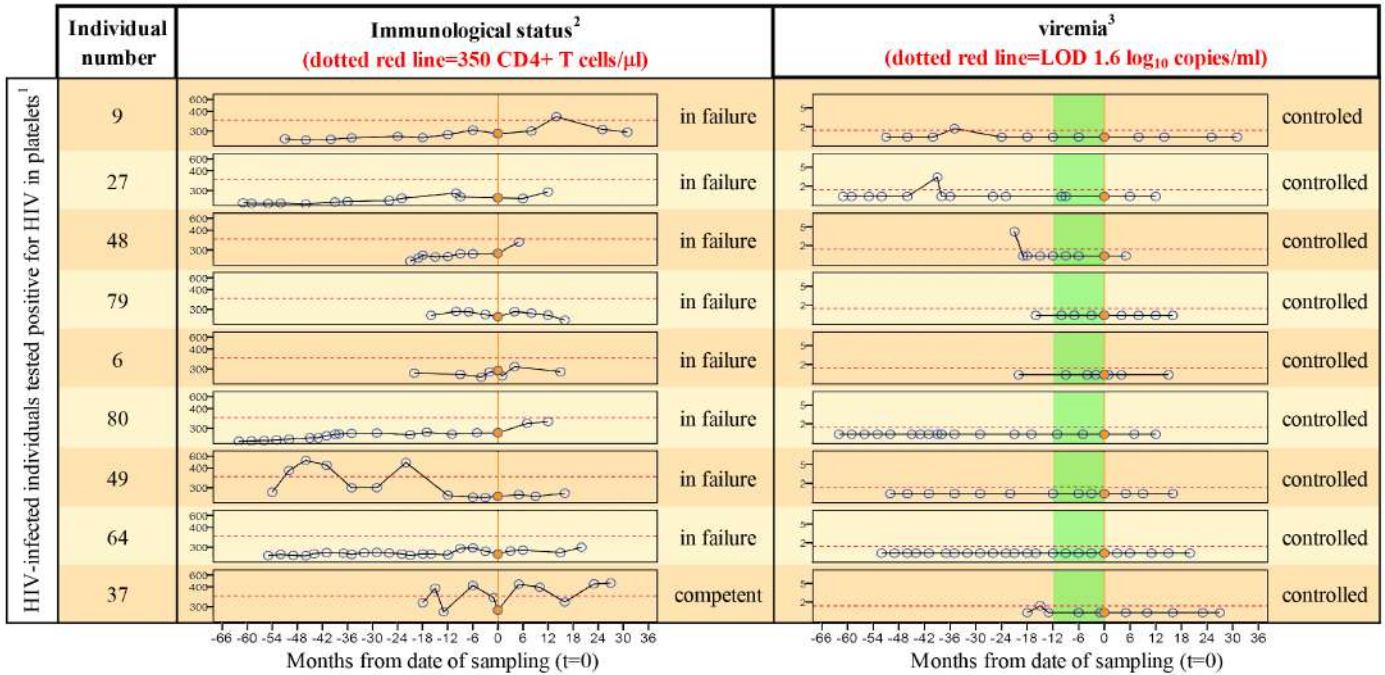
ART class	drug	Individuals tested negative for HIV in platelets*	Individuals tested positive for HIV in platelets*
RT inhibitor N nucleoside analogue	Emtricitabine or Eviplera		
	3TC or lamivudine		
	Abacavir or Kivexa or Ziagen		
	AZT or zidovudine		
RT inhibitor non nucleosidic analogue	Efavirenz or Sustiva		
	Nevirapin		
	Etravirin		
	Rilpivirin or Edurant		
RT inhibitor nucleotidic analogue	Tenofovir or Viread		
Integrase Inhibitor	Raltegravir or Isentress		
	Dolutegravir or Tivicay		
	Elvitegravir		
Protease inhibitor	Atazanavir or Reyataz		
	Ritonavir or Norvir		
	Darunavir or Prezista		
	Lopinavir		

*confirmed by at least two different techniques

Supplementary table S5: ART regimens for HIV-infected individuals classified as positive or negative for the presence of HIV in platelets.

Patients were arranged per column, classified as positive or negative based on similar results on at least two different techniques used employed for detection of HIV-containing platelets. Each row corresponds to an antiretroviral drug, organized by different ART functions (class). The use of a drug (rows) by a defined patient (columns) is spotted by a red square.

Table S6. CD4⁺ T cell counts and viral load measurements for HIV-infected individuals on ART with controlled viremia and positive for HIV in platelets



¹confirmed by at least two different techniques

²**competent immunological status:** >350 CD4+T-cells per ml for two or more consecutive measurements in blood samplings during at least 1 year including date of sampling for HIV in platelets; **immunological status in failure:** <350 CD4+T-cells per ml in all blood samplings during at least 1 year including date of sampling for HIV in platelets

³**controlled viremia:** HIV RNA log₁₀ copies/ml plasma always tested <1.60 log₁₀ copies/ml during at least 1 year prior sampling for HIV in platelets; **uncontrolled viremia:** HIV RNA log₁₀ copies/ml plasma tested >1.60 log₁₀ copies/ml at date of sampling or displaying less than 12 months of continuous suppression

Supplementary table S6: CD4⁺ T cell counts and viral load measurements for HIV-infected individuals on ART with controlled viremia and positive for HIV in platelets.

Longitudinal CD4⁺ T-cell count and plasma viral load measurements around the date of sampling in patients with sustained controlled viremia below LOD and platelets positive for HIV analyzed in Figure 4C (orange bar in the center, 88% [8 out of 9] of patients in immunological failure). Temporal data was normalized by the date of sampling, shown in the graph as time coordinate t=0 in x axis. Temporal negative values correspond to measures prior date of sampling, with the 1-year range of virological suppression prior sampling highlighted in green. Viral load in log₁₀ copies/ml or CD4⁺ T-cell count are expressed in y axis; dotted red lines refer to the viral load limit of detection (LOD) of 1.6 log₁₀ copies/ml or CD4⁺ T-cell count threshold of 350 cells/ μ l.

Table S7. List of Gag mRNA probe sequences used for FISH-flow cytometry

#	sequence	#	sequence
1	GGCCTTAACCGAATTTTTTC	25	TAGATTTCTCCTACTGGGAT
2	TTTATATTGTTTCTTTCCCC	26	TTTAATCCCAGGATTATCCA
3	CTTGCCATACTATATGTTT	27	TGGTAGGGCTATACATTCTT
4	AACTGCGAATCGTTCTAGCT	28	CCTTGTCTTATGTCCAGAAT
5	ATGTCTCTAAAAGGCCAGGA	29	TAGTCTCTAAAGGGTTCCTT
6	AGTATTTGICTACAGCCTTC	30	CTCGGCTCTTAGAGTTTTAT
7	TGAAGGGATGGTTGTAGCTG	31	TTTTTACCTCTTGTGAAGCT
8	TCTAAGTTCTTCTGATCCTG	32	CCAACAAGGTTTCTGTTCATC
9	TGCACACAATAGAGGACTGC	33	CAATCTGGGTTTCGCATTTTG
10	GTGTCTTTTACATCTATCCT	34	CTGGTCCCAATGCTTTTTAAA
11	CTCTTCCTCTATCTTATCTA	35	ATGCTGTCATCATTCTTCT
12	GCCTTTTTCTTACTTTTTGTT	36	TTCAGCCAAAACCTTTGCTT
13	TAGGGTAATTTGGCTGACC	37	GGATTTGTTACTTGGCTCAT
14	ATATGGCCTGATGTACCATT	38	GCCTTTCTGTATCATTATGG
15	ACCCATGCATTTAAAGTTCT	39	AGTCTTTCTTTGGTTCCTAA
16	GAAAGCCTTCTCTTCTACTA	40	CCTTCTTTGCCACAATTGAA
17	ACATGGGTATTACTTCTGGG	41	CCTGCAATTTTGGCTATGT
18	GCTCCTTCTGATAATGCTGA	42	AATCTTTCATTTGGTGTCTT
19	CACTGTGTTTAGCATGGTAT	43	AAATTAGCCTGTCTCTCAGT
20	TAACATTTGCATGGCTGCTT	44	AAGAAAATTCCTGGCCTTC
21	CATGCACTGGATGCAATCTA	45	CAAACCTGAAGCTCTCTTCT
22	TAGTTCCTGCTATGTCACTT	46	CTTCTGAGAGGGAGTTGTTG
23	ATTTGTTTCTGAAGGGTACT	47	ATACAGTTCCTTGTCTATCG
24	GTGGATTATGTGTCATCCAT	48	GAGTGATCTGAGGGAAGCTA

Probes targeting gag mRNA (HIV-1 vector pNL4-3; GenBank AF324493.2) were designed using the Stellaris Probe Designer program available at <http://www.singlemoleculefish.com>.

Supplementary table S7: List of Gag mRNA probe sequences used for FISH-flow cytometry

List of 48 gag mRNA probe sequences used for fluorescence *in situ* hybridization and FISH-flow cytometry analysis of HIV-containing platelets. Probes targeting gag mRNA (HIV-1 vector pNL4-3; GenBank AF324493.2) were designed using the Stellaris Probe Designer program available at <http://www.singlemoleculefish.com>.

Movie S1. Laser scanning confocal microscopy image of an HIV-containing platelet being engulfed by a macrophage

Movie refers to Figure 2B and shows fluorescence channels after immunostaining with antibodies against CD41 (green), p24-Gag (red) and merged images of the fluorescence channels with phase contrast. The movie first shows successive focal planes from the top of the cell until revealing one HIV-containing platelet inside the macrophage (0 to 8 seconds: phase contrast merged with green and red fluorescent channels; 9 to 20 seconds: zoom into HIV-containing platelet, red and green fluorescent channels merged and rotated in three-dimensional projection). Next, three-dimensional reconstruction of CD41 and p24-Gag fluorescent signals is also shown, highlighting HIV sheltered by platelet engulfed by the macrophage (20 to 29 seconds: CD41 and p24-Gag isosurfaces in green and red respectively).